Genome-wide Target Analysis of NEUROD2 Transcription Factor Reveals Potential Roles in Cortical Migration and Layer Formation

by

Gizem Güzelsoy

A Thesis Submitted to the
Graduate School of Sciences and Engineering
in Partial Fulfillment of the Requirements for
the Degree of

Master of Science
in
Molecular Biology and Genetics

Koc University
September 2015

Koc University

Graduate School of Sciences and Engineering

This is to certify that I have examined this copy of a master's thesis by

Gizem Güzelsoy

and have found that it is complete and satisfactory in all respects,
and that any and all revisions required by the final
examining committee have been made.

Committee Members:

_____

Gülayşe Ince Dunn, Ph. D. (Advisor)

_____

Tamer Önder, Ph. D.

_____

Aslı Kumbasar, Ph. D.

Date: _____

To My Dearest Family..

ABSTRACT

Specialized functions of cells and how they communicate with each other determine the functions of organs as well as organ systems. The nervous system consists of the brain, spinal cord and the peripheral nerves of the body and it allows an organism to perceive and respond to the environment. The brain is a complex organ that is composed of complex networks of neurons. Each neuron receives input from thousands of other neurons, so trillions of connections are created in the brain. This intricacy provides us to perform many sensory, motor and cognitive tasks.

Different types of transcription regulators play roles in the development of the nervous system. Prominent among them are the basic helix-loop-helix (bHLH) family of transcription factors that control a wide array of developmental process in different organisms. Neurogenic Differentiation Factor2 (NeuroD2), a member of the neurogenic bHLH transcription factors, contributes to neurogenesis significantly in the brain.

The complexity of the gene regulatory system that controls the development of the rich assortment of neurons is revealed by the identification of direct target genes of transcription factors. Despite the crucial role of NeuroD2 in neuronal differentiation and development, its transcriptional downstream target genes during development are not known. My goal in this study was to analyze the binding profiles of NeuroD2 transcription factor in whole genome as revealed by a previous Chromatin Immunoprecipitation followed by sequencing (ChIP-Seq) experiment conducted in our laboratory. My results demonstrated that NeuroD2 regulates a set of genes which are responsible for axon guidance, synaptogenesis, neuronal migration; cortical layer identity and dendritogenesis. Further I aimed to analyze the function of NeuroD2 in the

dendrite development and branching; however I found that NeuroD2 does not affect the morphology of dendrites in primary cortical neurons. In addition, I examined the mechanism by which NeuroD2 regulates the Inhibitor of Differentiation 2 (Id2) protein which inhibits E-box mediated gene expression by interfering with binding of neurogenic bHLH proteins to their target promoters. My results showed that the mRNA level of *Id2* does not change in the knockdown of *NeuroD2* suggesting that NeuroD2 does not regulate the expression of *Id2* gene at the conditions examined.

Taken together, my findings indicate that NeuroD2 is an effector transcription factor that targets key genes playing role in cortical migration and layer formation and required for major signaling pathways such as Reelin and Wnt pathways while it is not necessary for the dendrite morphology and regulation of *Id2* gene expression.

ÖZET

Hücrelerin özelleşmiş fonksiyonları ve birbirleriyle olan ilişkileri, organların hatta organ sistemlerinin işlevlerini belirler. Beyin, omurilik ve vücuttaki periferik sinirlerden oluşan sinir sistemi, bir organizmanın çevreyi algılamasını ve cevap vermesini sağlar. Beyin, karmaşık nöron ağlarından oluşan kompleks bir organdır. Her nöron binlerce diğer nörondan girdi alır böylece beyinde trilyonlarca bağlantı oluşur. Bu karmaşıklık bizim duyusal, fiziksel ve zihinsel görevleri yerine getirmemizi sağlar.

Yazılım düzenleyicilerinin farklı tipleri sinir sisteminin gelişiminde rol oynamaktadır. Aralarında öne çıkan temel heliks-lup-heliks (bHLH) yazılım faktörü ailesi, farklı organizmalardaki gelişimsel süreci kontrol etmektedir. Neurogenic Differentiation Factor 2 (NeuroD2), nörojenik bHLH yazılım faktörleri üyesi, beyinde nöron oluşumuna önemli derecede katkıda bulunmaktadır.

Nöronların zengin çeşitliliğinin gelişimini kontrol eden gen düzenleme sisteminin karmaşıklığı, yazılım faktörlerinin doğrudan hedef genlerinin tanımlanması ile ortaya çıkar. NeuroD2 nöronsal farklılaşma ve gelişiminde hayati rol almasına rağmen, NeuroD2'nin gelişim sırasındaki yazılım alt hedef genleri bilinmemektedir. Benim bu çalışmadaki amacım; laboratuvarımızca yürütülen kromatin imünpresipitasyon sonrasındaki dizinlemenin ortaya çıkardığı NeuroD2 yazılım faktörünün tüm genom içindeki genlere bağlanma profilini analiz etmekti.

Sonuçlarım NeuroD2'nun akson yöneliminden, sinaps oluşumundan, nöron göçünden, dendrit oluşumundan ve kortikal tabaka kimliği belirlenmesinden sorumlu bir dizi genin işlevini düzenleyen olduğunu göstermiştir. Bunun dışında, ben NeuroD2'nun

dendrit gelişimindeki ve dallanmasındaki işlevini incelemeyi amaçlamıştım; ancak NeuroD2'nin birincil kortikal nöronlarda dendritlerin morfolojisini etkilemediğini buldum. Buna ek olarak, NeuroD2'nin bHLH proteinlerinin hedef genlerinin yazılım başlatıcı bölgelerine bağlanmasına müdahale ederek E-kutu aracılığıyla gerçekleşen gen ifadesini engelleyen Inhibitor of Differentiation (Id2)'yi düzenlediği mekanizmayı inceledim. Sonuçlarım, *NeuroD2* susturulduğunda *Id2'*nin mRNA seviyesinin değişmemesinin, NeuroD2'nin *Id2* geninin işlevinin düzenlenmesinde görevli olmadığını gösterdi.

Birlikte ele alındığında, bulgularım NeuroD2'nin kortikal nöron göçü ve tabaka kimliği mekanizmalarında rol oynadığını ayrıca Reelin ve Wnt gibi başlıca sinyal yollarında gerekli olan önemli genleri hedefleyen efektör bir yazılım faktörü olduğunu fakat dendrit morfolojisinde ve *Id2* geninin işleyişinde gerekli olmadığını işaret etmektedir.

ACKNOWLEDGEMENTS

Firstly, I would like to deeply thank my advisor Gülayşe İnce Dunn, PhD for her knowledge, enthusiasm, creativity and great ideas. I am very grateful for her constant patience and persistent help during my research. She helped me modulating my scientific way of thinking, encouraged me and supported me.

I would like to express my gratitude to Tamer Önder, PhD not only for critical reading of my thesis but also for sharing constructs and equipment without hesitation. I would also like to thank Cory Dunn, PhD and Halil Kavaklı, PhD for helping me by sharing their constructs and Aslı Kumbasar, PhD for critical reading on my thesis.

I am hugely indebted to my postdoc Efil Bayam, PhD for her useful comments and assistance as this work would not have been accomplished without her support. Although she sometimes treated me like a "gestapo" in the laboratory, there was a different relationship between us called "tough love". She spend her all time to discuss my project and to create great ideas about my research. I have learned lots of valuable research techniques from her. Her assistance opened my mind by gaining different points of view and made me more excited in this scientific world. In addition to scientific field, I am thankful to her for enjoyful conversations about theatre, music and life.

I would like to thank not only my lab members but also friends, Semra Şahin and Gökhan Güner for all coffee breaks, gossips and fun. I would like to give my very special thanks to Cansu Akkaya for her help and support in the lab. I am also grateful to her for being with me in my sad times. I would like to thank Gülkız Baytek, Emel Akdoğan,

Abdurrahman Keskin and Zeynep Cansu Üretmen for being nice friends from METU to these days.

I would like to thank my best friends Oğuz Yaşar, Elif Dağaslan, Kağan Karataylı, Emre Eryiğit, Elif Çevik and Fırat Ergon for always being there for me. I am very lucky to have friendship with these perfect people.

I would like to say very special and deep thanks to my dear one, Deniz Mengü, without whom for sure life in this boring university especially in İstanbul would not have been the same. Thanks for sharing all the happy and hard moments of my life, never letting me feel alone, cheering me up every single time and making this school a sufferable place for me. Having met him has been my biggest chance during graduate school.

Last but definitely not least, I am grateful to my parents, Ayhan and Güzide Güzelsoy, my brother Hasan Güzelsoy and my aunt Aynur Küçükyılmaz for always supporting and believing in me throughout my life with their endless love, without them this work would have never been possible.

TABLE OF CONTENTS

LIST OF TABLES

LIST OF FIGURES

NOMENCLATURE

APS	Ammonium persulfate
ATP	Adenosine triphosohate
bHLH	Basic Helix-loop-helix
BSA	Bovine Serum Albumin
BME	Basal Medium Eagle
bp	Basepair
cDNA	Complementary Deoxyribonucleic acid
Ch-IP	Chromatin Immunoprecipitation
DAPI	4',6-diamidino-2-phenylindole
DMEM	Dulbecco's Modified Eagle Medium
DMSO	Dimethyl sulfoxide
DNA	Deoxyribonucleic acid
dNTP	Deoxynucleotide
DTT	Dithiothreitol
EDTA	Ethylenediaminetetraacetic acid
FBS	Fetal Bovine Serum
GFP	Green Fluorescent Protein
HBSS	Hank's Balanced Salt Solution
HEPES	4-(2-Hydroxyethly)piperazine-1-ethanesulfonic acid
HRP	Horseradish peroxidase
kDa	Kilodalton
LB	Luria Broth
MEM	Minimum Essential Media
mRNA	Messenger Ribonucleic acid

NEM	N-ethylmaleimide
PBS	Phosphate Buffered Saline
PEG	Polyethylene glycol
PCR	Polymerase Chain Reaction
PFA	Paraformaldehyde
P/S	Penicillin/Streptomycin
Q-PCR	Quantitative Polymerase Chain Reaction
RIPA	Radioimmunoprecipitation Assay Buffer
RNA	Ribonucleic Acid
RT-PCR	Reverse Transcription Polymerase Chain Reaction
shRNA	Short Hairpin Ribonucleic Acid
SDS-PAGE	Sodium Dodecyl Sulfate Polyacrylamide Gel Electrophoresis
TBS-T	Tris Buffered Saline-Tween
TEMED	Tetramethylethyleneamine

Chapter 1

INTRODUCTION

Nervous system is the major network that controls and regulates the communication in the body. It is the center of all mental activity including thought, learning, and memory. The central nervous system (CNS) includes the brain and the spinal cord. It consists of different types of tissues, including nerve, blood, and connective tissue and has billions of neural connections, which together carry out complex activities of the mind.

During early development, brain's three major vesicles called forebrain, midbrain and hindbrain is generated by the anterior part of the neural tube. During the development of the brain, diverse cell types are generated by neural stem cells and progenitor cells. This process starts with the proliferation of the cells, continues with cell cycle exit, cell fate determination and migration of the cells to settle to the proper place in the brain. Following migration, neurons initiate differentiation and form neurites called axon and dendrites to support synaptogenesis and the establishment of neuronal connectivity. The destiny of a particular cell type is determined by environmental cues and by an cell intrinsic program of gene expression [1].

Intrinsic genetic factors, for example, transcription factors (TFs) have important roles in determining the identity and the connectivity of neurons [2]. Helix-loop-helix (HLH) transcription factors are discovered to be critical in the regulation of differentiation and

development in numerous cell types including neurons, myocytes and hematopoietic cells [3][4]. Basic helix-loop helix (bHLH) proteins are capable of forming heterodimers and binding to specific DNA sequences called E-box sites. The roles of transcription factors of bHLH family in cell proliferation, determination and differentiation are essential for the brain. In addition, they have important roles in neuronal morphogenesis, neuronal polarization, axon development, dendrite development and synaptogenesis [5][6].

NeuroD family proteins include NeuroD1, NeuroD2, NeuroD4 and NeuroD6 and regulate neuronal differentiation of the telencephalon. These transcription factors start to get expressed in post-mitotic neurons at embryonic stages throughout adulthood. Expression of proneural bHLH transcription factors which are Neurog1 and Neurog2 determine the neuronal fate decision by regulating NeuroD1/2 [7]. There is limited information about their downstream pathways and how they regulate differentiation.

HLH repressors function in neuronal development and differentiation. These proteins antagonize bHLH transcription factors by binding to them and inhibit them from binding to DNA. Id family of inhibitory HLH factors additionally takes parts in neurogenesis. Each of four mammalian *Id* genes (*Id1-4*) are expressed in the developing brain. Moreover, the ectopic expression of Id2 has the capacity to promote premature neurogenesis and provide the conversion of ectoderm to neural crest cells [8].

To be able to solve the gene regulatory network, the direct target genes of the transcription factors were identified by genome-wide analysis. ChIP-Seq is a powerful method that determines the binding profile of transcription factors in the genome. The direct target genes of NeuroD2 bHLH transcription factor were analyzed by performing ChIP-Seq in embryonic and postnatal cerebral cortical tissues [9].

In this study, I confirmed a large set of the direct target genes of NeuroD2 identified by ChIP-Seq analysis in embryonic and postnatal stages of mice cortical development by performing Chromatin Immunoprecipitation Quantitative Polymerase Chain Reaction (ChIP-qPCR). I knocked down NeuroD2 in embryonic primary neuronal cell cultures and carried out Reverse Transcription Quantitative Polymerase Chain Reaction (RT-qPCR) confirmation to determine which genes expression are regulated by NeuroD2. I validated that NeuroD2 binds to a set of genes which act as key regulators of radial migration and axon pathfinding of cortical projection neurons. I further confirmed that NeuroD2 regulates genes which are responsible for synaptogenesis and dendritogenesis. According to the preliminary data (Ince-Dunn, unpublished) suggesting that in NeuroD2 knock-out samples, there is a significant reduction in the number of branches and dendrites compared to the wild type. Therefore, I specifically focused on the function of NeuroD2 in the dendrite development and analyzed the polarity and the branching of dendrites in embryonic stage. My results demonstrated that knockdown of NeuroD2 did not affect the dendrite morphology in embryonic primary neurons. In addition, I focused on Inhibitor of Differentiation 2 (Id2) which inhibits E-box mediated gene expression by interfering with binding of neurogenic bHLH proteins to their target promoters. According to the preliminary data (Ince Dunn, unpublished), *Id2* gene was identified as a top candidate gene in a microarray experiment comparing gene expression patterns between wild-type and NeuroD2 knockout mice. *In situ* hybridization and northern blot results demonstrated that *Id2* expression is significantly reduced in NeuroD2 knockout mice. Therefore, I examined the interaction between Id2 and NeuroD2 and also their expression and localization patterns on neuronal differentiation; however my results suggested that NeuroD2 did not regulate the expression of *Id2* gene. Also, I did not detect a protein-protein interaction between these two proteins.

In Chapter 2, the literature review of NeuroD2 bHLH transcription factor and its significance for neurogenesis and dendritogenesis are explained. In Chapter 3, the material and methods used in this study are explained. Finally, in Chapter 4 and 5, the results of my project, their importance and indications are described.

Chapter 2

LITERATURE REVIEW

2.1 Overview

The remarkable complexity of the brain is fundamental to sensory, motor and cognitive functions and the proper development of the brain.

Ectoderm, the outermost of the three germ layers, gives rise to the neural plate that forms the central nervous system (CNS). During embryonic neurodevelopment, neural plate folds to form the neural tube in a process called neurulation [10][1]. While the internal cavity of the neural tube comprises the ventricular system, the outer tissue of the neural tube differentiate progressively to give rise to the spinal cord and the brain with three primary vesicles called the prosencephalon (forebrain), mesencephalon (midbrain) and rhombencephalon (hindbrain) (Figure 2.1) Rostrally, the prosencephalon generates the telencephalon which is the precursor of cortex dorsally and ganglionic eminence ventrally.

The development of neural structure occurs in three major processes: cell proliferation, cell migration and cell differentiation. Before onset of the neurogenesis, the single layer of cells called neuroepithelial cells (NE) which are located in neural plate and neural tube divide symmetrically to proliferate and expand ventricular surface [11][12][13].

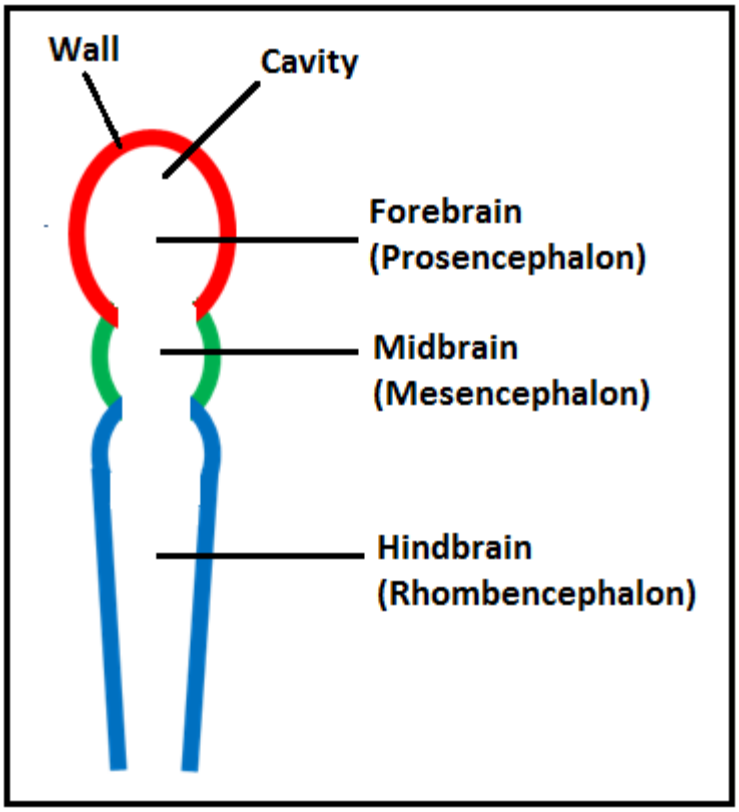

Figure 2.1 Division of the embryonic brain into three primary brain vesicles, known as the forebrain (prosencephalon), midbrain (mesencephalon), and hindbrain (rhombencephalon).

These earliest neural precursors change their style of division from symmetrical to asymmetrical and produce the highly polarized radial glial cells (RGC) which are the progenitors of nearly all glial cells and excitatory neurons in the mammalian cortex. Since the cortex becomes thicker progressively, RGCs keep contact with both apical and the pial surfaces. Besides, the cell bodies of RGCs are located in the ventricular zone (VZ) [14] [12] [15]. These cells also divide symmetrically to increase the number of their own progenitors however at mid-neurogenesis (E13.5) they start to divide asymmetrically to give rise to immature neurons or intermediate (basal) progenitors (BP) [16][17][18].

Immature neurons start differentiating into cortical projection neurons after migrating from VZ to the outer layers while BPs migrate to the subventricular zone (SVZ) where they divide and form more neurons. A new type of RGC is generated by neural precursor cells called outer radial glial cells located in outer VZ (Figure 2.2).

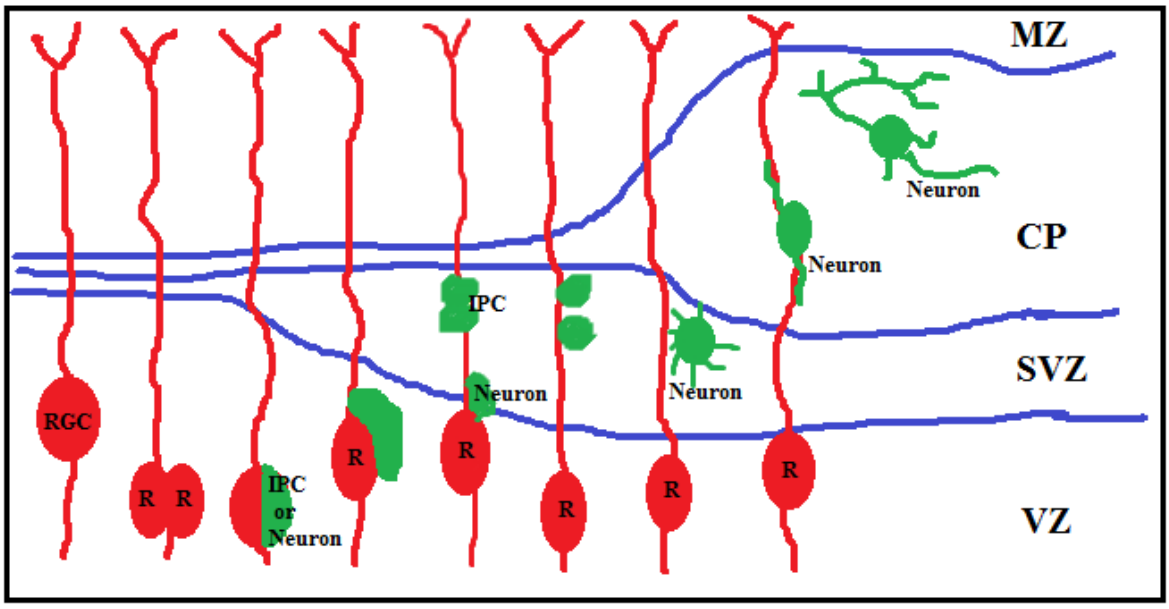

Figure 2.2 Schematic presentation of neuronal migration and differentiation during neurogenesis. Abbreviations: RGC and R, radial glial cells; IPC, intermediate progenitor cells; VZ, ventricular zone; SVZ, subventricular zone; CP, cortical plate; MZ, marginal zone

At the end of the neurogenesis, RGCs differentiate into post-mitotic ependymal cells in the ventricle or astrocytes and oligodendrocytes in the cortical layers but some of them keep their neurogenic identity and serve as adult neural stem cells [19] [20].

The largest part of the cerebral cortex is neocortex which has highly organized six layers containing various types of neurons and glia. The neurons including glutamergic excitatory projection (pyramidal) neurons and GABAergic inhibitory interneurons are unique in terms of their morphology, function and connection in each layer of neocortex [21]. Developmentally, the inhibitory neurons that are generated from progenitors in the ventral telencephalon migrate along multiple pathways to reach the cerebral cortex and connect to the already existing neural circuits [22] [23], whereas the excitatory neurons are generated from progenitors in the dorsal telencephalon, migrate radially to upper layers of the cortex resulting in an inside to outside manner [24]. The migration of the neurons to their final destination where they obtain different neuronal properties and connectivity provide the formation of six layers of the neocortex.

The projection neurons in different cortical layers have distinct morphologies and projection patterns. Layer I contains the apical dendrites of the pyramidal cell from lower layers whereas layer II and III comprising small and medium sized densely packed pyramidal neurons are the main origin and termination of intercortical connections. Layer 4 has spiny stellate excitatory interneurons and pyramidal neurons that connect to the thalamocortical neurons. Lastly, layer V and VI contain the largest pyramidal neurons that connect with basal ganglia, brain stem, spinal cord and thalamus by forming long distance projections [25][12][26].

It has been demonstrated that the mechanism of neurogenesis is intrinsically regulated. Intrinsic effectors such as transcription factors play vital roles in proliferation of neural precursor cells, fate determination of neurons, astrocytes, oligodendrocytes and also development and layer identity of neocortex [19][21]. Especially, cell specific basic helix-loop-helix transcription factors determine many mechanisms during development. For

example, differentiation of oligodendrocytes from glial cells is guided by Olig1/2 bHLH factors [27][28] and two types of HLH proteins, Hes and Id family proteins [3]. Hes factors inhibit neuronal differentiation by direct transcriptional repression and physical interaction by binding to specific DNA region of a target gene. On the other hand, due to the lack of a basic domain, Id family members do not bind to DNA thus act as a dominant-negative regulator by sequestering E proteins needed heterodimerization with proneural bHLH factors [29]. The proneural bHLH transcription factors that are expressed in progenitor cells are key regulators for initiation of differentiation. Ascl1 (Mash1) is known to generate GABAergic neurons by expressing in the ventral telencephalon whereas Neurog1 and Neurog2 expressed in dorsal telencephalon produce all cortical projection neurons by directing the expression of cascades of neuronal differentiation bHLH transcription factors such as NeuroD and Nscl family [30]. Like proneural factors, differentiation factors also bind to specific DNA regions called E-box site and promote gene expression required for polarization, synaptogenesis, dendritogenesis or migration [31]. Projection neurons located in different cortical layers are under control of distinct groups of bHLH transcription factors. For example, Neurog2 is essential for early-born deep layer neurons specification [32] with its downstream effectors such as Tbr1 and NeuroD1/2 [9][30]. Furthermore, while the upper layers II, III and IV express Cux1/2 and Brn1/2, neurons in deep layers V and VI express Ctip2 and Fezf2 [25][33][1][34].

Taken together, the cortex is comprised of progenitor cells limited in their potential to give rise to specific neurons during different developmental processes.

2.2 NeuroD Family

NeuroD family that belongs to basic helix-loop-helix transcription factors plays important roles in the control of neurogenesis [3]. There are four members of this family: NeuroD1, NeuroD2, NeuroD4 and NeuroD6. NeuroD1, the first identified one, is highly expressed in the regions containing differentiating neurons in both frog and mice [3]. The ectopic overexpression of NeuroD1 in Xenopus embryos make ectodermal cells differentiate into neurons. Other NeuroD-related factors have been classified subsequently as NeuroD2 and NeuroD4 [4].

Specifically, NeuroD2 (NDRF) shows %53.4 similarity with NeuroD1 based on sequence. In addition, like NeuroD1, NeuroD2 has capability of formation of ectopic neurons when it is overexpressed in Xenopus embryos [4]. Moreover, these two transcription factors bind to specific E-box sequences (CANNTG) of a target gene after forming heterodimers with ubiquitously expressed E proteins. It is suggested that there is an upstream/downstream cascade among NeuroD bHLH transcription factor family that directs neuronal development [3].

2.3 Expression Pattern of NeuroD2 in the nervous system

McCormick *et al.* demonstrated that NeuroD2 was expressed in both newborn and adult mice. The expression of NeuroD2 starts at embryonic day 11 (E11), increases at E12.5 and persists in the post mitotic neurons through the adult nervous system (Figure 2.3). It has been discovered that NeuroD2 is expressed in the neocortex, cerebellum, amygdala, optic tectum, spinal cord and the brainstem during the development but in the adult stage the expression is detected only in hippocampus and the region of Purkinje cells [35] [36] [4].

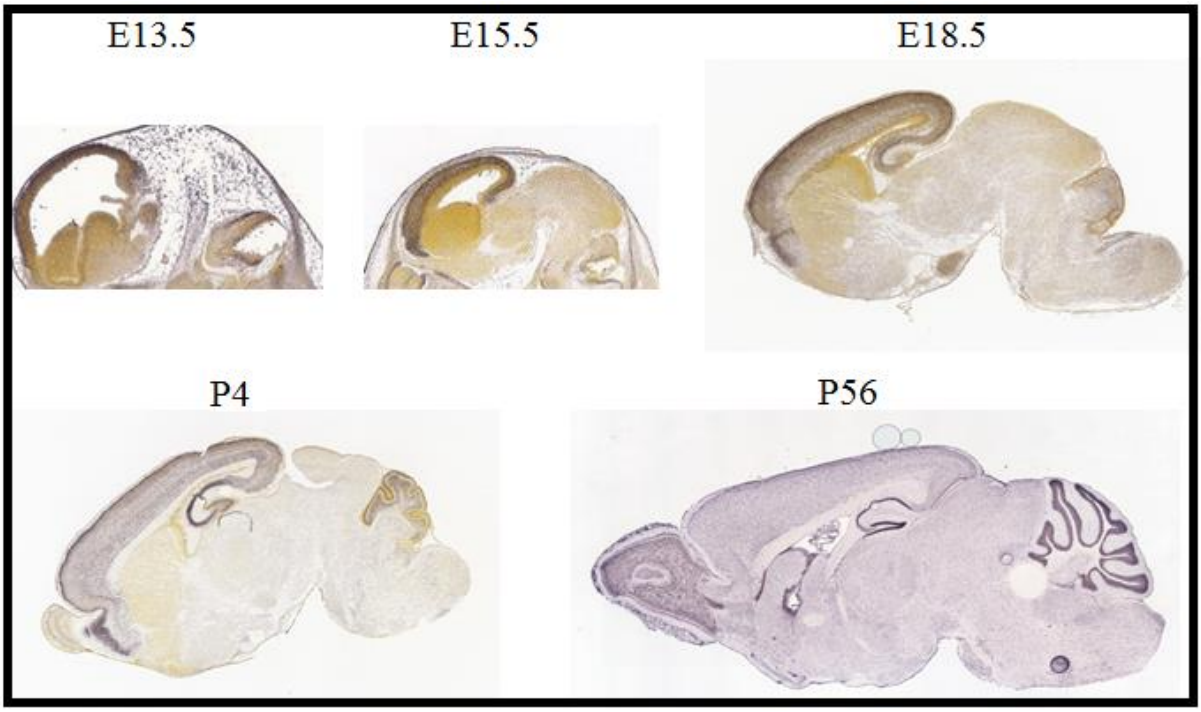

Figure 2.3 Expression patterns of NeuroD2 from embryonic stage to the adulthood (Allen Brain Atlas).

2.4 Regulation of Expression and Activity of NeuroD2

The proneural bHLH proteins Neurog1 and Neurog2 which are expressed in dorsal telencephalon progenitors control the specification and differentiation of neuronal phenotypes [7] [35]. Y.Sun et al. showed that the exogenous expression of Neurog1 in E14 rat cortical precursor cell culture increase the generation of neurons. In addition, decrease in number of neuronal population in *Neurog2* single mutant embryos indicates the importance of Neurog2 for neurogenesis [37] [38]. The genes that are downregulated in the presence of mutant form of Neurog1 and Neurog2 were identified by microarray analysis.

This study demonstrated that NeuroD2 expression is promoted by these proneural proteins [30] [39].

The activation of NeuroD2 by Neurog1 was found by co-transfection of *NeuroD2* gene promoter driven luciferase reporter and the different bHLH expression vectors to P19 embryonal carcinoma cells. H.Oda et al. demonstrated that only Neurog1 has the ability to trans-activate the reporter construct [40]. Additionally, Lin *et al*. affirmed the role of Neurog1 proneural protein on *NeuroD2* gene expression [41]. In this study, breeding *Neurogenin1*-null mice with *NeuroD2*+/- mice expressing *lacZ* gene under the control of the *NeuroD2* promoter resulted in the loss of lacZ expression in neurons where *NeuroD2* is expressed normally [41].

The significance of Neurog2 to induce the expression of *NeuroD2* gene was revealed by the mis-expression of Neurog2 in the dorsal telencephalon. Mattar et al. showed that NeuroD2 is a downstream protein of Neurog2 pathway [42].

2.5 Regulation of Transcriptional Activity of NeuroD2

Throughout the development of the cerebral cortex, the stabilization and assembly of the neurons are provided by neuronal activity patterns [43]. As the neurons are activated, the connections between them become permanent and specific resulting in the establishment of the mature of the nervous system. Moreover, neuronal activity affects cell proliferation, synaptogenesis, axon and dendrite formation [44]. Calcium mediates many of the neuronal activity-dependent development, differentiation and plasticity of the nervous system [45].

NeuroD2 is one of the calcium-regulated transcription factors that were identified by the use of “transactivator trap” strategy [44].

2.6 Role of NeuroD2 in Neuronal Development and Differentiation

The neurospecific transcription factor NeuroD2 has the ability to differentiate the neural precursor cells into neurons [4][35]. Farah *et al.* found that transient expression of NeuroD2 achieves the differentiation of pluripotent mouse P19 embryonal carcinoma cells into neurons. In this study, expression of NeuroD2 with its binding partner E12 lead to cell cycle exit, induction of electrical excitability and neurite growth. Furthermore, Noda *et al.* showed that mouse neuroblastoma cell line N1E-115 adopts neural morphology after transduction of NeuroD2 protein [46].

NeuroD2 also plays an essential role in the normal brain development by controlling the cell maintenance, population as well as migration and synaptic plasticity. Olson et al. analyzed the transgenic mice lacking NeuroD2 has neurodevelopmental abnormalities such as ataxia [47]. They realized that the brain regions of transgenic mice that expressed NeuroD2 were smaller compared to the wild-type. In addition, they suggested that brain-derived neurotrophic factor, BDNF, which is responsible for cerebellar neuron survival might be a target gene of NeuroD2 since its expression was decreased in NeuroD2 null mice brain [47].

2.7 Role of NeuroD2 in Thalamocortical Communication

Sensory input from peripheral systems is transmitted to the cortex through the brainstem and thalamus. In cortical layer IV, cells surround the individual thalamocortical

axon clusters which result in the formation of whisker related structures called “barrels”. Signals are carried to each barrel from the one corresponding whisker follicle [36] [48].

Ince-Dunn *et al.* showed that the pre and post-synaptic mechanisms of thalamocortical interactions were regulated by NeuroD2. As NeuroD2 is a calcium-activated transcription factor [36] and the thalamocortical connections are regulated by neuronal activity [49], they analyzed the thalamocortical connections in *NeuroD2* knockout mice. They observed that the barrels were disorganized and the maturation of synaptic transmission was damaged in *NeuroD2* knockout mice, leading to abnormal thalamocortical development. Therefore, they concluded that NeuroD2 acts as a key regulator for the formation of proper thalamocortical axon segregation [36].

2.8 Role of NeuroD2 in synaptogenesis

In the cerebral cortex, neurons are divided into two major types according to the neurotransmitters that they release. The neurons releasing GABA neurotransmitter is called inhibitory neurons which cause the inhibition of post-synaptic neurons. However, excitatory pyramidal neurons release glutamate neurotransmitters to activate the post-synaptic neurons. For the neuronal activity of the excitatory pyramidal neurons, glutamergic synapses are required. Therefore, there are metobotropic and ionotropic glutamate receptors located in the post-synaptic membranes [48]. Ionotropic glutamate receptors are composed of NMDA, AMPA and kainate receptors and affect the establishment and the function of development of thalamocortical synaptic connections [48]. While the NMDA receptors take role in the early development of the synapse, AMPA receptors regulate the transmission of currents in the mature synapses [50]. Lu and his colleagues determined that the relation between AMPA currents and the barrel formation

by showing that the AMPA/NMDA receptors are reduced when the mice has impaired barrel formation. Besides this findings, Ince-Dunn et al. demonstrated that the contribution of AMPA receptors are decreased comparing to the NMDA receptors in *NeuroD2* knockout mice demonstrating the significance of NeuroD2 in the regulation of synaptic maturation [36][51].

Glutamergic synapses are mediated by post-synaptic protrusions called dendritic spines that are regulated by activity–dependent changes in calcium [48] resulting in morphological changes. NeuroD2 is one of the transcription factors that are expressed in excitatory post-mitotic neurons and regulated by calcium signaling [4][36][48]. Wilke et al. analyzed the assembly of neural circuits of hippocampal region in *NeuroD2* knock out mice. They studied the transmission between the mossy fibers and dentate gyrus relayed to CA3 parts of the hippocampus. Wilke et al. demonstrated a role of NeuroD2 in the formation CA3 dendritic spines knockdown of *NeuroD2* in vivo and using *NeuroD2* knock out mice. Thorny excrences (TE) head numbers that are the characteristics of the dendritic sites of the mossy fibers are less in *NeuroD2* knock out mice than wild-type. Furthermore, like thalamocortical synapses, they discovered a decrease in the ratio of AMPA to NMDA receptors in *NeuroD2* null mice. They showed that this regulation of maturation occurred by the expression of PSD95 (post synaptic density protein) controlled by NeuroD2. In the absence of NeuroD2, PSD95 was downregulated leading to CA3 neuronal spine defects so they concluded that NeuroD2 regulates maturation of glutamatergic synapses through PSD95 protein [52].

2.9 NeuroD2 might play role in dendrite development and morphology

For the establishment of the neural circuits and connections in the brain, the proper arrangement and morphogenesis of dendrites are required. Dendrite morphology including dendritic arbor growth, retraction and pruning occurs after cell cycle exit and migration in the neurons. Particularly, numerous that play role in the regulation of dendrite development and specification have been identified including several transcriptional regulators [6] [5].

Hand et al. implicated that in the mammalian cortex, several distinct transcription factors direct the different phases of dendrite development by the activation of calcium dependent signaling pathways. For example, CREB activation is necessary for CaM Kinase IV induced dendrite growth [45]. In addition, bHLH transcription factor Neurog2 induces the specification of unipolar apical dendrite morphology in cortical pyramidal neurons [53]. Moreover, another bHLH transcription factor NeuroD1 enhances the dendrite arbor. Gaudilliere et al. found that knockdown of *NeuroD1* causes a dramatic reduction of dendrite growth and branching in primary cerebellar granule neurons. Gao et al. supported this finding in *NeuroD1* knock out mice by showing shorter dendrite formation. The activity of NeuroD1 is regulated by calcium signaling and neuronal activity [6]. CaMKIIα which is an activity–regulated protein kinase phosphorylates NeuroD1 to stimulate NeuroD1 dependent transcription and dendrite growth [5] suggesting that NeuroD1 act downstream of neuronal activity.

Preliminary data (Ince Dunn, unpublished) suggested that, NeuroD2 is required for calcium and CaM Kinase IV induced development of dendrites. At postnatal 7 (P7) stage, *NeuroD2* knock out mice shows significant reduction in the number of dendrite branches compared to the wild type. On the other hand, the number of dendrites does not change in

NeuroD2 knockout samples. In primary cortical neurons of wild-type and knockout mice, the basal level of dendritic growth is also not affected in *NeuroD2* knockouts. It has been showed that KCI is an activator of calcium channels. Furthermore, KCl treatment stimulates dendritic growth in both wild-type and *NeuroD2* knockouts suggesting that calcium activated dendritic growth does not require NeuroD2. Also, Ince Dunn demonstrated that the overexpression of the constitutively active form of CaM Kinase IV leads to the increase in the number of dendrites and branches in wild-type cultures but this increase is reduced in *NeuroD2* knockout cultures suggesting that the absence of NeuroD2 disrupts the CaM Kinase IV stimulated dendritic elaboration.

In accordance with this findings, NeuroD2 might have regulatory effects on dendrite morphology with or without activity. However, the contribution and importance of NeuroD2 on dendrite morphogenesis remains to be elucidated.

2.10 Role of NeuroD2 in formation of commissural fiber tracts

The cerebrum is composed of two cerebral hemispheres linked by the commissural fiber tracts which are hippocampal commissure, anterior commissure and corpus callosum [54]. Neocortical pyramidal projecting neurons that arise from the neocortex and the hippocampus form these axonal fiber bundles at the same developmental time with NeuroD2 expression [55].

Bormuth and his coworkers illustrated that *NeuroD2* and *NeuroD6* double mutant mice have both corpus callosum and anterior commissural fiber tracts deficiency [56]. Furthermore, the double mutation of *NeuroD2/6* causes a dramatic reduction in GAP-43 positive axon bundles and glutamergic synaptic activity [56]. As a result, NeuroD2 and

NeuroD6 which are co-expressed in post-mitotic projecting neurons play important roles in the generation of commissural fiber bundles and connectivity of two hemispheres [56][57].

2.11 Role of NeuroD2 in learning and memory

The amygdala is the brain structure responsible for the processing of emotional memory, learning and responses [47]. Lin et al. showed that *NeuroD2 +/-* mice display abnormal emotional learning behavior due to the fewer neurons in amygdala region [58]. They also supported this findings in *NeuroD2* null mice by showing completely loss of neurons in lateral and basolateral amygdala [58]. Furthermore, they achieved standard unconditioned anxiety tests on *NeuroD2 +/-* mice which is constructed by two open and two closed armed plus shaped maze [58]. As a result, heterozygous *NeuroD2* mice fail to behave appropriately in fearful situations suggesting that NeuroD2 transcription factor is required for the regular activity of basolateral amygdala. On the other hand, in the lateral amygdala, conditioned fear is regulated by the glutamergic receptors such as AMPA receptors which are synthesized and placed at the postsynaptic membrane during fear conditioning [59]. They indicated that compared to the wild-type, heterozygous NeuroD2 mice have dramatically less AMPA receptors concluding that haploinsufficiency of *NeuroD2* gene leads to amygdala deficiency.

2.12 Gene targets of NeuroD2

There are different studies reporting NeuroD2 bHLH transcription factor putative gene targets. GAP-43 protein expressed in presynaptic axonal regions is one of them [4]. According to the study of Ince Dunn et al., in *NeuroD2* null mice, the expression level of

GAP-43 significantly decreases. Supporting this result, there is abnormal barrel cortex formation in GAP-43 mutant mice like in *NeuroD2* null mice [36][60]. Likewise, PSD-95, a postsynaptic scaffold protein, highly expressed in glutamergic synaptic regions is revealed as a target gene of NeuroD2 since its expression level diminishes in *Neurod2* knock out mice [52]. Moreover, Konishi et al. demonstrated that binding of NeuroD2 to E-box consensus sequence of Ca^{+2} channel protein, type 1 inositol 1, 4, 5-triphosphate receptor leads to activation of this gene in Purkinje neurons and hippocampus [61].

The study conducted in *NeuroD2* null mice to find the alterations in gene expression by expression array analysis indicated that 27 of nearly 6000 mRNAs are reduced [47]. *BDNF, tyro3/sky, ras-p21, MAPK, c-fos, c-jun* which are important for the neuronal survival in the cerebellum are diminished in the absence of NeuroD2 [47]. Fong *et al.* revealed genome-wide transcription profiles of NeuroD2 by transducing NeuroD2-expressing lentivirus into the pluripotent mouse cell line P19 converted to neurons [62]. After expression of NeuroD2, 532 genes were upregulated and 278 genes were downregulated. Gene ontology analysis revealed that the upregulated genes were related to neuronal development and differentiation [62]. Since this study was achieved in cell culture, it may not reflect the *in vivo* targets of NeuroD2.

Bayam et al. identified the genome-wide targets of NeuroD2 during mid-embryogenesis by carrying out chromatin immunoprecipitation followed by high-throughput sequencing (CHIP-Seq) in cortex tissue [9]. They demonstrated that there are large numbers of target genes of NeuroD2 that play roles in major pathways. They also found that the target genes involved in layer identity and axon pathfinding of cortical projection neurons during cortical development. In this study, they first identified NeuroD2 binding sites in embryonic cortices which were mapped onto 94,621 peaks. They revealed

that the binding profile of NeuroD2 occurred mostly on the first 5'UTR exon. Next, they observed NeuroD2 peaks accumulation within 1000bps from Transcription Start Site (TSS) after generating a NeuroD2 binding map relative to annotated TSS suggesting that TSS proximal sequences located within or upstream of 5'UTR are the binding sites of NeuroD2. To assign the individual peaks to genes and clarify the TSS distant peaks, they used ClosestGene method. In this method, the number of associated peaks and their closeness to TSS are calculated to give a score to the individual gene. For each gene, they calculated normalized ClosestGene score by subtracting the random score from the NeuroD2 score. After Gene Ontology analysis, they identified target genes controlled the processes of two major developmental processes; cortical radial migration and axon guidance. They also clarified the signaling pathways that were regulated by NeuroD2 and found Reelin signaling (Figure 2.4) which play role in the regulation of neuronal migration and reorganization of actin cytoskeleton. They showed that NeuroD2 targeted *Fyn, Lrp8, Cdk5r1* and *Dab1* are the key components of this pathway [9].

In Reelin signaling, a secreted protein Reelin located on the surface of the developing cortex. It binds to the receptors Lrp8 and Vldlr on migrating neurons and provides the reorganization and regulation of actin cytoskeleton resulting neuronal migration [63]. In addition, they found that NeuroD2 regulated layer specific transcription factors that are important for differentiation and axonal guidance. The deep layer markers such as *Ctip2, Fezf2, Tbr1* and the upper layer markers such as *Cux1/2* and *Satb2* were identified as targets of NeuroD2 [9]. Next, they determined the role of NeuroD2 in this cortical development process by comparing the set of target genes against KEGG (Kyoto Encyclopedia of Genes and Genomes) pathway database and found that among 132 genes which are involved in different axon path finding pathways in KEGG, 30 were targets of NeuroD2 including *Epha3 , Plxna2* and *Robo2* at embryonic stages [9].

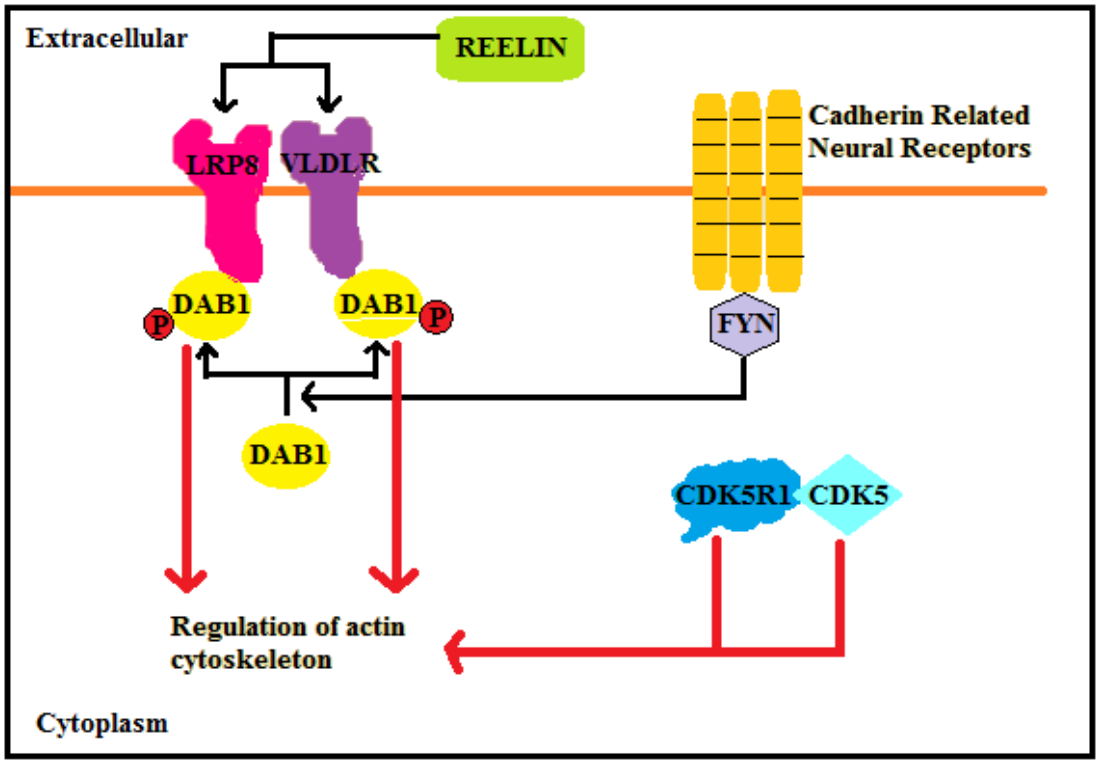

Figure 2.4. Schematic representation of Reelin signaling pathway

They also identified the genome wide targets of NeuroD2 at postnatal stage by using same methods and indicated that these target genes perform in other major pathways. MTOR pathway, one of the major ones, is important for the regulation of cell cycle, growth and proliferation. They found key components involved in this signaling such as *Eif3a*, *Pkd1*, *Rps6kb1* and *Tsc1*. Furthermore, they determined that NeuroD2 also targets other genes such as *Fzd4, Fzd8, Fzd9, Gsk3* and *Dvl3* regulating canonical Wnt pathway (Figure 2.5) which controls cell fate specification, cell proliferation and cell migration. (Bayam et al., unpublished).

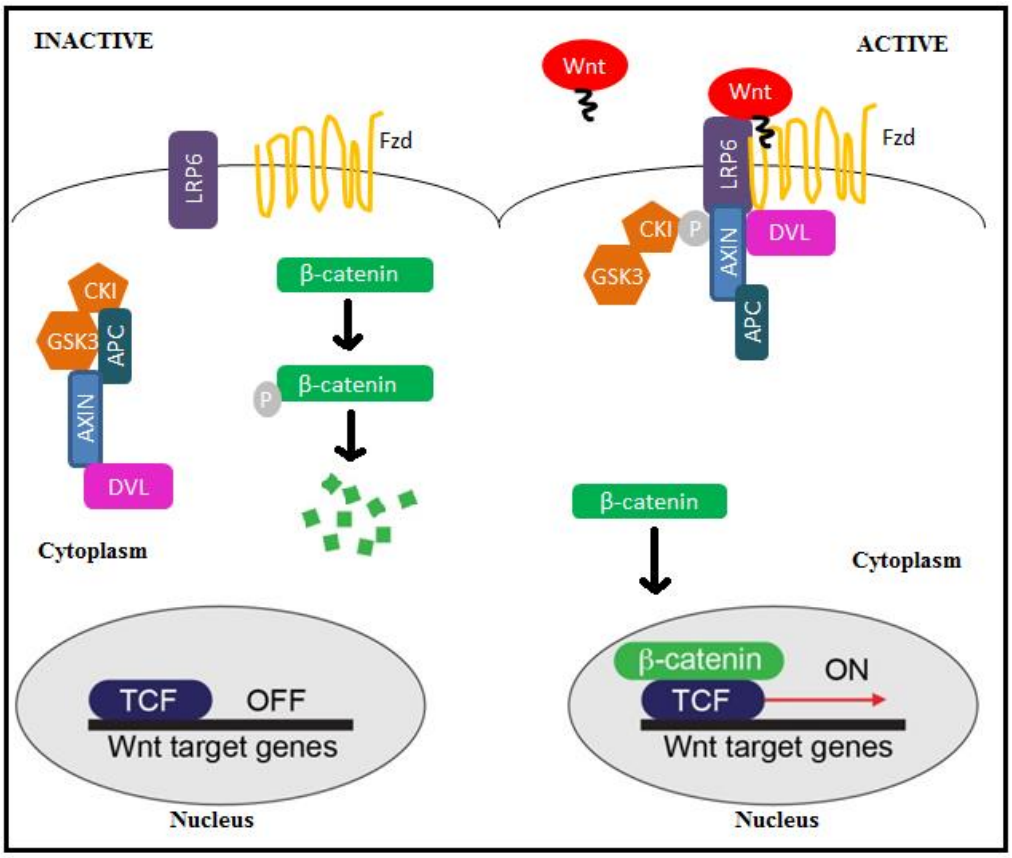

Figure 2.5. Schematic representation of canonical Wnt signaling pathway

In addition, they revealed *Id2* as a target gene of NeuroD2 at both embryonic and postnatal stages. Previous study (Ince Dunn, unpublished) showed the comparison of the expression profiles of the postnatal cortex of wild-type and *NeuroD2* knock-out mice by using microarray and found that *Id2* was one of the down regulated transcripts that showed two fold decreases in the mRNA level (Table 2.1). They confirmed these changes by northern blotting and *in-situ* hybridization analysis. In Northern Blot analysis, the RNA

level of *Id2* decreased dramatically in the knockouts compared to the wild type and heterozygote controls (Figure 2.6). In addition, the expression pattern of *Id2* was performed in control and *NeuroD2* knockout cortex by *in-situ* hybridization showing that Id2 was highly expressed in the cortex in control mice; however the expression of Id2 was strongly reduced in the knockout mice (Figure 2.6)

Entrez Definition	GenBank	Fold Change	p-value
Neurogenic differentiation factor 2 (NeuroD2)	NM_010895	4.3	0.000046
CXC chemokine MIP-2gamma precursor (MIP-2γ)	AF252873	2.0	0.002032
Suppressor of bimD6 homolog (SudD)	AK004748	2.0	0.002753
Inhibitor of DNA binding (Id2)	BF019883	2.1	0.00002
Angiogenin-like (Angl)	NM_007448	4.6	0.00225

Table 2.1. List of mRNAs that are decreased in the knockout cortex relative to the wild type at age P4 (fold change > 2; p-value > 0.997) (Ince Dunn, unpublished).

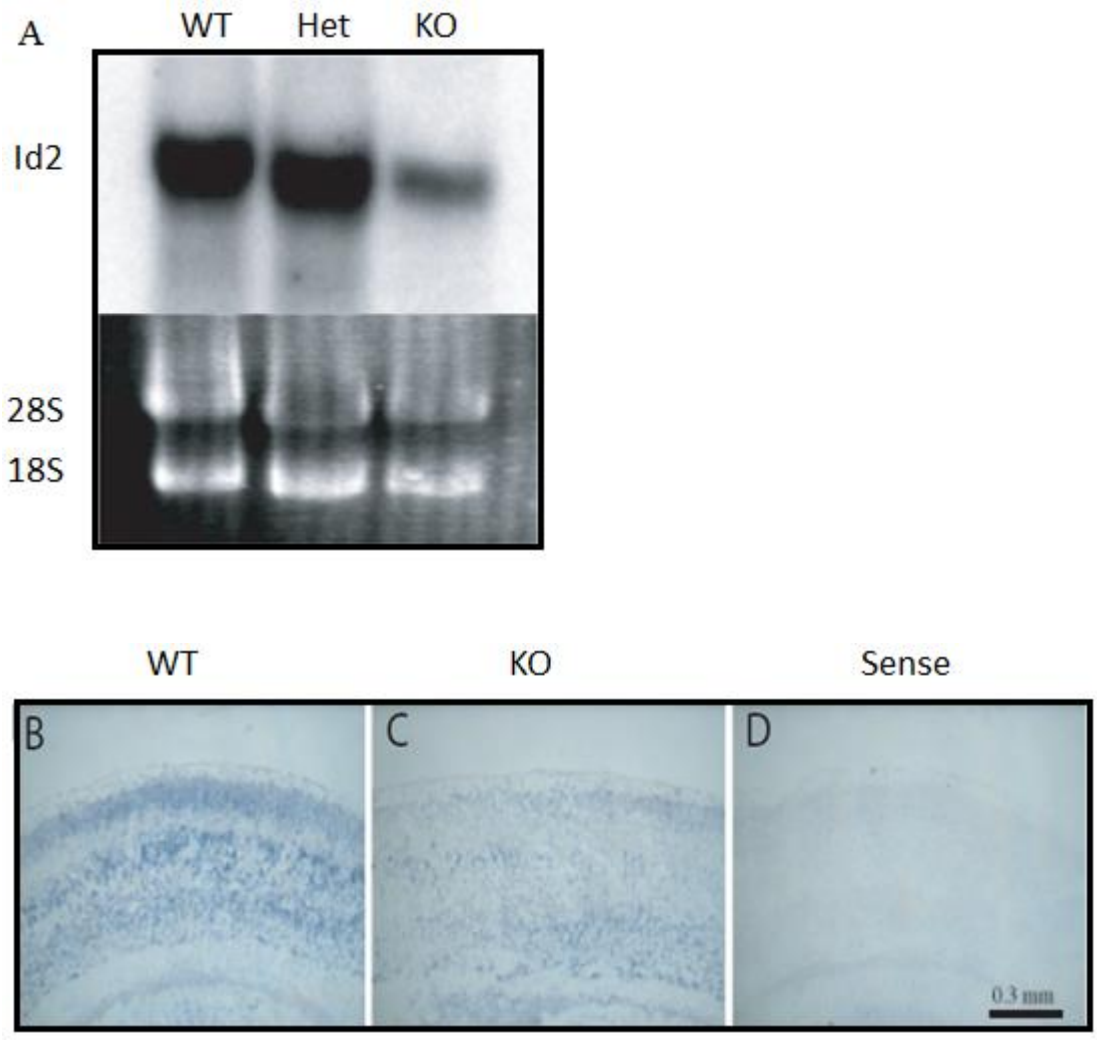

Figure 2.6. mRNAs that are down regulated in *NeuroD2* knock out cortex by northern blot and *in-situ* hybridization (Ince Dunn, unpublished).

2.13 Id family

Id proteins are one of the helix-loop-helix (HLH) transcription factors that function primarily as dominant-negative regulators of basic helix-loop-helix (bHLH) proteins through the formation of Id-bHLH heterodimers [29] [64]. This family is orthologous to the *Drosophila melonogaster* gene *extramacrochaetae* [64]. Four family members of Id gene family are identified as Id1, Id2, Id3 and Id4 [64] [65].

Id encoded proteins are known to inhibit lineage specific gene expression. According to the studies, the introduction of Id expression vectors to the cultured cells causes the inhibition of differentiation [29]. The mutation in Id1 makes the brain smaller due to the critical roles of Id proteins in the cell cycle regulation of neural precursor cells [66]. In addition, Jung et al. demonstrated that Id1, Id2 and Id3 induce self-renewal and proliferation of neural precursor cells while inhibiting neuronal differentiation by interfering with the complex of E proteins and proneural bHLH transcription factors [66]. Therefore, it is conceivable that Id proteins act as positive- regulators in the proliferation of undifferentiated neural stem cells but negative- regulators in the diffentiation of the neurons.

2.14 Id2

Id2 is one of the members of Id family which play role in the regulation of nervous system development. The expression of Id2 starts in the ventricular zone during early development of nervous system, and then continues through the neocortex, olfactory bulb and the cerebellum as development progresses [29]. Martinsen et al. showed that in chick-embryo surface ectoderm, the overexpression of Id2 resulted in turning of the ectodermal

precursor cells into neural crest and neurogenic fates [67]. Furthermore, Bai et al. investigated that the expression of Hes1, a negative bHLH transcription factor, is upregulated by the overexpression of Id2 in chick hindbrain leading to the blockage of proneural gene expression and neuronal differentiation [64]. In addition, Wang et al supported the negative regulatory role of Id2 by indicating the inhibition of oligodendrocyte differentiation due to the overexpression of Id2 [68].

Chapter 3

MATERIALS AND METHODS

3.1 Chromatin Immunoprecipitation

Cerebral cortices of postnatal day 0 (P0) mice were dissected in cold 1X HBSS containing 100mM HEPES. After one-time trituration in 1X HBSS containing 100mM HEPES, tissues were placed into petri dishes. The crosslinking was done by 1% formaldehyde for 10 minutes at room temperature on slow shaker. 125mM glycine was added to quench the crosslinking reaction for 10 minutes at room temperature on slow shaker. Then, tissue was washed with cold 1X HBSS containing 10mM HEPES twice and centrifuged at 4000rpm at 4˚C for 4 minutes each. Lysis step was applied by 1X RIPA (0.05 M Tris-HCl pH 7.5, 0.15M NaCl, 1% Triton-X 100, 1% Na-DOC, 0.1% SDS) containing freshly added 1 tablet of protease inhibitor cocktail (Roche cOmplete Mini, EDTA-free) and the sonication was performed in cold room by Bandelin Sonopus HD2070 with the power of 93 and 70% output for 20 seconds , 30 times. Between each cycle, the samples were chilled on ice to cool down. At the end of the sonication, the samples were centrifuged at 14000rpm at 4˚C for 20 minutes and 100 µl of supernatant was separated as input while the rest of the supernatants were collected as lysates into new eppendorf tubes containing Protein A/G Magnetic Beads (Thermo Scientific, , Cat. #88802). 75 µl of Protein magnetic beads was used for sample pre-cleaning which was carried out in cold

room for 1 hour while continuously rotating and 1X RIPA was added three times for washing. After that, lysates were transferred into new eppendorf tubes and appropriate antibodies were put into the same tubes and rotated from 2 hours to overnight in the cold room. Then, 50 µl of Protein A/G magnetic beads were washed again with 1X RIPA lysis buffer three times and lysate-antibody samples were added onto washed magnetic beads. The incubation was applied in cold room by rotating the eppendorf containing magnetic beads, lysate and antibody for 1 to 1.5 hours. By the use of magnetic stand, the supernatants of the samples were separated from the beads and stored at -20 ˚C. The beads having antibody-protein complexes were washed with seven different washing buffers for 10 minutes, twice for each in the cold room by rotating. (Wash Buffer 1: 1X PBS, 0.1% SDS, 0.5% Na-DOC, 0.5% NP-40. Wash Buffer 2: 5X PBS, 0.1% SDS, 0.5% Na-DOC, 0.5% NP-40. Wash Buffer 3: 15mM Tris-HCl, pH 7.5, 5mM EDTA, 2.5mM EGTA, 1% Triton X-100, 1% Na-DOC, 0.1% SDS, 120mM NaCl, 25mM KCl. Wash Buffer 4: 15mM Tris-HCl, pH 7.5, 5mM EDTA, 2.5mM EGTA, 1% Triton X-100, 1% Na-DOC, 0.1% SDS, 1M NaCl. Wash Buffer 5: 15mM Tris-HCl, pH 7.5, 5mM EDTA. Wash Buffer 6: 50mM Tris-HCl, pH 7.5, 150mM NaCl, 1mM MgCl2, 0.05% NP-40. Wash Buffer 7: 50mM Tris-HCl, pH 7.5, 10mM MgCl2, 0.5% NP-40). After adding Elution Buffer 1 (sterile 1% SDS, 0. 1M NaHCO3 onto Protein A/G magnetic beads and input sample in the amount of 200 and 300 µl, samples were incubated at 65 ˚C , 1 hour by shaking for reverse crosslinking. Then, the eluate was seperated from the beads and incubated at 65 ˚C again maximum 15 hours. 200 and 300 µl of Elution Buffer 2 (sterile 100mM Tris-HCI, 20mM EDTA pH 8.0) was put into the ChIP samples and input sample. Before incubation at 37˚C for 1 hour, 1 µl of RNaseA (Thermo Scientific, Cat. #R1253) was added into the samples. Then, 4µl of 20mg/ml Proteinase K (Thermo Scientific, Cat. #EO0491) was added and incubated at 50˚C for 2 hours. ChIP DNA samples were purified by the standard phenol-chloroform extraction in which 500µl of phenol-chloroform solution was put onto the samples and

mixed slowly for 10 minutes. The samples were centrifuged at 14000rpm, 5 minutes and upper parts of the solutions were separated into new eppendorf tubes. After repeating the extraction step one more time, Na-Acetate pH 5.2 was added onto the samples in the amount of 1/3 volume together with the 100% isopropanol in the amount of 10X volume of samples. They were incubated at -20˚C for 2 hours. After incubation, the centrifugation was applied at 14000rpm at 4˚C for 20 minutes to discared the supernatants. The pellets were washed with 70% ethanol, twice and air dried under the hood. After evoporation, the pellets were dissolved in 30µl of ultrapure water (RNase and DNase free).

3.2 ChIP-Quantitative PCR

By the use of standard phenol-chloroform extraction and ethanol precipitation method, input chromatin DNA was prepared from 10% of the cross-linked lysate. Input and ChIP DNA were dissolved in 30 µl sterile water and 2 µl of each was diluted in 18 µl sterile water. Then, 1 µl from each was used for quantitative PCR experiments. 3.32 (log210) representing a 10% of input chromatin was subtracted from the input Ct value to generate the adjusted input Ct. Following formula was used to calculate the input normalized ChIP DNA amount: $100x2^{(\text{Adjusted input Ct} - \text{ChIP Ct})}$. Quantitative Real Time PCR was performed using Luminaris HiGreen qPCR Master Mix (Thermo scientific, Cat. #K0991) according to manufacturer's recommendations.

3.3 Cell Lysate Collection of Primary Neuronal Culture and Neuro2A Cell Lines

Cells were lysed with freshly prepared 1X RIPA lysis buffer containing protease inhibitor tablet for 10 minutes on ice. For 24-well plates, 100 µl lysis buffer was used per well and 200 µl lysis buffer was used for one well in 12-well plates. Samples were spun

down for 20 min at 14,000 g, 4°C. The supernatant was transferred to a fresh tube and stored at -20°C or used for SDS-PAGE.

3.4 Co-Immunoprecipitation

Neuro2A cells were collected in ice-cold SDS-free lysis buffer (150mM NaCl, 50mM Tris-HCl ph.7.4, 1% Nonidet P-40, 0.25% Sodium Deoxycholate, and 1mM EGTA, 1 tablet of protease inhibitor cocktail). Cell lysates were incubated for 10 minutes in ice and centrifuged at 14,000rpm, 4°C for 20 minutes. The supernants were transferred to new eppendorfs. 50 µl of Protein A/G magnetic beads were washed with lysis buffer 3 times and added onto lysates. Lysates with beads were incubated in roller at 4°C for 1 hour. After that, samples were placed in a magnetic stand and the beads were discarded. 50 µl of lysates were aliquoted as input control. Then, the antibody was added onto lysates and antibody-lysate mixture was incubated in roller at 4°C overnight. 50 µl of magnetic protein A/G beads were washed 3 times with lysis buffer and added onto antibody-lysate mix. After the whole mixture was incubated at 4°C for 1 hour, the samples were placed in magnetic stand and 50 µl of supernatant was taken to new eppendorf as post IP control. Then, the rest of the lysate was discarded and the beads were washed with lysis buffer for 15 minutes at 4°C room roller. The beads were eluted with 10 µl SDS-PAGE loading buffer and the samples were run on 12% SDS-PAGE and continued with western blotting.

3.5 SDS-PAGE

A 5% stacking SDS-PAGE (5% Acrylamide-Biasacrylamide (29:1), 126mM Tris-HCl, pH 6.8, 0.1% APS, 0.1% SDS, 0.1% TEMED) gel was added on top of a 12% separating SDS-PAGE (12% Acrylamide-Bisacrylamide (29:1), 375mM Tris-HCl, pH 8.8, 0.2% APS,

0.2% SDS, 2.5% TEMED) gel. Appropriate amounts of proteins were mixed with 2X SDS-Loading Buffer (100mM Tris-HCl pH 6.8, 2% β-mercaptoethanol, 4% SDS and 0.02% bromophenol blue, 20% glycerol) and boiled for 5 minutes and loaded to wells. Samples were run at 80V for 30 minutes and 120V for 2 hours in SDS running buffer (10X, pH 8.3; 30g Tris Base, 187.6g Glycine, 1% SDS in total volume of 1L). After gel electrophoresis was completed, gels were further processed for western blot analysis.

3.6 Western Blot Analysis

After SDS-PAGE, gels were transferred to a polyvinyl difluoride membrane, PVDF, (Thermo Scientific, Cat. #88518) using wet-transfer method (1.45 g Tris Base, 7.25 g Glycine, 150 ml Methanol in total volume of 1L). Wet-transfer was performed at 50mA , 4°C. Then, membrane was blocked in 5% Nonfat Dried Milk Powder (AppliChem, Cat. #A0830) in TBS-T (10mM Tris-HCl pH7.5, 150mM NaCl, 0.05% Tween) for 1 hour. Membrane was exposed to primary antibody in 5% Nonfat Dried Milk Powder in TBS-T for 2h at room temperature to overnight at 4°C. Membrane was washed with TBS-T (10mM Tris-HCl pH7.5, 150mM NaCl, 0.05% Tween) three times for 30 minutes. Membrane was incubated with appropriate secondary antibody for 1h at room temperature. Membrane was washed with TBS-T for 30 minutes, three times. Membrane was incubated in Western Bright™ Sirius western blotting detection kit (Advansta, Cat. #K-12043-D20) for 4 minutes at room temperature and visualized under Gel Logic 2200 Imaging System (Molecular Imaging System CareStream Health Inc.).

Table 3.1: Primary Antibodies used in western blotting and immunoprecipitation

Antibody	**Host**	**Company**	**Catalogue Number**	**Dilution**
Myc	Mouse	Santa Cruz	sc-40	1:1000
NeuroD2	Rabbit	Abcam	ab104430	1:1000
NeuroD2	Rabbit	Abcam	ab109406	1:1000
NeuroD2	Mouse	Abcam	ab168932	1:1000
Id2	Rabbit	Santa Cruz	B2013	1:1000
Id2	Mouse	Abcam	ab166708	1:1000
HA	Rabbit	Cell Signaling	C29F4	1:1000
GFP	Rabbit	Santa Cruz	H0612	1:1000
Beta-Actin	Rabbit	Thermo Scientific	PA5-16914	1:1000
Turbo-GFP	Rabbit	Evrogen	AB513	1:1000

Table 3.2: Secondary Antibodies used in western blotting immunoprecipitation

Antibody	**Host**	**Company**	**Catalogue Number**	**Dilution**
Anti-Mouse IgG HRP-linked	Mouse	Cell Signalling	7076S	1:2500
Anti-Rabbit IgG HRP-linked	Rabbit	Cell Signalling	7074S	1:2500

3.7 Coating of Plates

0.5mg of Poly-D-lysine Hydrobromide (Sigma Life Sciences, Cat. #P9155) and 0.05mg Mouse Laminin (Millipore, Cat. #CC905) were added to 15ml sterile 1X PBS. Cover glasses (Heinz Herenz Medizinalbedarf GmbH, Cat. #1051204) was placed into the wells for 24-well plates and 500µl of the coating solution was added into each well. For 12-well plates, 1ml of the coating solution was used for one well. Plates were incubated for 12-16 hours at 37°C, 5% CO_2 in the tissue culture incubator. Next day, plates were washed three times with sterile ddH_2O. They were stored in 4°C for 2-3 weeks or used for culturing immediately.

3.8 Primary Neuronal Cultural Preparation

Embryos were removed from time-pregnant mice euthanized by cervical dislocation. The meninges were removed; the telencephalic hemispheres separated, the hippocampus and the olfactory bulbs were removed. Cortices were dissected from mice embryos at embryonic days 14 (E14) and 18 (E18) of development. Cortices were dissected in cold 1X Hanks balanced salt solution (HBSS, GIBCO) with 10mM HEPES (pH 7.4) and then incubated in the enzyme solution containing cysteine (3.2mg) and papain (200 units) in dissociation media (82mM Na2SO4, 30mM K2SO4, 5.8mM MgCl2, 0.252mM CaCl2, 1mM HEPES (pH 7.4), 20mM glucose, 0.001% phenol red, 0.2mN NaOH in ddH2O) for 10 minutes at 37°C. The tissues were put into the light inhibitor (6mg BSA and 6mg trypsin inhibitor in dissociation media, adjusting the pH with 0.1N NaOH) and incubated for 1 minute at room temperature. Then, they were transferred to the heavy inhibitor (60mg BSA and 60mg trypsin inhibitor in dissociation media, adjusting pH with 0.1N NaOH) for another 1 minute. Tissues were placed into fresh BME (Lonza, Cat. #BE12-105F)

containing 1% P/S, 0.5% L-glutamine, and 5% FBS (BF) and washed twice. Then, mechanical trituration was done three to four times using serological pipettes in BF and tissues were settled down in the bottom of the falcon. The upper cell suspension were filtered to eliminate the large tissue particles and transferred into a new falcon tube. All the washing, trituration and counting steps of the tissues were done in BME (1% P/S, 0.5% L-glutamine) without FBS only for the nucleofection experiment. Cells were counted and 300.000 cells per one well of 24-well plates were plated in 500 µl volume in BF. Two hours later, medium was aspirated and 500µl of N-2 (Gibco Life Technologies, Cat. #17502-048) and B-27 (Gibco Life Technologies, Cat. #12587-010) supplemented fresh BF media (BNBF) was added per well. Two days after, half of the media were aspirated and freshly prepared media (BNBF) were added into plates. This procedure was continued until cells were collected for following analyses.

3.9 Neuronal Culture and Nucleofection

Dissociated cortical neuron cultures were prepared as previously described. In short, embryonic day 14 (E14) mice pups were sacrificed, and cortices were isolated and digested using papain protease. Neurons were dissociated and resuspended in BME (Lonza, Cat. #BE12-105F) containing 1% P/S, 0.5% L-glutamine. 500 µl BF was added into Poly-D-Lysine and laminin coated wells of 12-wells plate and pre-warmed at 37°C. Cells were counted and 1.5 million of them were transferred to a new falcon tube. They were centrifuged at 1500rpm, 4°C and 3 minutes. After preparation of cells, nucleofection step was performed by the use of Amaxa™ P3 Primary Cell 4D-Nucleofector X Kit L (Lonza, Cat. #V4XP-3024). The upper cell suspension part was aspirated and the pellet was dissolved in 100 µl P3 nucleofection solution (Lonza, Cat. #V4XP-3024) gently. 20µg DNA was added into the solution and the solution was mixed by pipetting gently. Then,

100µl of the solution was transferred to the nucleofection cuvette and nucleofection was applied by CU133 program in the nucleofection machine. After that, the cells were incubated at room temperature for 10 minutes. 1 ml of BF was added into the cuvette by pipetting and 500µl of nucleofected cell solution (750.000 cells /well) was plated into pre-warmed one well of 12-well plates in 1ml BF volume. Two hours later, medium was aspirated and 1ml of N-2 (Gibco Life Technologies, Cat. #17502-048) and B-27 (Gibco Life Technologies, Cat. #12587-010) supplemented fresh BF media (BNBF) was added per well. Three days after, half of the media were sucked and freshly prepared media (BNBF) were added into plates. This procedure was continued until cells were collected for following analyses.

3.10 Neuronal Culture and Transfection

Cells were plated into 24-well plates on Poly-D-lysine-treated support. Cortical neurons were transfected at 2 days in vitro (2DIV) with 1 µg DNA using 2 µl Lipofectamine 2000 (Invitrogen). Following the product protocol, the media in the wells (conditional media) were replaced with 500µl Opti-MEM®I and collected into a new falcon tube to incubate at 37°C. The plate with 500µl Opti-MEM®I was put into the tissue culture incubator. 1µg of DNA was dissolved in 250 µl Opti-MEM®I and 2 µl Lipofectamine 2000 was added into another 250 µl Opti-MEM®I for one well of 24-well plates. They were incubated for 10 minutes at room temperature. Then, these two solutions were mixed with each other and incubated for 20 minutes at room temperature. After incubation, 500µl of the mixture was added dropwise into the one well of 24-well plate. The plate was incubated 2 hours and the Opti-MEM®I was sucked and 1 ml fresh media (50% BNBF + 50% conditional media) was added into the well. The plate was for 2 more days before analysis in the tissue culture incubator (37˚C, 5% CO_2).

3.11 Neuro2A Cell Line and Transfection

Neuro2A cell line was grown in 500 µl MEM (Gibco Life Technologies, Cat. #31095029) containing 10% FBS (HyClone), 1% P/S (Gibco Life Technologies, Cat. #15140122), 0.5% L-Glutamine (HyClone) in one well of 24-well plate. The confluency of the cells was expected to be 70-80% for the transfection. Following the protocol, 1 µg amount of DNA was diluted in 50 µl Opti-MEM®I and 2 µl Lipofectamine 2000 was added into another 50 µl Opti-MEM®I for one well of 24-well plates. After incubation for 5 minutes at room temperature, they were mixed with each other and again incubated for 20 minutes at room temperature. Then, 100 µl of the mixture was added into the one well of 24-well plate drop by drop. Transfected Neuro2A cells were incubated in incubator (37˚C, 5% CO_2) for 48 hr.

3.12 Immunofluorescence of Primary Neuronal Culture and Neuro2A Cell Line

The wells with the coverslips were fixed with 4% Paraformaldehyde (dissolved in ddH_2O with heating and stirring, adjusted pH to 7.2) after two days of the transfection. The amount of added 4% PFA was equal to the media in one well of the 24-well plate. After PFA treatment, the plate was incubated at room temperature for 20 minute. Then, PFA was aspirated and wells were washed with 1X cold PBS for three times. 500 µl of 1X PBS with 2 % azide (100X) was added into the wells and the plate was stored at 4˚C for long-term or used for immunostaining experiments. Primary antibodies were diluted in 1X PBS containing 0.5 % Triton-X-100, 3% BSA and coverslips were incubated with this solution 2 hours at room temperature or overnight at 4°C. Coverslips were washed in 1X PBS three times for 15minutes and then incubated in a dark environment at room temperature for 50 minutes with specific secondary antibodies conjugated to a fluorescent dye, diluted also in

1X PBS containing 0.5 % Triton-X-100 and 3% BSA. After three times washes in 1X PBS, DAPI was used at a concentration of 0.1µg/ml in 1X PBS to visualize the nuclei by incubating coverslips for 10 minutes. Then coverslips were placed on glass slides by the use of mounting media (Thermo Scientific, Cat. #TA-060-UG). After drying, slides were stored at 4^{o}C or examined to take the images under Nikon Eclipse 90i confocal microscope equipped with a 60x and 100x oil emersion objectives.

Table 3.3: Primary Antibodies used in immunofluorescence

Antibody	**Host**	**Company**	**Catalogue Number**	**Dilution**
Myc	Mouse	Santa Cruz	sc-40	1:1000
NeuroD2	Rabbit	Abcam	ab104430	1:1000
NeuroD2	Rabbit	Abcam	ab109406	1:1000
NeuroD2	Mouse	Abcam	ab168932	1:1000
Id2	Rabbit	Santa Cruz	B2013	1:1000
Id2	Mouse	Abcam	ab166708	1:1000
HA	Rabbit	Cell Signaling	C29F4	1:250
GFP	Chick	Aves Labs	GFP-1020	1:800
Flag	Mouse	SantaCruz	sc-807	1:1000

Table 3.4: Secondary Antibodies used in immunofluorescence

Antibody	**Host**	**Company**	**Catalogue Number**	**Dilution**
Donkey Anti-Mouse IgG (H+L) Alexa Fluor®488	Mouse	Invitrogen	A21202	1:1000
Donkey Anti-Rabbit IgG (H+L) Alexa Fluor®488	Rabbit	Invitrogen	A21206	1:1000
Goat Anti-Chick IgG (H+L) Alexa Fluor®488	Chick	Life Technologies	A11039	1:1000
Donkey Anti-Rabbit IgG (H+L) Alexa Fluor®594	Rabbit	Invitrogen	A21207	1:1000
Donkey Anti-Mouse IgG (H+L) Alexa Fluor®594	Mouse	Invitrogen	A21203	1:1000

3.13 Sholl Analysis

After immunostaining experiments, images of neurons were captured by using 60X objective with fluorescence microscopy. To detect dendrite development and branching, sholl analysis was used. By using Image J software , concentric circles that were separated

from each other by a distance that correspond to 10μm in the scale bar were drawn from the center of the soma to dendrites. The number of dendrites that intersected each of concentric circles was counted.

3.14 Total RNA Isolation

Absolutely RNA Microprep Kit (Agilent Technologies, Cat. #400805) was used as per the instructions in the manual to isolate total RNA from 4 DIV and 8 DIV E14 primary neurons. First, 0.7 μl of beta-mercaptoethanol was added into 100 μl Lysis buffer for one well of 12-well plate. Lysis solution was added directly onto cells and the sample was homogenized by pipetting. Then, the same volume of 70% ethanol was put into the cell lysate. After vortexing for 5 seconds, the mixture was transferred into a RNA-binding spin cup seated within 2ml collection tube and spinned down for 1 minute at maximum speed. The filtrate was discarded and 600 μl of 1X low salt wash buffer was added. Again, the tube was spinned down for 1 min at maximum speed. After discarding the filtrate, the sample was spinned down for 2 minutes at maximum speed to dry the matrix. Then, 30 μl of DNase solution (5 μl RNase-free DNase I with 25 μl DNase Digestion Buffer) was added directly onto the center of the matrix and incubated at 37°C for 15 minutes. After the incubation, 500 μl of 1X High Salt Wash Buffer was added and the sample was spinned down for 1 min at maximum speed. The filtrate was discarded and 600 μl of 1X Low-Salt Wash Buffer was added and the same spin technique was applied. Then, 300 μl of 1X Low-Salt Wash Buffer was added and the sample was spinned down for 2 minutes at maximum speed. After that, the Spin cup was transferred into new collection tube and 30 μl of Elution Buffer was put directly onto the matrix. After 2 minutes incubation at room temperature, the sample was spinned down for 1minute at maximum speed. The purified RNA in the Elution Buffer was stored at -20°C up to one month or at -80°C for long-term storage.

3.15 cDNA synthesis

Transcriptor High Fidelity cDNA Synthesis Kit (Roche, Cat. #05081955001) was applied to synthesize cDNA from 10ng total RNA. Random primers were used to synthesize cDNA according to manufacturer's protocol. First, in a sterile, nuclease free PCR tube, the components which are total RNA (10ng), Random Hexamer (600pmol/ µl) and water were mixed. Denaturation was done at 65°C for 10 minutes and the tubes were immediately cooled down in the ice. Then, the other components which are 5X Transcriptor High Fidelity Reverse Transcriptase Reaction Buffer, Protector RNase Inhibitor, 10mM Deoxynucleotide mix, DTT and Transcriptor High Fidelity Reverse Transcriptase were added into the mixture to 20 µl final volume. The tubes were placed into the block cycler with a heated lid and incubated at 29°C for 10 min., 48°C for 1 hour and 85°C for 5 min. Then, the reaction was stopped by putting the tubes on ice. The samples were stored at -20°C for longer periods.

3.16 Standard PCR

PCR experiment was performed with 0.01-1 ng range for plasmids and 0.1-1 µg range for genomic DNA templates, 1X *Taq* Buffer with KCl, 0.5µM of forward and 0.5µM of reverse primers, 200µM dNTP's, 2mM MgCl2 and 2.5 Unit *Taq* DNA Polymerase in 50µl reaction mixture (Thermo Scientific, Cat. #EP0402). PCR conditions for denaturing, annealing and extension were set to 95°C for 30 seconds, 58°C for 30 seconds and 72˚C for 30 seconds respectively and repeated 40 cycles. The samples were run in the 1.2% agarose gel by electrophoresis and visualized under UV-light box.

3.17 Real Time PCR (Q-PCR)

Quantitative Real Time PCR was performed using Luminaris HiGreen qPCR Master Mix (Thermo scientific, Cat. #K0991) according to manufacturer's recommendations in which the 20 µl reaction master mix was prepared by adding 10 µl of 2X Luminaris Color Q-pcr Master Mix, 0.6 µl of each primers and 7.8 µl water for each q-pcr reaction at room temperature. The mixture was dispensed appropriate volumes into PCR tubes and 1 µl of DNA template was added into the tubes. Three-step cycling protocol was applied as denaturation 95 ˚C 15 seconds, annealing 60˚C for 30 seconds and extension 72˚C for 30 seconds and repeated 45 cycles.

3.18 Cloning of *Id2* into pcDNA3 backbone vector

PCR was performed with 1X Phusion HF reaction buffer, 300µM dNTP's, 0.5µM forward primer and 0.5µM reverse primers (Appendix C), 1µl of template DNA and 1 Unit Phusion Hot Start Flex DNA Polymerase (New England BioLabs, Cat. #M0535L) in 30µl reaction mixture. Conditions of PCR for denaturing, annealing and extension were set to 98^{o}C for 15 seconds, 57^{o}C for 30 seconds, and 72^{o}C for 2 minutes respectively and the cycle number was 40. Confirmation of the PCR was done by agarose gel electrophoresis by the use of 5µL of the PCR product. Remaining PCR products was purified with EZ-10 Spin Column PCR Purification Kit (Bio Basic Inc. Cat. #BS363). Since BamHI restriction enzyme site was added to the forward primer and reverse primer was to contain XhoI restriction enzyme, double-digestion was achieved in 20µl reaction mixture containing 2X Tango Buffer (Thermo Scientific, Cat. #BY5), 5 Unit BamHI (Thermo Scientific, Cat. #ER0051), 5 Unit XhoI (Thermo Scientific, Cat. #ER0691) and 10µl PCR purified DNA or 1µl plasmid DNA which is pcDNA3A at 37^{o}C overnight. Next day, 1µl of FastAP

(Alkaline phosphatase) was added to the reaction mixture containing plasmid DNA to avoid the self-ligation of the plasmid at 37 ^{o}C for 1h. Then, they were purified again with PCR purification kit. In order to ligate the sample DNA to the pcDNA3A vector, 10µl reaction mixture was prepared with 1X T4 Ligase Buffer, 5 Unit T4 ligase and incubated at 16 ^{o}C overnight.

Transformation of 1µl of ligation product into chemically competent DH5α *E.coli* cells was achieved by heat shock method. cell-plasmid mixture was chilled on ice for 10 minutes and incubated at 42°C for 1 minute. Then, 500ml of LB medium with was added into them and incubated at 37°C for 60 minutes. After that, cells were plated on LB/ampicillin plates since ampicillin was a selective marker for pcDNA3A. Miniprep cultures were incubated at 37^{o}C overnight with constant shaking and plasmid DNA's were purified by GeneJET Plasmid Miniprep Kit (Thermo Scientific, Cat. #K0503). Diagnostic digestion was set up to confirm the success of the cloning and miniprep DNA's were sent to direct sequencing for validation. After confirmation of miniprep DNA's had correct insertions, maxi-prep cultures were incubated at 37^{o}C overnight with constant shaking and plasmid DNA containing Id2 were purified with GeneJet Plasmid Maxiprep Kit (Thermo Scientific, Cat.#K0491).

3.19 Subcloning of *Id2 from Id2*-pcDNA3 *into* pcDNA4 backbone vector

Since BamHI and XhoI restriction enzyme sites were the common restriction enzyme sites in both Id2-pcDNA3A and pcDNA4A, double-digestion wasset up in 20µl reaction mixture containing 2X Tango Buffer (Thermo Scientific, Cat. #BY5), 5 Unit BamHI (Thermo Scientific, Cat. #ER0051) , 5 Unit XhoI (Thermo Scientific, Cat. #ER0691), 1µl Id2-pcDNA3A vector DNA or 1µl pcDNA4A at 37^{o}C for 2h. 1µl of FastAP (Alkaline

phosphatase) was added to the reaction mixture containing pcDNA4A to avoid the self-ligation of the plasmid at 37 ^{o}C for 1h. Then, samples were purified by PCR Purification kit. Ligation was performed as 10µl reaction mixture was prepared with 1X T4 Ligase Buffer, 5 Unit T4 ligase at 16 ^{o}C overnight. Transformation of 1µl of ligation product into chemically competent DH5α *E.coli* cells was achieved by heat shock method. cell-plasmid mixture was chilled on ice for 10 minutes and incubated at 42°C for 1 minute. Then, 500ml of LB medium with was added into them and incubated at 37°C for 60 minutes. After that, cells were plated on LB/ampicillin plates since ampicillin was selective marker for pcDNA4A. Miniprep cultures were incubated at 37^{o}C overnight with constant shaking and plasmid DNA's were purified by GeneJET Plasmid Miniprep Kit (Thermo Scientific, Cat. #K0503). Diagnostic digestion was set up to confirm the success of the cloning .After confirmation of miniprep DNA's had correct insertions, maxi-prep cultures were incubated at 37^{o}C overnight with constant shaking and plasmid DNA containing Id2 were purified with PureLink™ HiPure Plasmid Maxiprep Kit (Invitrogen by Life Technologies, Cat. #K2100-06).

Chapter 4

RESULTS

4.1 NeuroD2 knockdown in embryonic primary cortical neurons

In order to test whether NeuroD2 is necessary for the expression of target genes identified by ChIP-Seq analysis, I aimed to knockdown NeuroD2 expression in primary cortical neurons. NeuroD2 and the non-targeting shRNAs were cloned into pSUPER-neo-GFP backbone vector. shRNA containing plasmids were transfected into primary cortical neurons at embryonic stage 14 (E14) before plating by nucleofection. After plating, protein lysates were collected both at 4 and 8 DIV (days in vitro) and western blots were done to confirm the knockdown of NeuroD2 at two different time points (Figure 4.1 and 4.2). The blots were incubated with three primary antibodies α-NeuroD2, α-GFP and α-Beta-actin at the same time. GFP was used to check the efficiency of transfection and Beta-actin was the loading control. Western blot results showed that NeuroD2 was knocked down in both 4 DIV and 8 DIV neurons transfected with NeuroD2 shRNA compared to the non-targeting shRNA.

Next, the confirmation of NeuroD2 knockdown was shown by immunofluorescence. Primary cortical neurons were transfected with NeuroD2 shRNA, non-targeting shRNA

and NeuroD2 shRNA resistant plasmids two days after plating. Transfected neurons were cultured for two days more and fixed at 4 DIV. Cells were co-immunostained with α-GFP and α-NeuroD2. Also, cell nuclei were stained with DAPI. GFP was used to detect the transfected cells successfully. All GFP positive cells were selected and counted to detect whether NeuroD2 was expressed or not. Immunofluorescence results demonstrated that the expression of NeuroD2 in GFP positive cells significantly decreases in NeuroD2 shRNA transfected cells comparing to the non-targeting one. Moreover, according to the rescue experiment, NeuroD2 was strongly expressed in both NeuroD2 shRNA and resistant NeuroD2 plasmids transfected cells suggesting that NeuroD2 was knocked down in 4 DIV E14 primary cortical neurons (Figure 4.3). Both western blot and immunofluorescence experiments indicated that the knockdown of NeuroD2 with NeuroD2 shRNA was done successfully in primary cortical neurons.

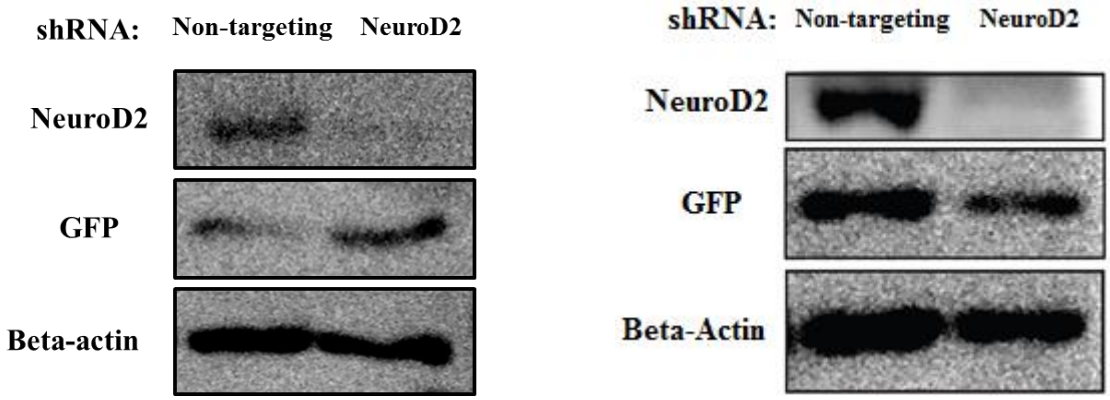

Figure 4.1 Western Blot analysis of NeuroD2 knockdown in 4 DIV primary cortical neurons. NeuroD2 western blotting with two different anti-NeuroD2 antibodies(left and right panels) confirms knockdown in 4 DIV E14 primary cortical neurons transfected with NeuroD2 shRNA as compared to a non-targeting shRNA. GFP is used to detect transfection efficiencyand Beta-Actin is used as a loading control.

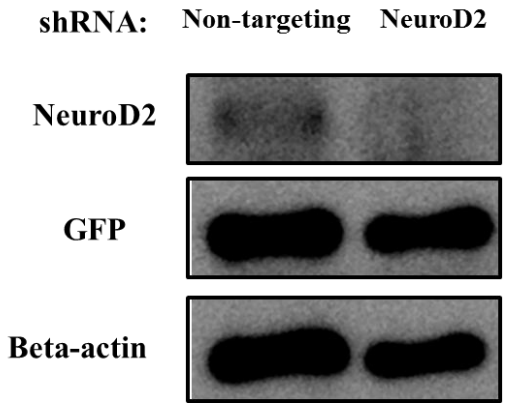

Figure 4.2 Western Blot analysis of NeuroD2 knockdown in 8 DIV primary cortical neurons. NeuroD2 western blotting with anti-NeuroD2 antibodies confirms knockdown in 8 DIV E14 primary cortical neurons transfected with NeuroD2 shRNA as compared to a non-targeting shRNA. GFP is used to detect transfection efficiency and Beta-Actin is used as a loading control.

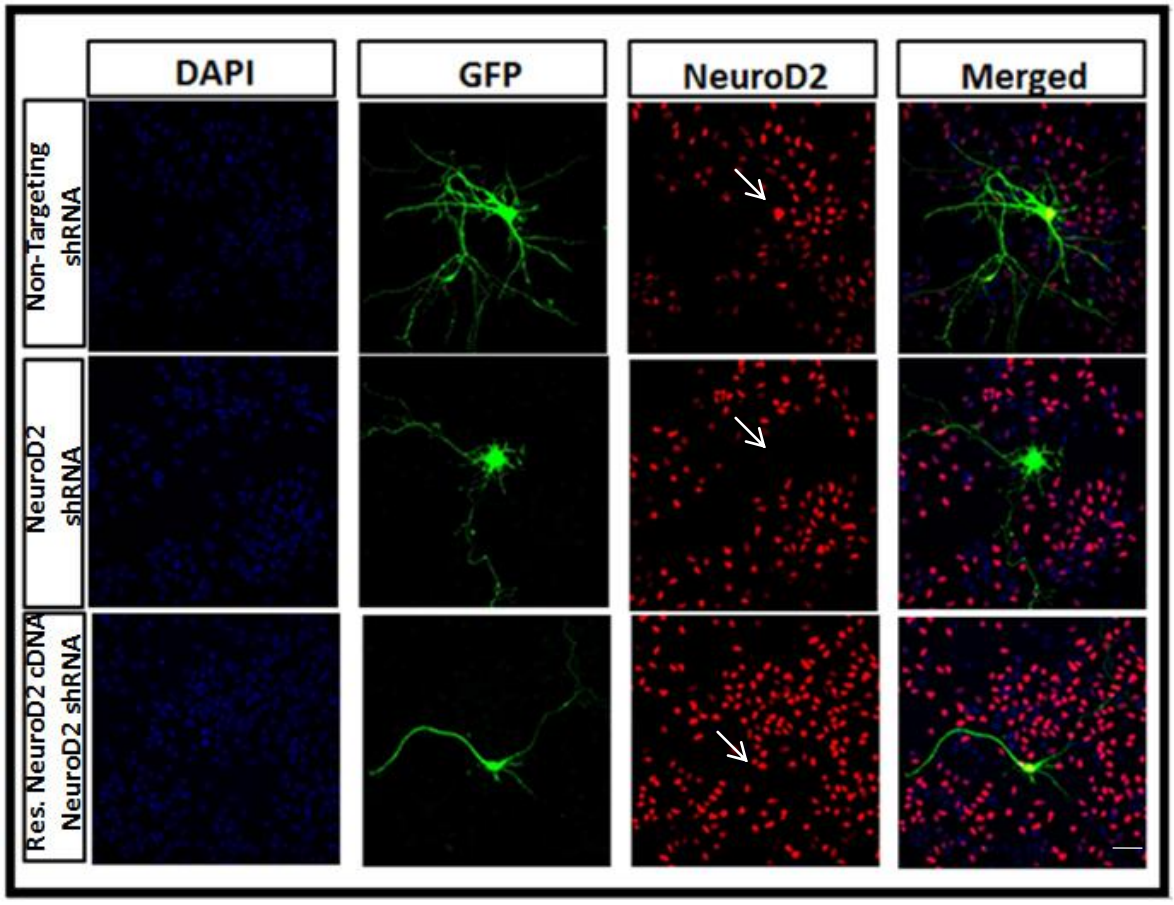

Figure 4.3 Immunofluorescence analysis of NeuroD2 knockdown in 4 DIV primary cortical neurons. 2 DIV E14 primary cortical neurons were transfected with non-tergeting, NeuroD2 shRNA and both NeuroD2 shRNA and resistant NeuroD2 cDNA. The neurons were fixed at 4 DIV and NeuroD2 was almost completely knocked down by NeuroD2 shRNA as compared to a non-targeting shRNA. GFP (green), NeuroD2 (red) and DNA (blue). Scale bar, 10μm.

4.2 NeuroD2 binding profile of target genes

ChIP-Seq analysis was carried out to find out the genome wide targets of NeuroD2 transcription factor at embryonic (E14) and postnatal (P0) stages. Three different NeuroD2 antibodies were used in this study, to match the species differences we separately generated GFP ChIP DNA with two different GFP antibodies. Depending on the species of the antibody used, NEUROD2 ChIP-Seq reads from each experiment were normalized to the respective GFP ChIP-Seq reads. In order to identify the binding profiles of NeuroD2 transcription factor in the whole genome and to understand the regulatory mechanism of it both at embryonic and postnatal stages, closest gene scores were assigned to each gene using both the number of associated peaks and their closeness to the transcription start site. Next, in the embryonic dataset, top 1,045 target genes were identified based on their high scores and gene ontology analysis was done to determine the biological functions of them in the mouse genome. According to this analysis, NeuroD2 has a key role in the regulation of major developmental processes; cortical radial migration and axonal path finding for the embryonic stages [9] and synaptogenesis and dendritogenesis for the postnatal stages. (Bayam et al., unpublished)

4.3 NeuroD2 target genes play role in cortical neuronal migration

To find the signaling pathways those were controlled by NeuroD2, pathway analysis with NeuroD2 targets against all pathways were carried out. Reelin Signaling pathway was identified as the most targeted one among the others at embryonic stage. Several components of this pathway such as *Cdk5r1* and *Lrp8* were revealed as NeuroD2 regulated targets. In order to confirm these genes as being *in vivo* targets of NeuroD2, NeuroD2 peaks that mapped onto genetic loci of all candidate target genes were overlaid

with whole brain enhancer (H3K4me1) and promoter regions (H3K4me3) [9]. Next, to further confirm NeuroD2 association with the promoter regions of the target genes, primers that were specific to binding regions of NeuroD2 were designed. Then, NeuroD2 ChIP coupled with quantitative PCR was performed. Then, we determined whether NeuroD2 is necessary for the target genes. Total RNAs were isolated from 4 DIV embryonic primary cortical neurons electroporated with NeuroD2 shRNA and non-targeting shRNA. Next, by RT-qPCR the transcript level abundance of *Cdk5r1* and *Lrp8* were tested. The results showed the reductions in the mRNA level of these target genes (Figure 4.4). In sum, our results demonstrated that NeuroD2 controls Reelin signaling pathway through direct regulation of the target genes.

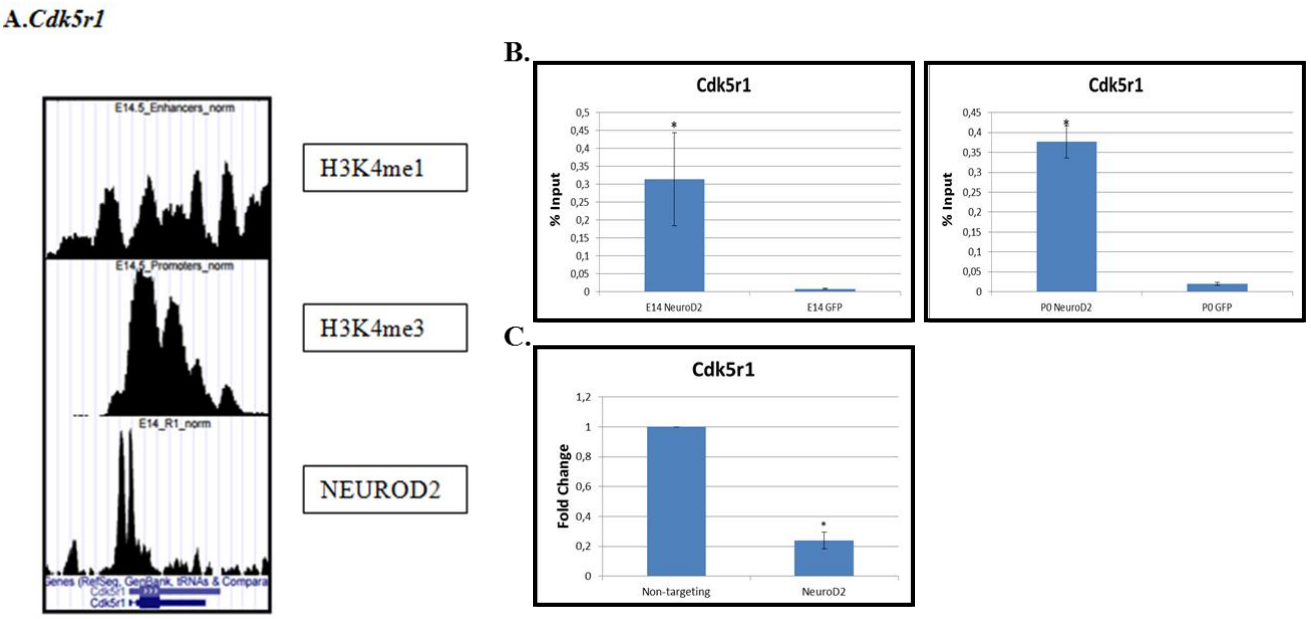

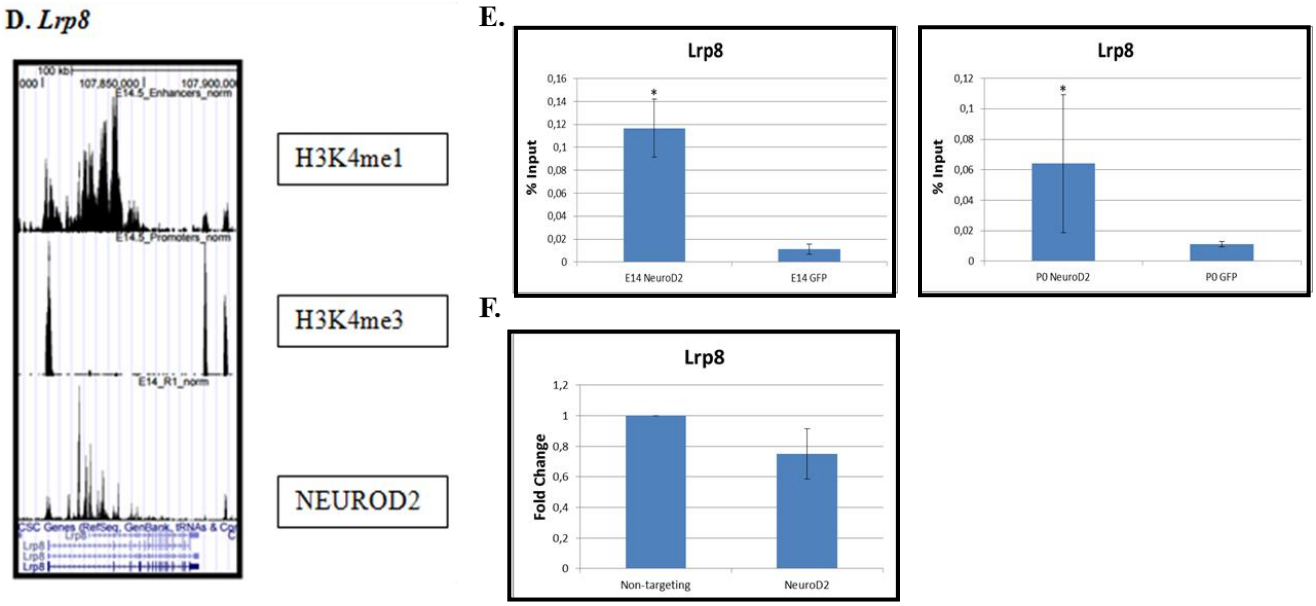

Figure 4.4 NeuroD2 targets *Cdk5r1* and *Lrp8* genes. (A and D) NeuroD2 peaks associated with Cdk5r1 and Lrp8 are plotted relative to enhancer (H3K4me1) and promoter (H3K4me3) marks. (B and E) NeuroD2 binding to the promoter regions of these target genes relative to a negative control (GFP ChIP) are confirmed by ChIP-qPCR. Data is normalized to the amount of input DNA, (p-value<0.05) and represents two biological and five technical replicates. Bars represent standard error of mean. (C and F) Reverse transcription and q-PCR analysis shows reduction in mRNA levels of Cdk5r1(p-value<0.05) and Lrp8. Data represents three biological replicates and each has three technical replicates. Data is presented as fold change of control sample . A non-targeting shRNA was used as control. Bars are standard error of mean.

4.4 NeuroD2 target genes are associated with cortical differentiation and axon guidance of cortical projection neurons

According to embryonic ChIP-seq analysis, NeuroD2 was shown to control the important transcription factors that play role in differentiation and axon guidance of cortical projection neurons [9]. The upper layer markers such as *Cux1/2, Satb2* and deep layer markers such as *Ctip2, Fezf2, Tbr1,Tle1* were revealed in NeuroD2 target gene list [9]. In order to confirm these genes as being *in vivo* targets of NeuroD2, NeuroD2 binding profile of these genes were examined and demonstrated the overlapping NeuroD2 peaks with whole brain enhancer (H3K4me1) and promoter regions (H3K4me3) of all candidate genes [9]. Next, I further confirmed NeuroD2 association with the promoter regions of the target genes by ChIP-qPCR. Then, the mRNA levels of the target genes were quantified RT-qPCR after knockdown of NeuroD2 in primary cortical neurons (Figure 4.5). Taken together, our results showed that NeuroD2 regulates a set of genes that play role in layer identity determination of cortical projection neurons.

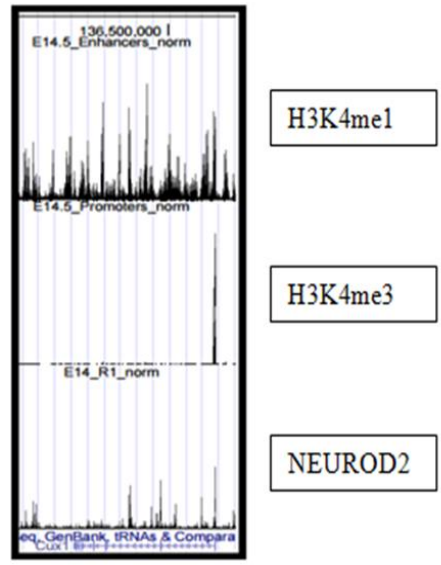

A. *Cux1*

B.

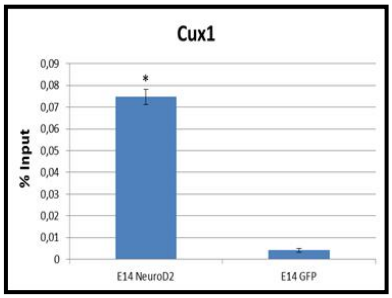

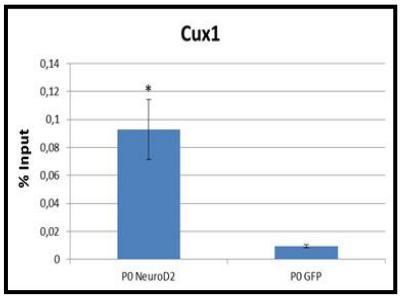

C.

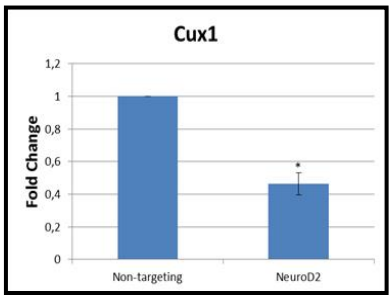

D. *Satb2*

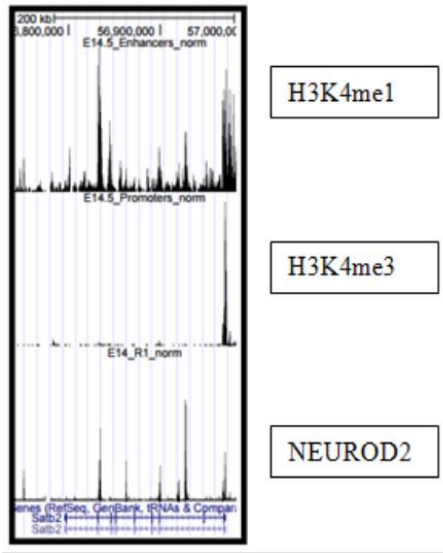

E.

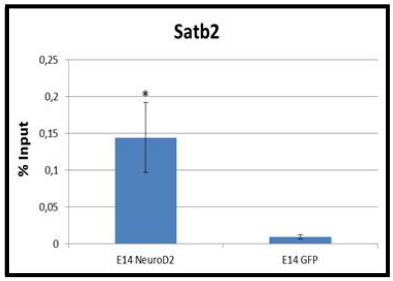

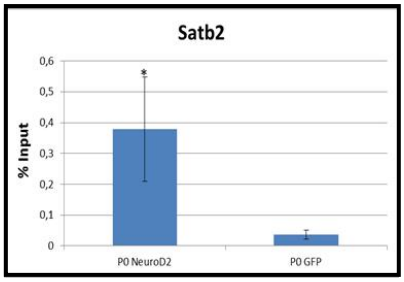

F.

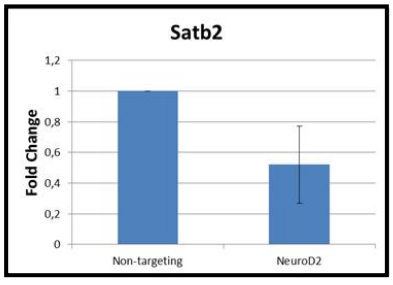

G. *Fezf2*

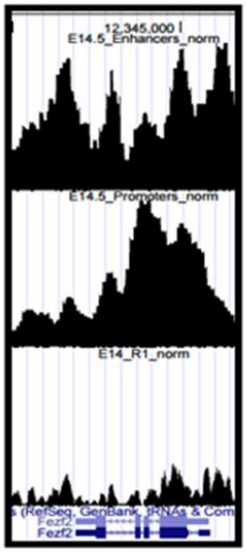

H3K4me1

H3K4me3

NEUROD2

H.

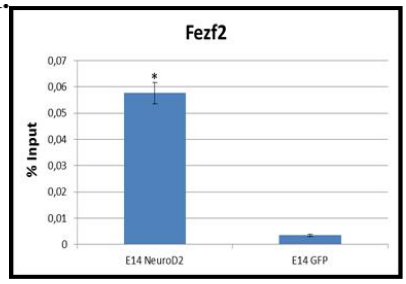

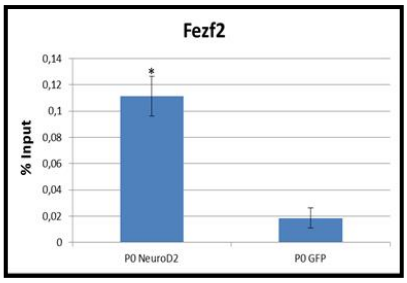

I.

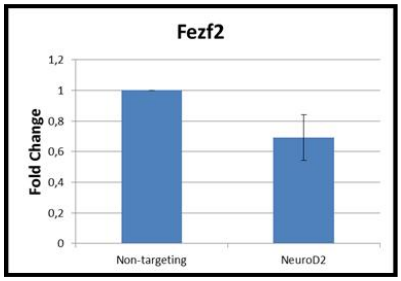

J. *Ctip2*

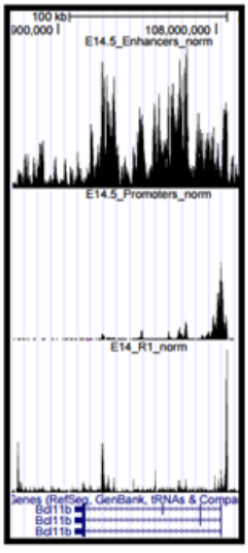

H3K4me1

H3K4me3

NEUROD2

K.

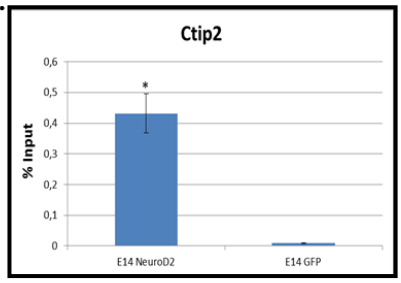

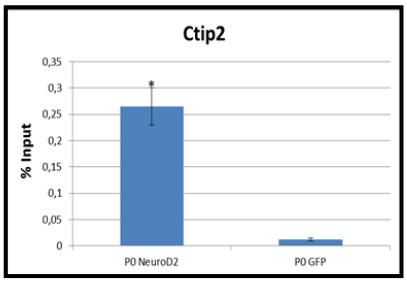

L.

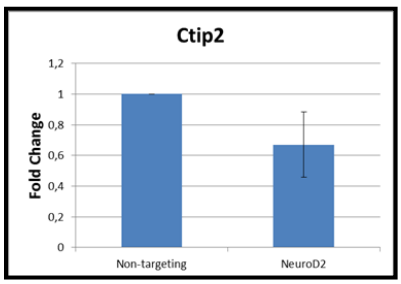

M. *Tbr1*

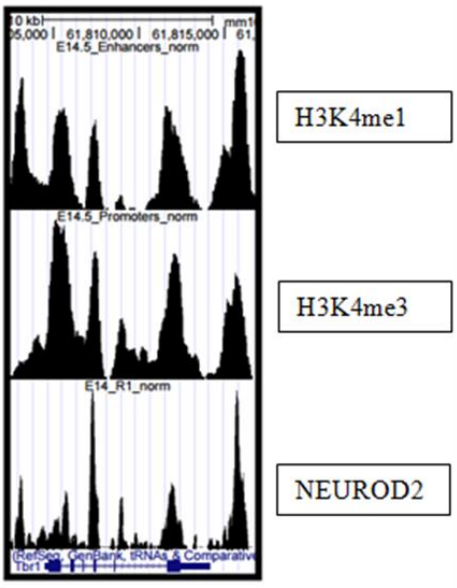

N.

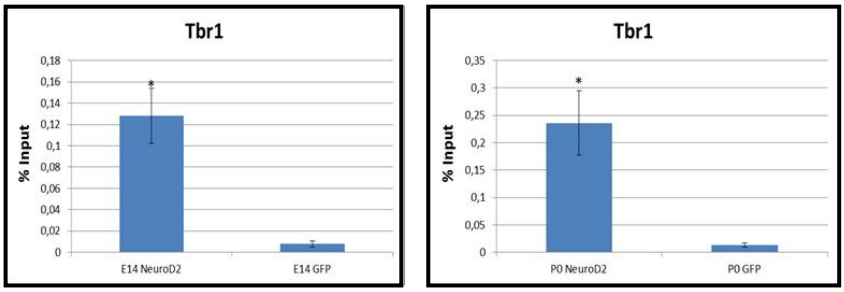

O. *Tle1*

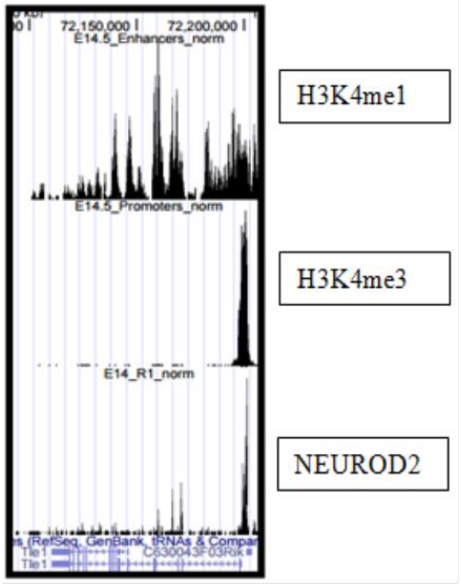

P.

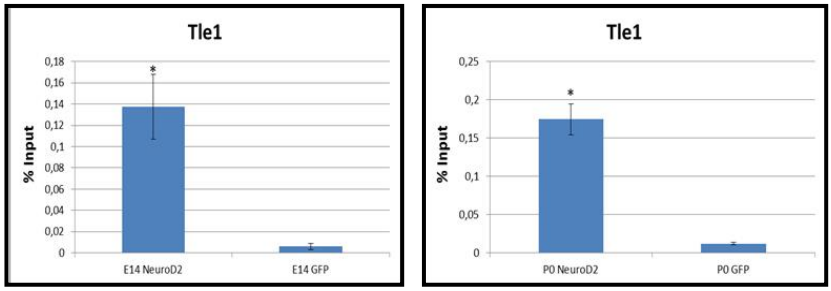

Figure 4.5 NeuroD2 targets cortical layer markers. (A, D, G, J, M, O) NeuroD2 peaks associated with *Cux1, Satb2, Fezf2, Ctip2, Tle1* and *Tbr1* are plotted relative to enhancer (H3K4me1) and promoter (H3K4me3) marks [9]. (B, E, H,K, N, P) NeuroD2 binding to the promoter regions of these target genes relative to a negative control (GFP ChIP) are confirmed by ChIP-qPCR. Data is normalized to the amount of input DNA, (p-value<0.05) and represents two biological and five technical replicates. Bars represent standard error of mean. (C, F, I, L,) Reverse transcription and q-PCR analysis shows reduction in mRNA levels of target genes, (* denotes p-value<0.05). Data represents three biological and three technical replicates. Data is presented as fold change of control sample . A non-targeting shRNA was used as control. Bars are standard error of mean.

4.5 NeuroD2 target genes are involved in Wnt signaling pathway

After postnatal ChIP-seq results and signaling pathway analysis, our laboratory identified several key components of Wnt pathway that are controlled by NeuroD2 (Bayam E et al., unpublished). *Fzd4*, *Fzd8*, *Fzd9* and *Dvl3* were revealed as the target genes of NeuroD2. To confirm these genes as being *in vivo* targets of NeuroD2, NeuroD2 peaks that mapped onto genetic loci of all candidate target genes were overlaid with whole brain enhancer (H3K4me1) and promoter regions (H3K4me3) (Bayam et al., unpublished). Then, NeuroD2 association with the promoter regions of the target genes were verified by ChIP-qPCR. Next, the mRNA levels of the target genes were quantified by RT-qPCR after knockdown of NeuroD2 in primary cortical neurons (Figure 4.6). To sum up, our results showed that NeuroD2 binds a group of genes that act in Wnt signaling pathway.

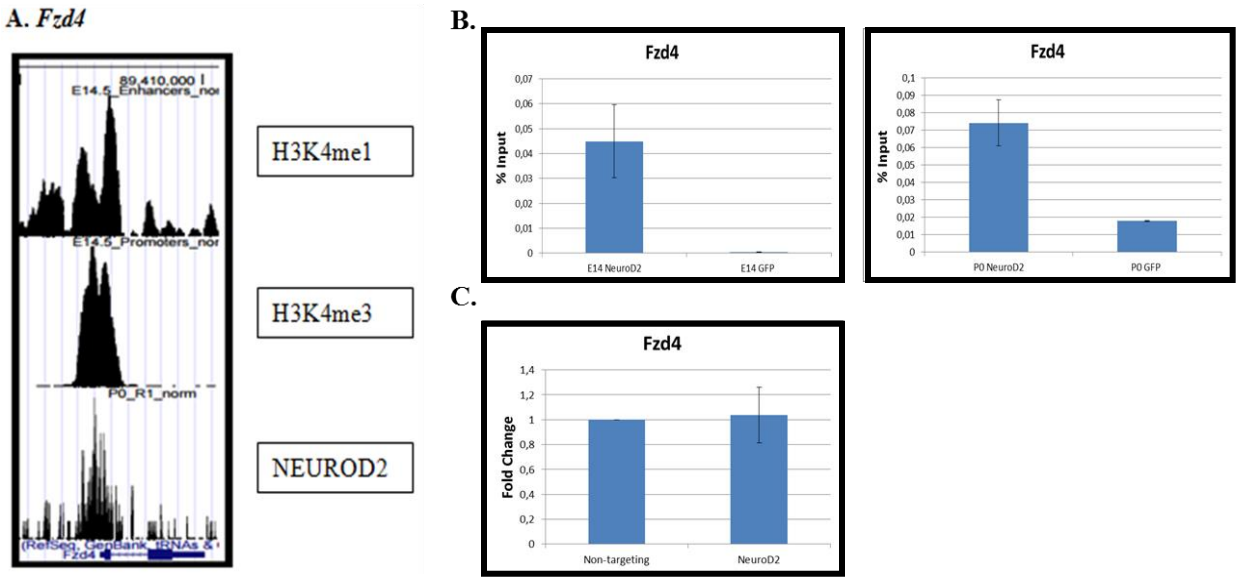

D. ***Fzd8***

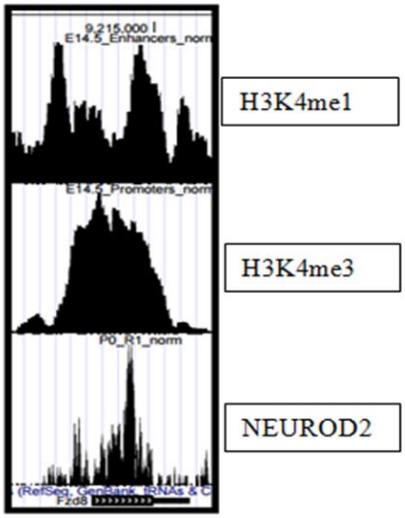

E.

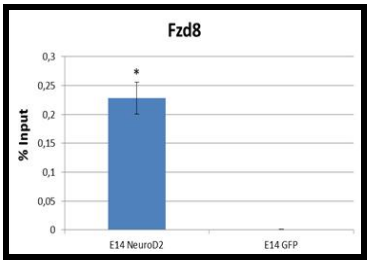

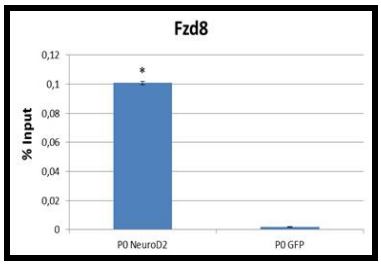

F.

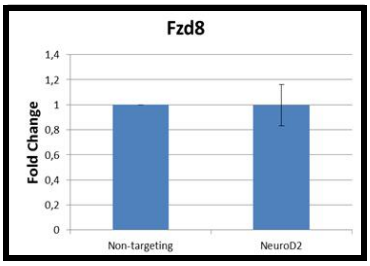

G. ***Fzd9***

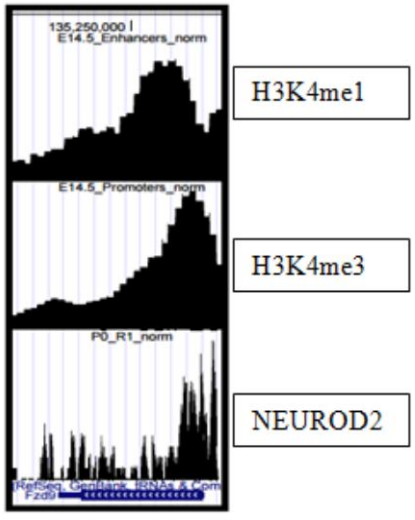

H.

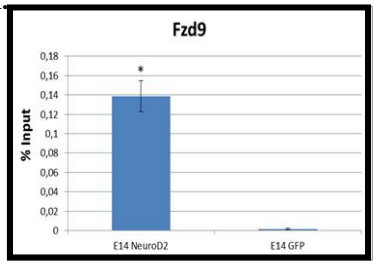

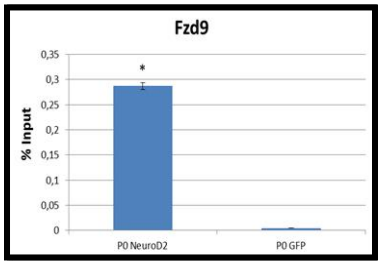

I.

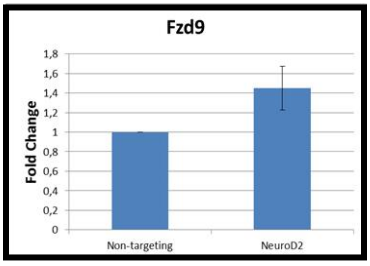

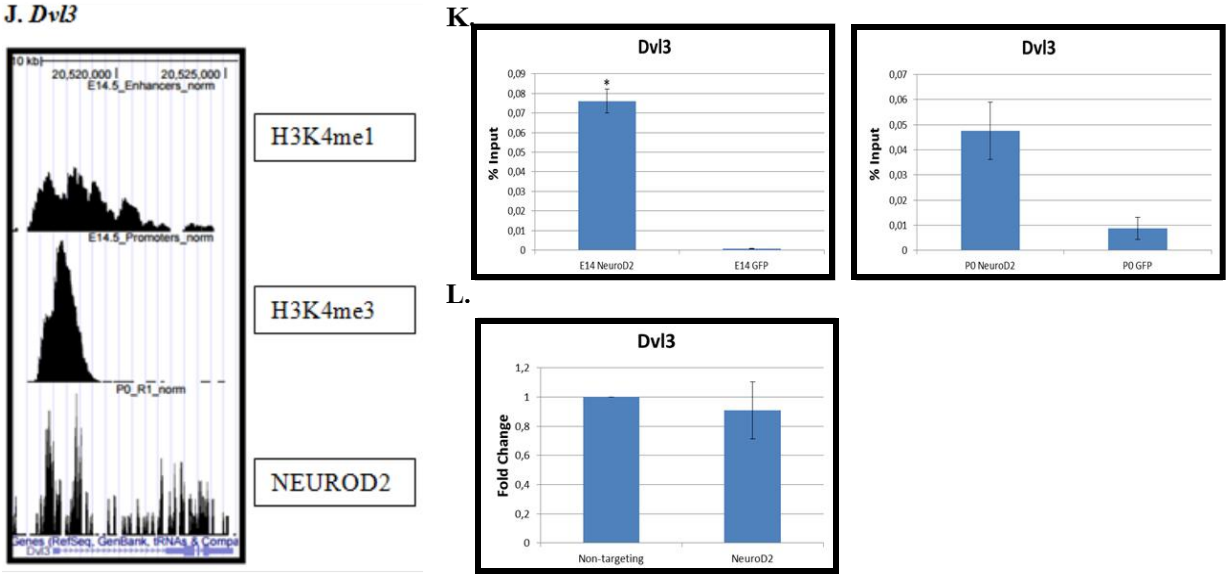

Figure 4.6 NeuroD2 target genes play role in Wnt signaling pathway. (A, D, G, J) NeuroD2 peaks associated with *Fzd4, Fzd8,Fzd9 and Dvl3* are plotted relative to enhancer (H3K4me1) and promoter (H3K4me3) marks. (B, E, H, K) NeuroD2 binding to the promoter regions of these target genes relative to a negative control (GFP ChIP) are confirmed by ChIP-qPCR. Data is normalized to the amount of input DNA, (* denotes p-value<0.05) and represents to one biological and three technical replicates. Bars represent standard error of mean. (C, F, I, L) Reverse transcription and q-PCR analysis shows no reduction in mRNA levels of target genes. Data represents two biological and three technical replicates. Data is presented as fold change of control sample . A non-targeting shRNA was used as control. Bars are standard error of mean.

4.6 NeuroD2 target genes are associated with mTOR pathway

After analyzing postnatal ChIP-seq data, to gain better understanding of the signaling pathways that were controlled by NeuroD2 we performed pathway analysis and found mTOR pathway as the targeted pathway. Our analysis revealed that NeuroD2 targets included several key members of this pathway such as *Eif3a, Tsc1, Rsb6kb1* and *Pkd1* genes. In order to confirm these genes as being *in vivo* targets of NeuroD2, NeuroD2 binding profile of these genes were examined and demonstrated the overlapping NeuroD2 peaks with whole brain enhancer (H3K4me1) and promoter regions (H3K4me3) of all candidate genes (Bayam et al., unpublished). Next, I further confirmed NeuroD2 association with the promoter regions of the target genes by ChIP-qPCR (Figure 4.7). Taken together our results illustrated that NeuroD2 targets a set of genes that play role in mTOR pathway.

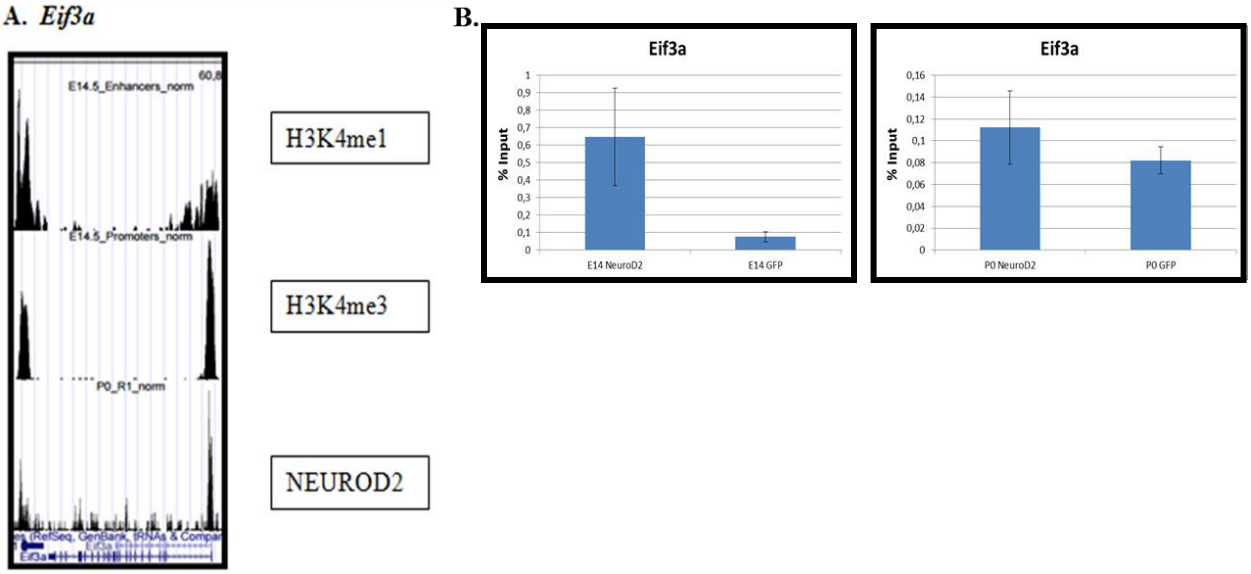

C. *Tsc1*

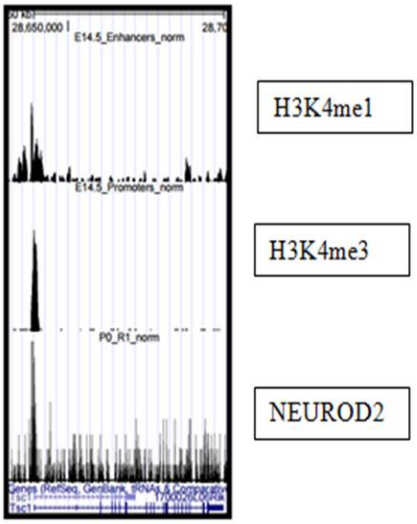

D.

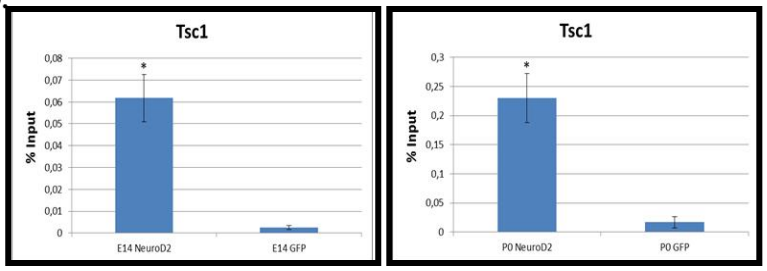

E. *Pkd1*

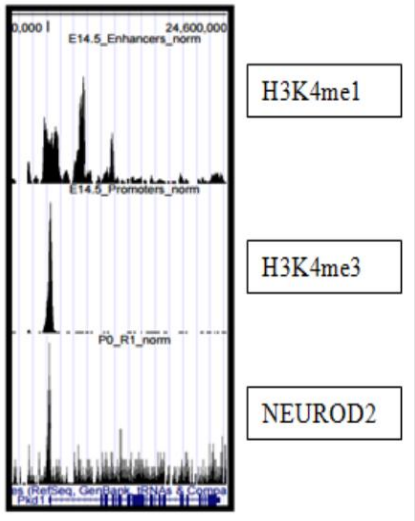

F.

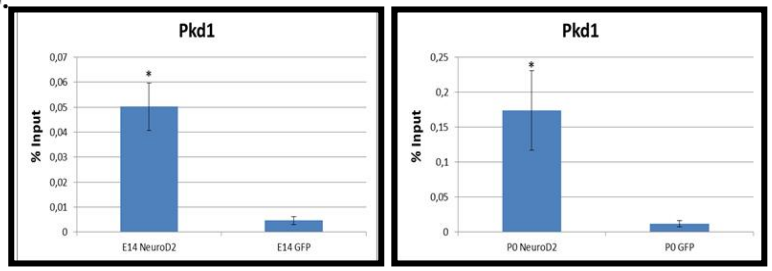

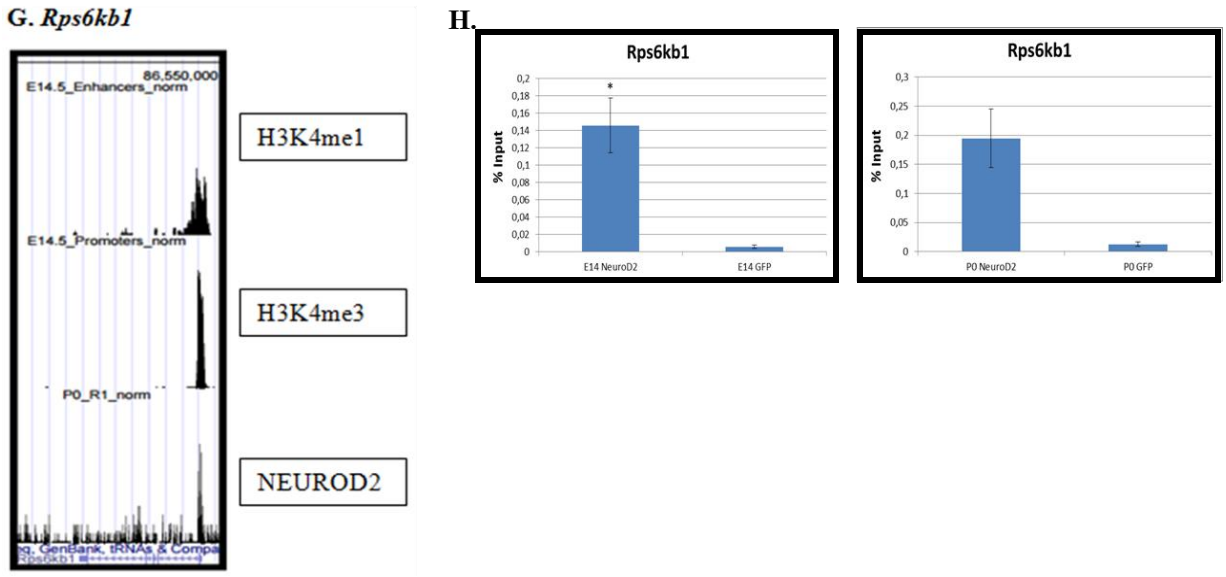

Figure 4.7 NeuroD2 target genes play role in mTOR signaling pathway. (A,C,E,G) NeuroD2 peaks associated with *Eif3a,Tsc1,Rps6kb1 and Pkd1* are plotted relative to enhancer (H3K4me1) and promoter (H3K4me3) marks. (B,D,F, H) NeuroD2 binding to the promoter regions of these target genes relative to a negative control (GFP ChIP) are confirmed by ChIP-qPCR. Data is normalized to the amount of input DNA, (p-value<0.05) and represents two biological and five technical replicates. Bars represent standard error of mean.

4.7 Other genes that are identified as targets of NeuroD2 transcription factor

After analyzing both the embryonic and postnatal ChIP-seq data, there were some genes idenfied as top targets of NeuroD2. While NeuroD6 and Nrcam were identified at embryonic stage, Stim1 and bHLHe22 were revealed at postnatal stage as significantly targeted genes by NeuroD2 (Bayam et al., unpublished). The confirmation of NeuroD2 binding profile was carried out by overlapping NeuroD2 peaks with whole brain enhancer (H3K4me1) and promoter regions (H3K4me3) of all candidate genes (Bayam et al., unpublished). Next, I aimed to confirm NeuroD2 association with the promoter regions of the target genes by ChIP-qPCR. Then, the mRNA levels of *NeuroD6* and *Stim1* were examined by RT-qPCR after knockdown of NeuroD2 in primary cortical neurons (Figure 4.8). The results showed that NeuroD2 targets *NeuroD6, Nrcam, Stim1* and *bHLHe22.*

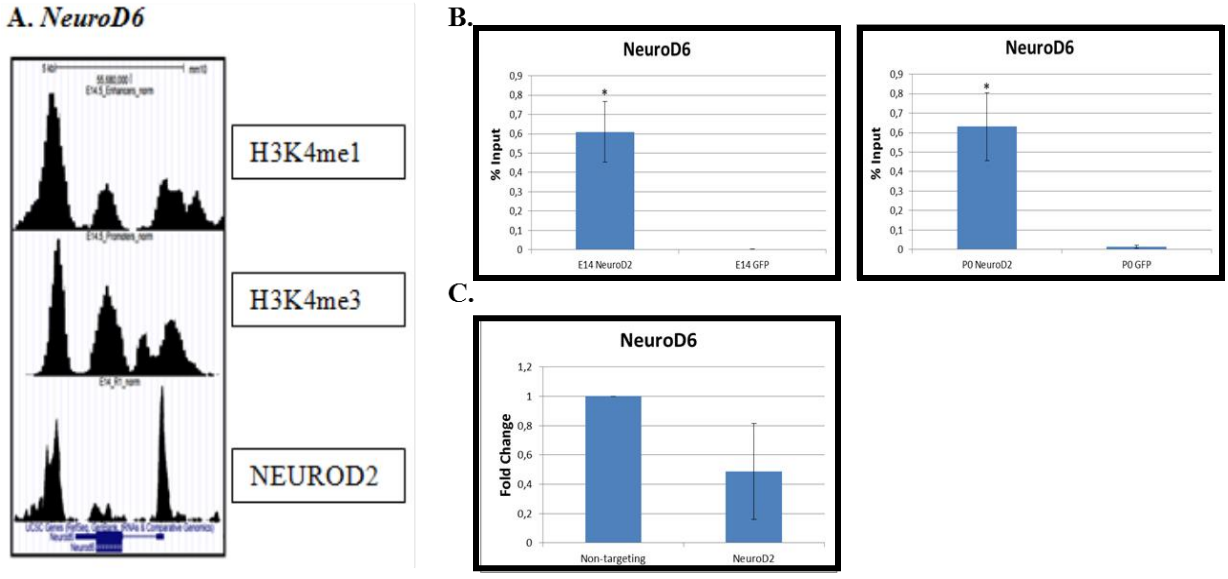

D. ***Nrcam***

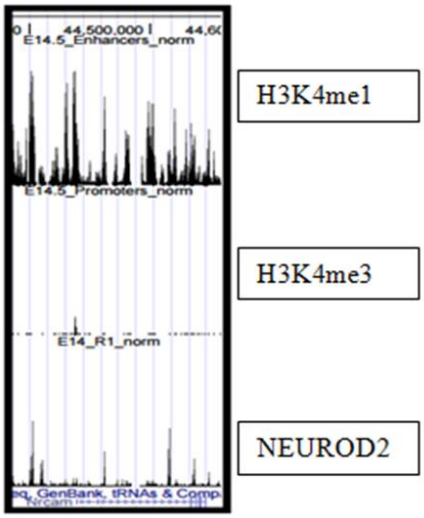

E.

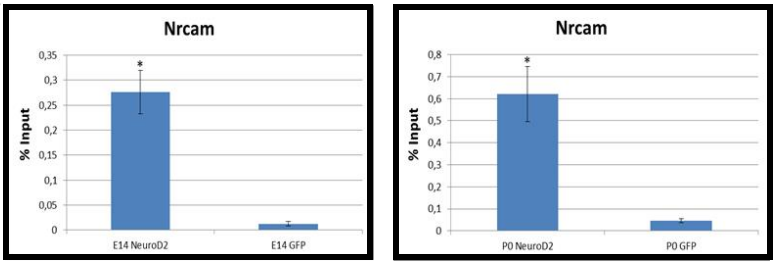

F. ***Stim1***

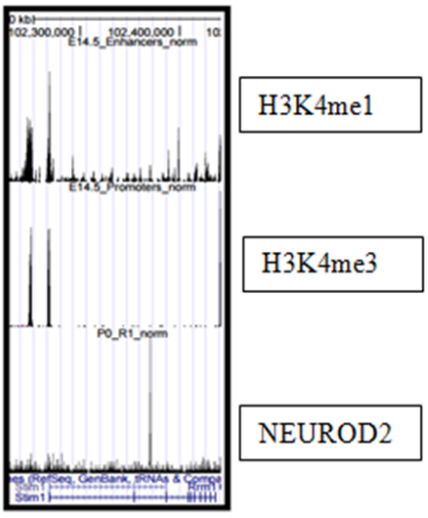

G.

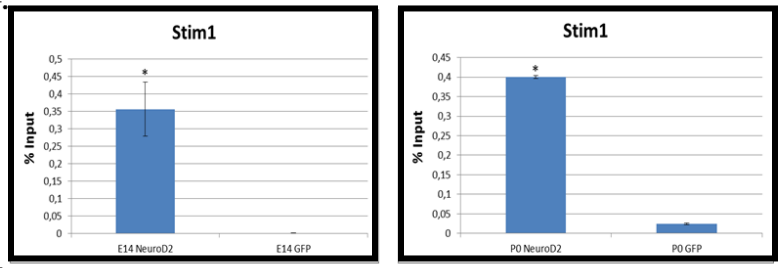

H.

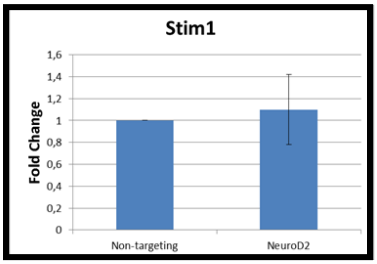

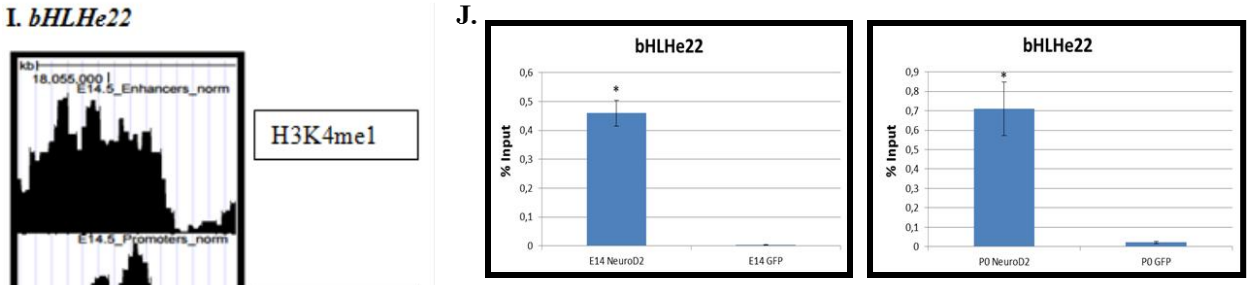

Figure 4.8 *NeuroD6, Nrcam, Stim1* and *bHLHe22* are the targets of NeuroD2.
(A, D, F, I) NeuroD2 peaks associated with *NeuroD6, Nrcam, Stim1* and *bHLHe22* are plotted relative to enhancer (H3K4me1) and promoter (H3K4me3) marks. (B, G, J) NeuroD2 binding to the promoter regions of these target genes relative to a negative control (GFP ChIP) are confirmed by ChIP-qPCR. Data is normalized to the amount of input DNA, (p-value<0.05) and represents two biological and five technical replicates.Bars represent standard error of mean. (C and H) Reverse transcription and q-PCR analysis shows no reduction in mRNA levels of *Stim1* but a trend in reduction of *NeuroD6* target genes. Data represents two biological and three technical replicates. Data is presented as fold change of control sample . A non-targeting shRNA was used as control. Bars are standard error of mean.

4.8 Genes that are not identified as targets of NeuroD2 transcription factor

In order to demonstrate high confirmation rate of NeuroD2 binding to target genes, we chose five genes as negative controls which were not identified as NeuroD2 targets in our embryonic and postnatal ChIP-Seq analysis. Selected genes, Gsx2, Dlx2, Gad1 and Calb2, are expressed in interneurons but not in cortical projection neurons. In addition, NeuroD2 peaks were overlapped with the zones of these genes resulting that there was no NeuroD2 binding. To further corfirm, I performed ChIP-qPCR and did not observe any enrichment in NeuroD2 binding to the non-target genes but only Gsx2 showed an insignificant enrichment (Figure 4.9).

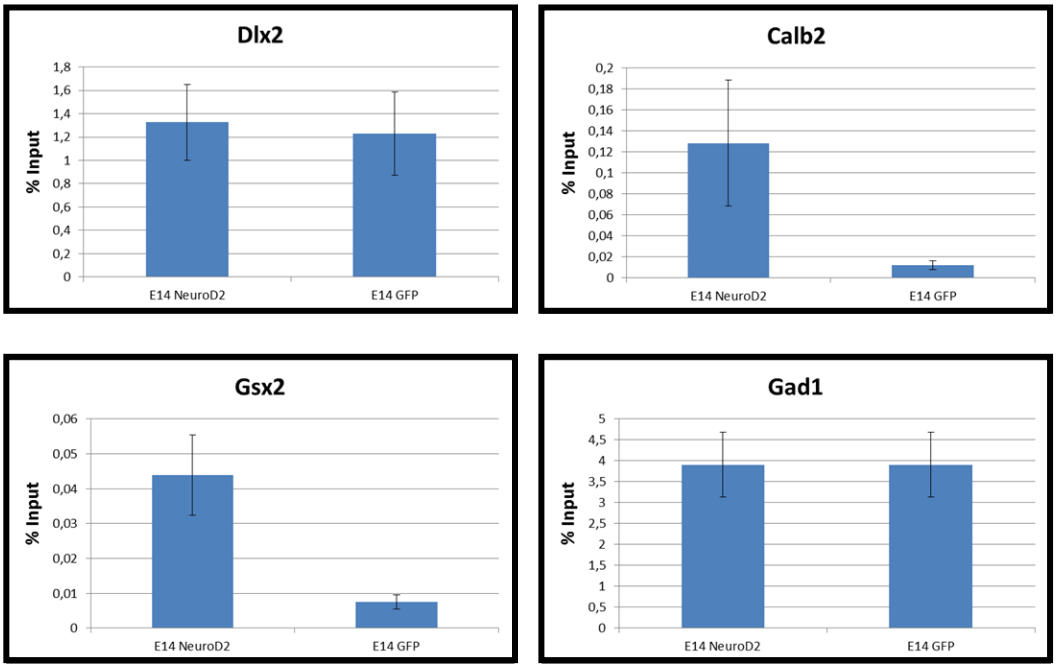

Figure 4.9 There is no enrichment in NeuroD2 binding to non-target genes. Data is normalized to the amount of input DNA, and represents two biological and five technical replicates for *Dlx2* and *Gsx2* but three technical replicates for *Gad1* and *Calb2*. Bars represent standard error of mean.

4.9 Regulation of Dendrite Development by NeuroD2

Several studies clarified that the proper control of dendrite morphology is regulated by several transcription factors and their downstream signaling pathways. For example, CREB activation is necessary for CaM Kinase IV induced dendrite growth [45]. Our preliminary data suggested that dendrites of cortical neurons were not properly developed in *NeuroD2* knockout mice. Therefore, we aimed to examine the dendritogenesis of embryonic primary cortical neurons in control and NeuroD2 knockdown cultures. We cultured cortical neurons both at E14 and E18 stages, transfected NeuroD2 shRNA, non-targeting shRNA and resistant NeuroD2 including pSUPER-neo-GFP plasmids at 2 div and fixed the cultures at 5 div with paraformaldehyde. Cultures were co-immunostained with anti-NeuroD2 and anti-GFP antibodies. DAPI was used for nuclei staining (Figure 4.10 and 4.11). Next, both NeuroD2 knockdown and GFP expressed cells were selected and imaged. We quantified dendrites morphology using Scholl analysis, a method counting the number of dendrites and their branch points based on the distance from the neuronal soma. Our results showed that there was no difference between wild-type and NeuroD2 knockdown samples according to the number of dendrites and the branch points (Figure 4.12)

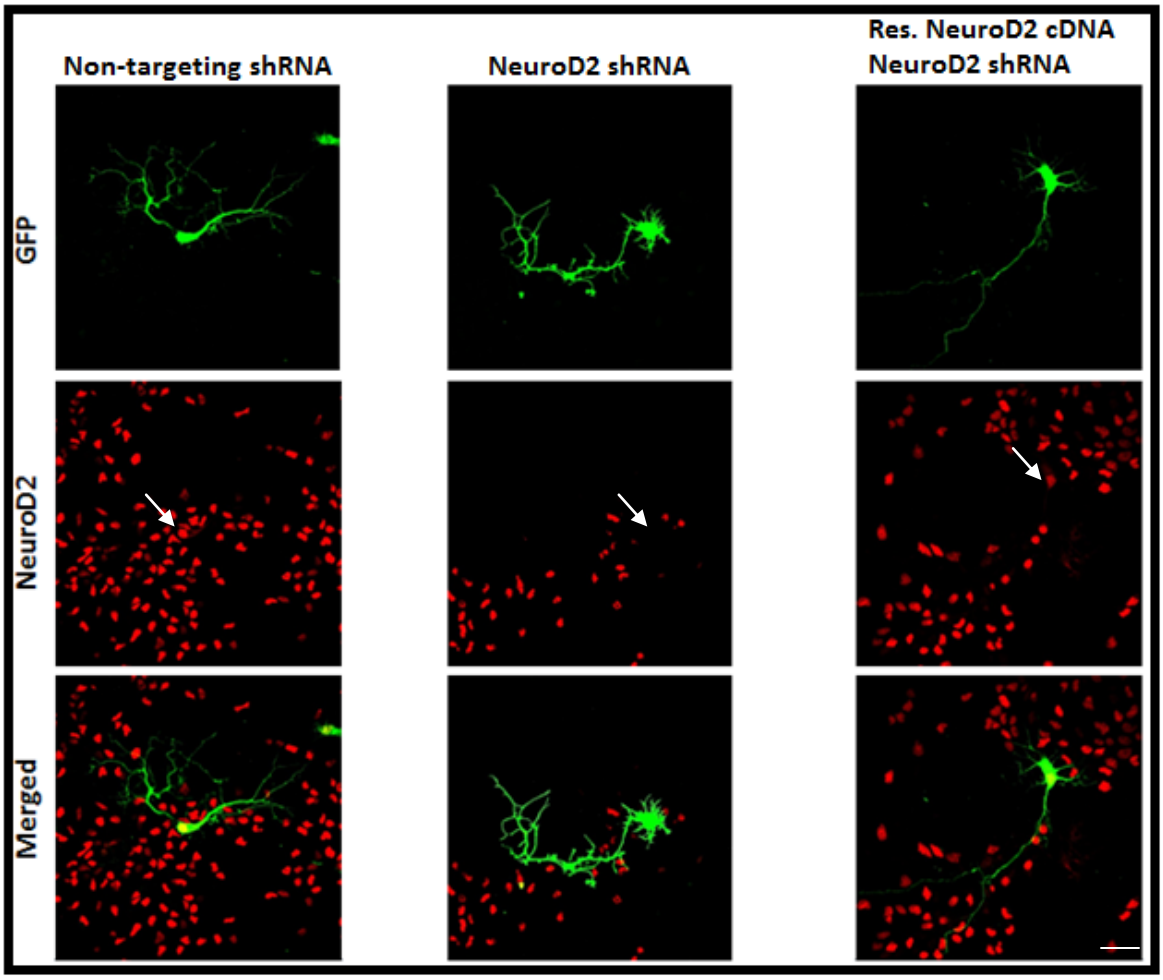

Figure 4.10 Immunofluorescence analysis of dendrite morphology of non-targeting and NeuroD2 shRNA transfected E14 primary cortical neurons. 2 DIV E14 primary cortical neurons were transfected with non-tergeting, NeuroD2 shRNA and both NeuroD2 shRNA and resistant NeuroD2 cDNA. The neurons were fixed at 4 DIV and analyzed based on their dendrite morphology. GFP (green) and NeuroD2 (red). Scale bar, 10μm

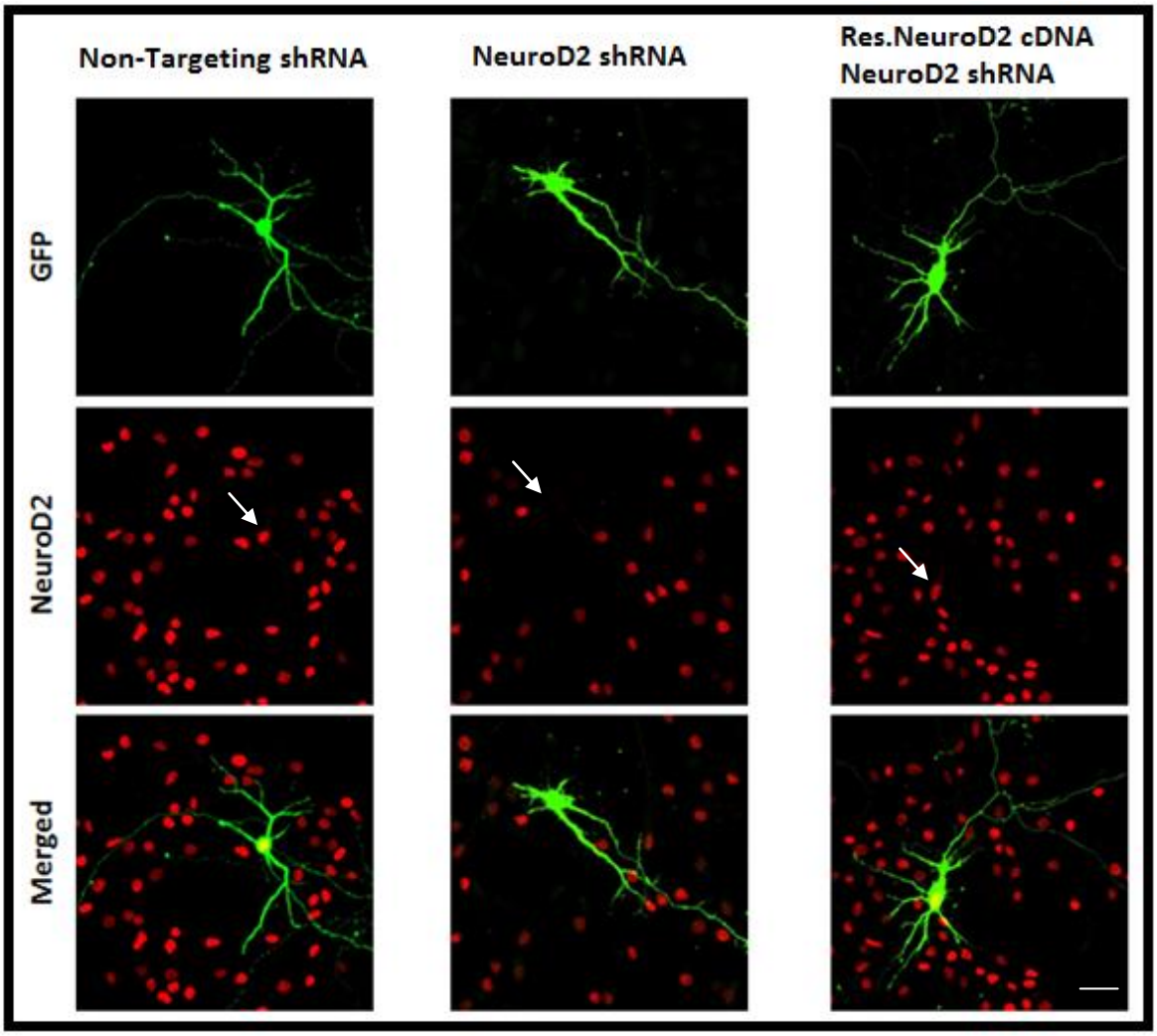

Figure 4.11 Immunofluorescence analysis of dendrite morphology of non-targeting and NeuroD2 shRNA transfected E18 primary cortical neurons. 2 DIV E14 primary cortical neurons were transfected with non-tergeting, NeuroD2 shRNA and both NeuroD2 shRNA and resistant NeuroD2 cDNA. The neurons were fixed at 4 DIV analyzed based on their dendrite morphology. GFP (green) and NeuroD2 (red). Scale bar, 10µm

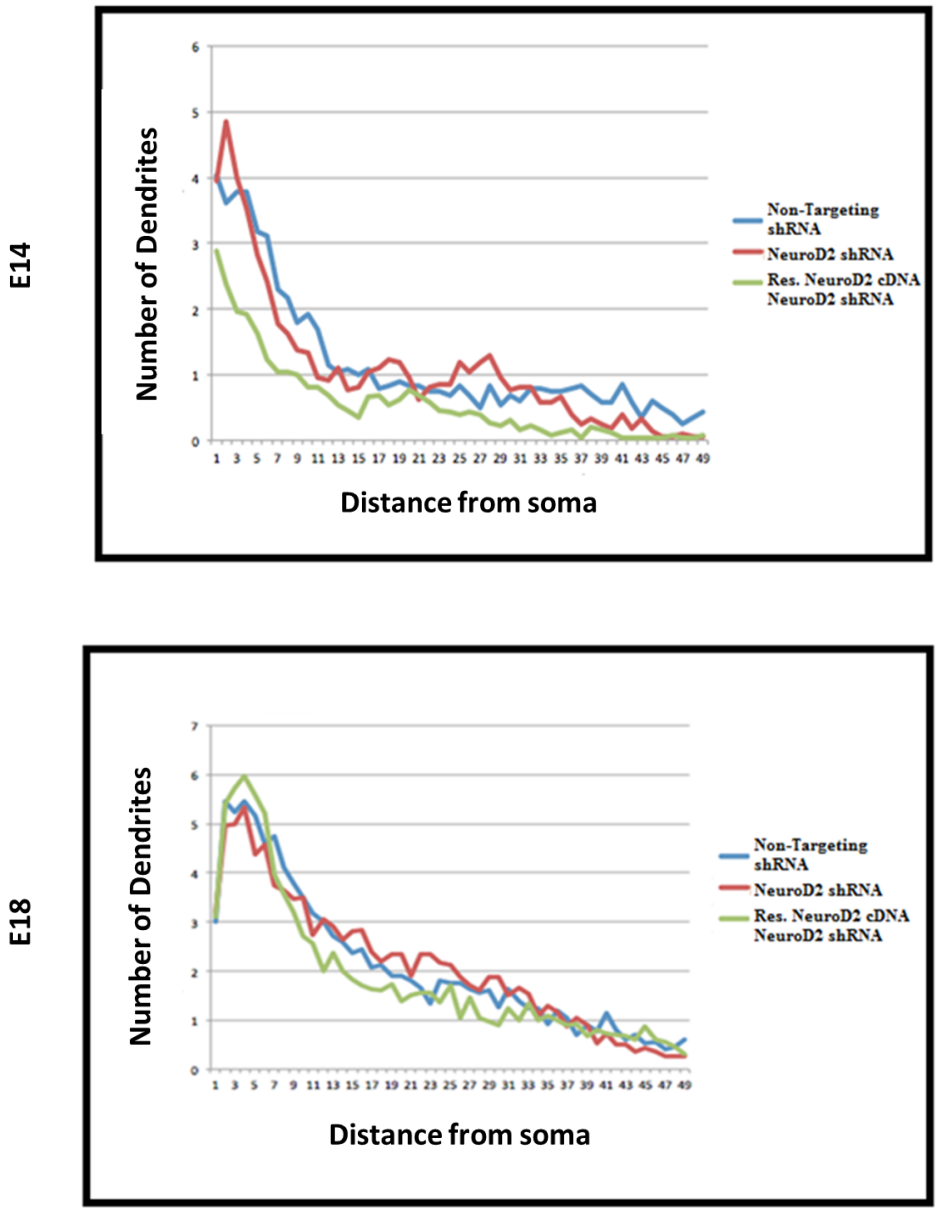

Figure 4.12 Quantification of dendrite development of E14 and E18 primary cortical neurons. Sholl analysis plugin of ImageJ software was used to analyze the dendrite development of E14 and E18 primary cortical neurons. Images were captured under 60X focus and they were 1024x1024 pixels. Unit scale: 1Pixel= 1,0 pixels

4.10 NeuroD2 binding profile of *Id2* gene

Following the preliminary data from microarray results (Ince-Dunn, unpublished) suggesting that *Id2* transcripts were two fold down-regulated in *NeuroD2* knockout samples compared to wild type. In addition, northern blot and *in situ* hybridization analysis indicated the dramatic decrease for the RNA level of *Id2* in the knockout one compared to the wild-type (Ince-Dunn, unpublished). Therefore, we wondered to test whether NeuroD2 transcription factor regulates the gene expression of *Id2*. Chip-Seq analysis was performed at both embryonic and postnatal stages and *Id2* was identified as one of the top target genes of NeuroD2. NeuroD2 peaks that mapped onto genetic loci of *id2* were overlapped with whole brain enhancer (H3K4me1) and promoter regions (H3K4me3) [9] (Figure 4.13). The peak results demonstrated that NeuroD2 binds to the promoter region of *Id2* gene.

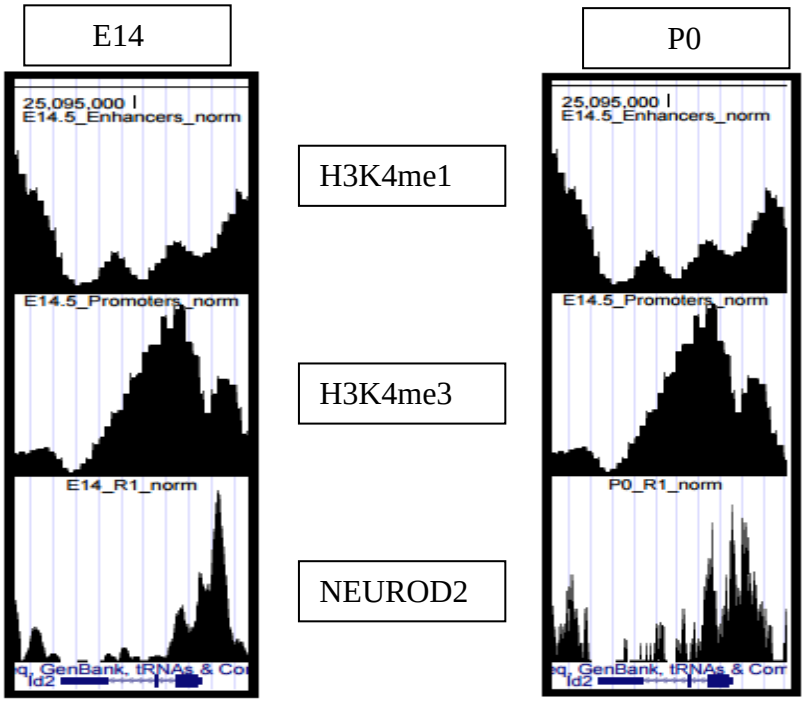

Figure 4.13 NeuroD2 binding profile of *Id2* gene at embryonic and postnatal stages. NeuroD2 peaks associated with *Id2* are plotted relative to enhancer (H3K4me1) and promoter (H3K4me3) marks both at embryonic and postnatal stages.

4.11 Enrichment of *Id2* promoter region

Next, we tried to confirm the enrichment of *Id2* promoter region due to the binding of NeuroD2 transcription factor. First, standard PCR was done using primers designed against promoter region of *Id2*. *Id2 gene* promoter was enriched in ChIP samples from the three anti-NeuroD2 antibodies but not from the anti-GFP antibody. One PCR was set up with no DNA template for the negative control. I performed NeuroD2 ChIP coupled with q-PCR again using *Id2* promoter region specific primers for further confirmation. The results revealed that NeuroD2 associated with the promoter region of *Id2* gene (Figure 4.14).

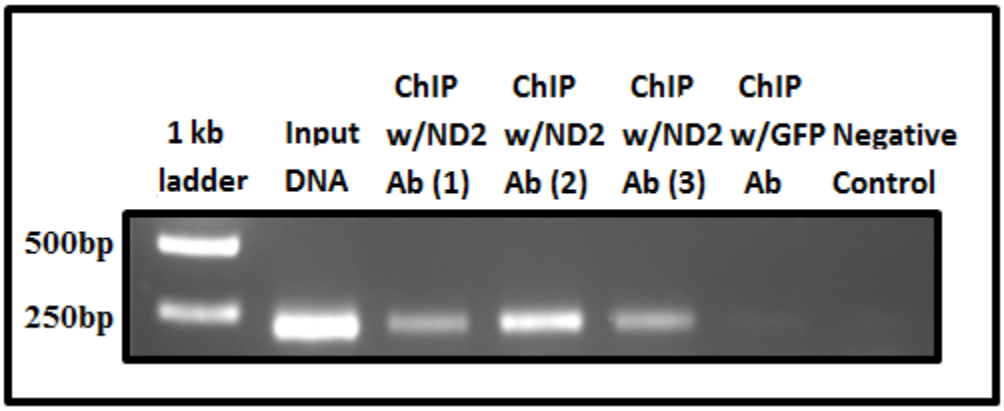

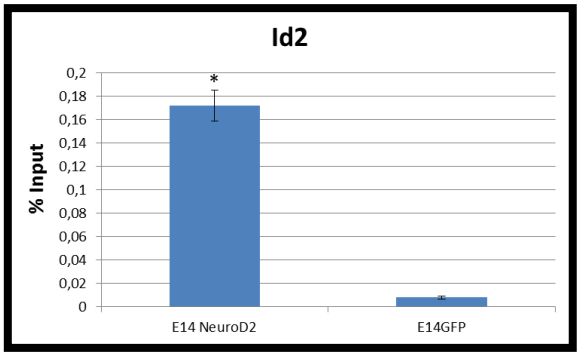

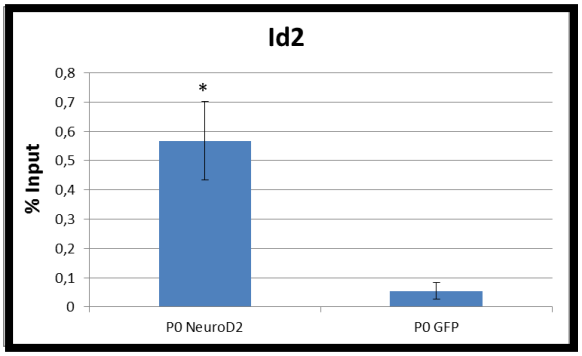

Figure 4.14 NeuroD2 binds to the promoter region of *Id2* gene. Standart PCR and ChIP-qPCR were performed to confirm the binding of NeuroD2 transcription factor to the promoter region of Id2 gene relative to negative control GFP both at embryonic and postnatal stages (p value<0.05). Bars represent standard error of mean.

4.12 Cloning of *Id2* into pcDNA3 backbone vector

In order to analyze the localization, expression and interactions of Id2, first of all, Id2 cDNA was cloned into pcDNA3A-HA/FLAG vector by using PCR based cloning method. After amplification of Id2 cDNA by standard PCR, restriction enzyme digestion was applied and ligation was done to pcDNA3-HA/FLAG vector. Chemically competent DH5alpha *E.coli* cells were transformed with this constructs and the colonies were selected to do miniprep experiment. Next, diagnostic digestion was carried out and samples were run on 1% agarose gel to find an insert in a correct size. After that, samples were analyzed by direct sequencing for the confirmation of cloning (Figure 4.15) Our result showed that Id2 cDNA was cloned successfully into pcDNA3-HA/FLAG vector.

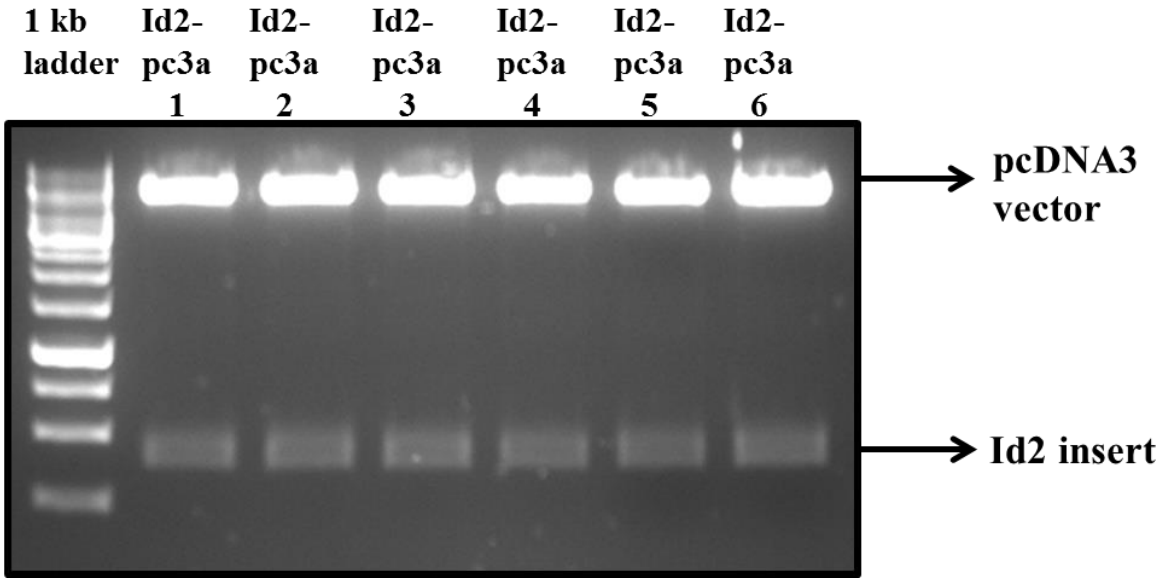

Figure 4.15 Diagnostic digestion result of Id2 cloning into pcDNA3-HA/FLAG vector. Agarose gel electrophoresis result after diagnostic digestion. Lanes 1-6 had correct insert.

4.13 Sub-cloning of *Id2 from Id2*-pcDNA3-HA/FLAG into pcDNA4-myc backbone vector

It has been showed that Id2 interacts with one of bHLH transcription factor, Bmal1. We decided to use this protein as a positive control while we were examining the interaction between Id2 and NeuroD2. However, our positive control construct (Bmal-pcDNA4-FLAG had the same tagged proteins with Id2-pcDNA3-HA/FLAG which was FLAG tagging. As a result, we needed to clone Id2 into another vector, pcDNA4-myc, containing different tagged protein. Briefly, we did sub-cloning of Id2 from Id2-pcDNA3-HA/FLAG vector by restriction enzyme digestion and ligation into pcDNA4-myc vector properly by using chemically competent DH5alpha E.coli cells. After these steps, again miniprep and diagnostic digestion were done. The samples were run on 1% agarose gel to check the presence of insert at a correct size (Figure 4.16). The result demonstrated that sub-cloning of Id2 was achieved properly.

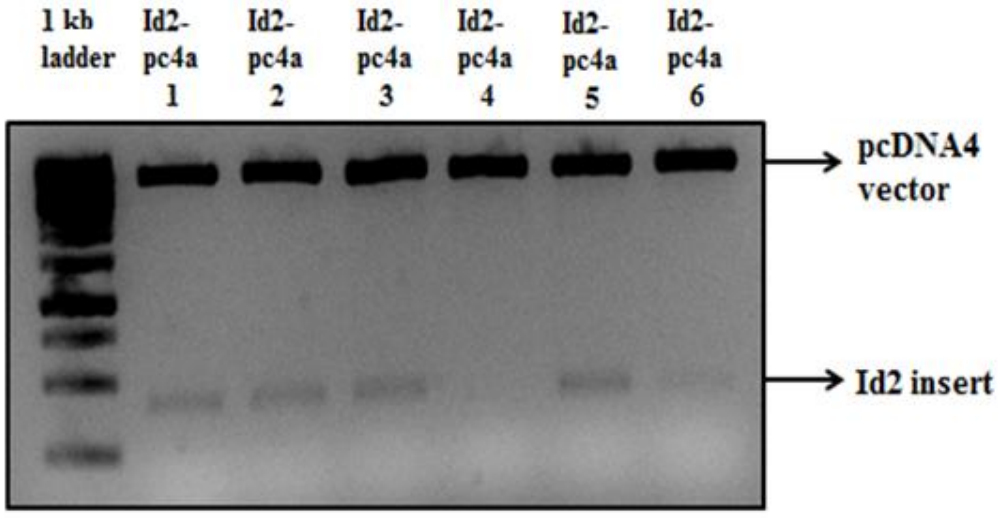

Figure 4.16 Diagnostic digestion result of Id2 sub-cloning into pcDNA4 vector. Lanes 1, 2, 3 and 5 had correct insert.

4.14 Expression of Id2-pcDNA4-myc in NeuroD2 cell line

To be sure that Id2-pcDNA4-myc construct was successfully cloned and expressed , we transfected Neuro2a cell line with this vector and collected cell lysates two days after transfection for western blot. The blots were incubated with anti-myc antibody. The western blot result showed our construct is expressed in Neuro2A cell line successfully (Figure 4.17).

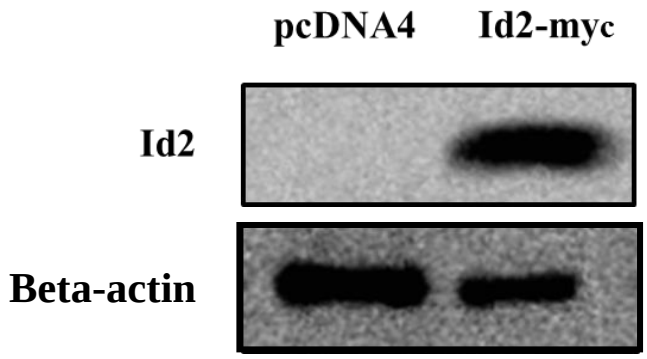

Figure 4.17 Western blot analysis of expression of Id2-pcDNA4-myc construct in Neuro2 cell line. The membrane was blotted with anti-myc and anti-beta-actin antibodies separately. Id2-pcDNA4-myc construct was successfully transfected to Neuro2a cell line.

4.15 Expression of Id2-pcDNA3-HA/FLAG and NeuroD2-pcDNA4-myc constructs in NeuroD2 cell line

To be sure that Id2-pcDNA3-HA/FLAG and NeuroD2-pcDNA4-myc constructs were successfully cloned and expressed, I transfected Neuro2a cell line with these vectors separately and collected cell lysates two days after transfection for western blot. The blots were incubated with anti-HA, anti-Id2, anti-NeuroD2 and anti-myc antibodies (Figure4.18 and 4.19). The western blot results showed that the transfections of these constructs were achieved properly.

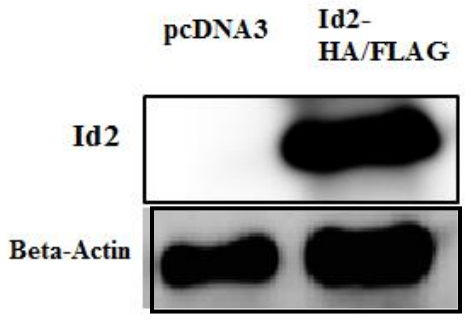

Figure 4.18 Western Blot analysis of expression of Id2-HA/FLAG in Neuro2a cell line. The membrane was blotted with anti-HA and anti-beta-actin antibodies separately. Id2-pcDNA3-HA/FLAG construct was successfully transfected to Neuro2a cell line.

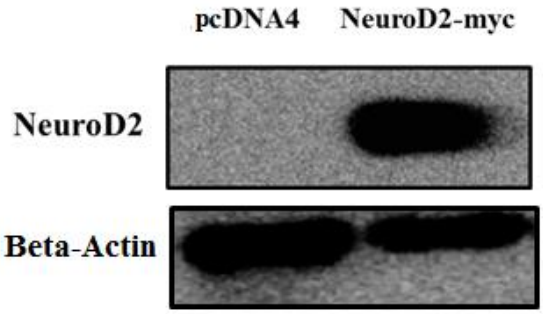

Figure 4.19 Western Blot analysis of expression of NeuroD2-myc in Neuro2a cell line. The membrane was blotted with anti-myc and anti-beta-actin antibodies separately. NeuroD2-pcDNA4-myc construct was successfully transfected to Neuro2a cell line.

4.16 Co-localization and expression of NeuroD2 and Id2 in Neuro2a cell line

According to the study that showing the interaction between Id2 and two bHLH proteins, Bmal1 and Clock, the localizations of Id2 with these proteins were overlapped in the cytoplasm. However, the overexpression of Clock and Bmal1 in the presence of Id2 resulted in a significant reduction in their nuclear localization, indicating that Id2 sequesters Clock and Bmal1 to the cytoplasm [69]. Since Id2 has a role in the nuclear-cytoplasmic shuttling that affects the localization of Bmal1 and Clock proteins, we wondered that whether there was a localization mechanism between NeuroD2 and Id2 proteins. Therefore, first of all, we did confirmation of localization change of Id2 and Bmal1 which was our positive control. We transfected Neuro2a cell lines with Id2-pcDNA4-myc and Bmal-pcDNA4-FLAG and and fixed the cells two days after transfection. Co-immunostaining was done with anti-FLAG and anti-myc antibodies (Figure 4.20). In addition, NeuroD2-pcDNA4-myc and Id2-pcDNA3-HA/FLAG constructs were transfected into Neuro2a cell lines and fixed cells were co-immunostained with anti-HA and anti-myc antibodies. DAPI staining was done to observe the nuclei (Figure 4.21).

Immunofluorescence results demonstrated that Bmal1 changed their localization from nucleus to cytoplasm due to the presence of Id2 however there was no change in the localization of NeuroD2 and Id2. NeuroD2 was always observed in the nuclear part of the cells while Id2 localized both cytoplasmic and nuclear.

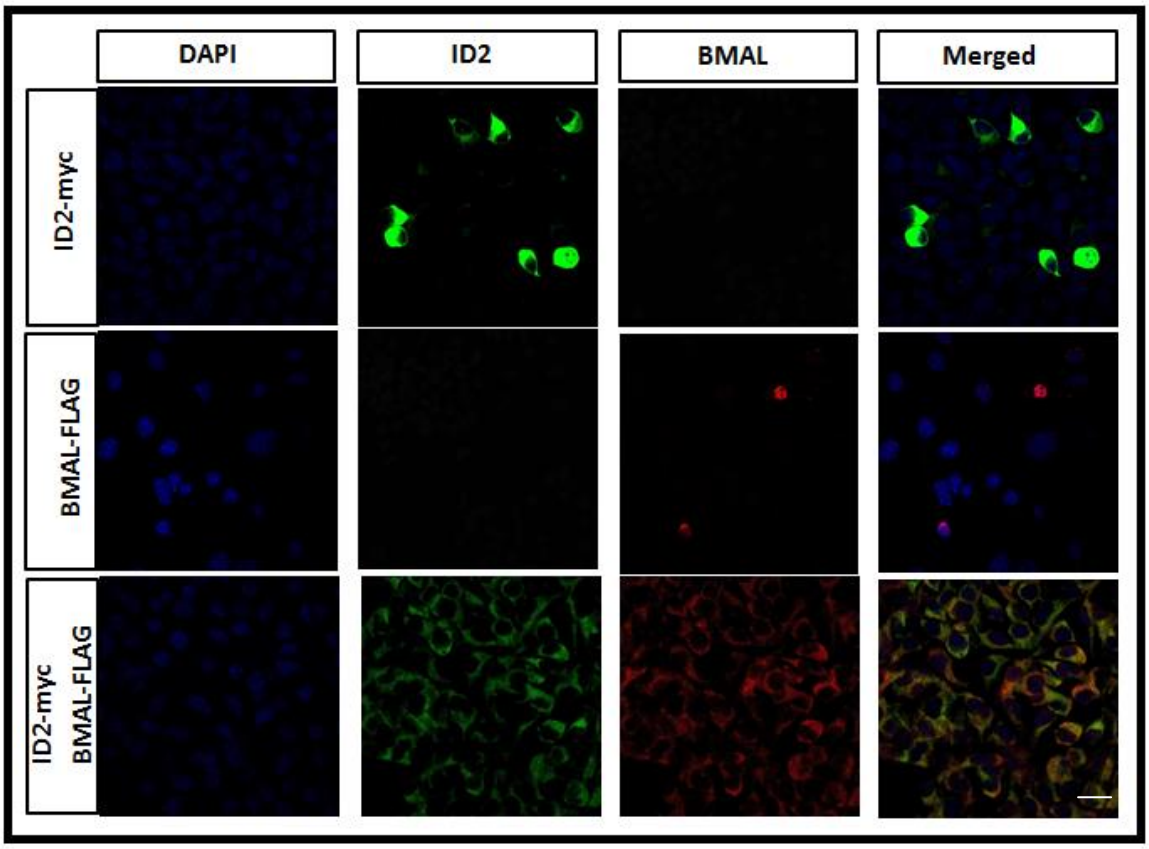

Figure 4.20 Immunofluorescence analysis of co-localization and expression of Id2-myc and Bmal-Flag in Neuro2a cell line. Neuro2a cell line was co-transfected with Id2-myc and Bmal-Flag constructs and immunostained with anti-myc and anti-Flag antibodies. Id2 (green), Bmal (red) and DAPI (blue). Scale bar, 10μm

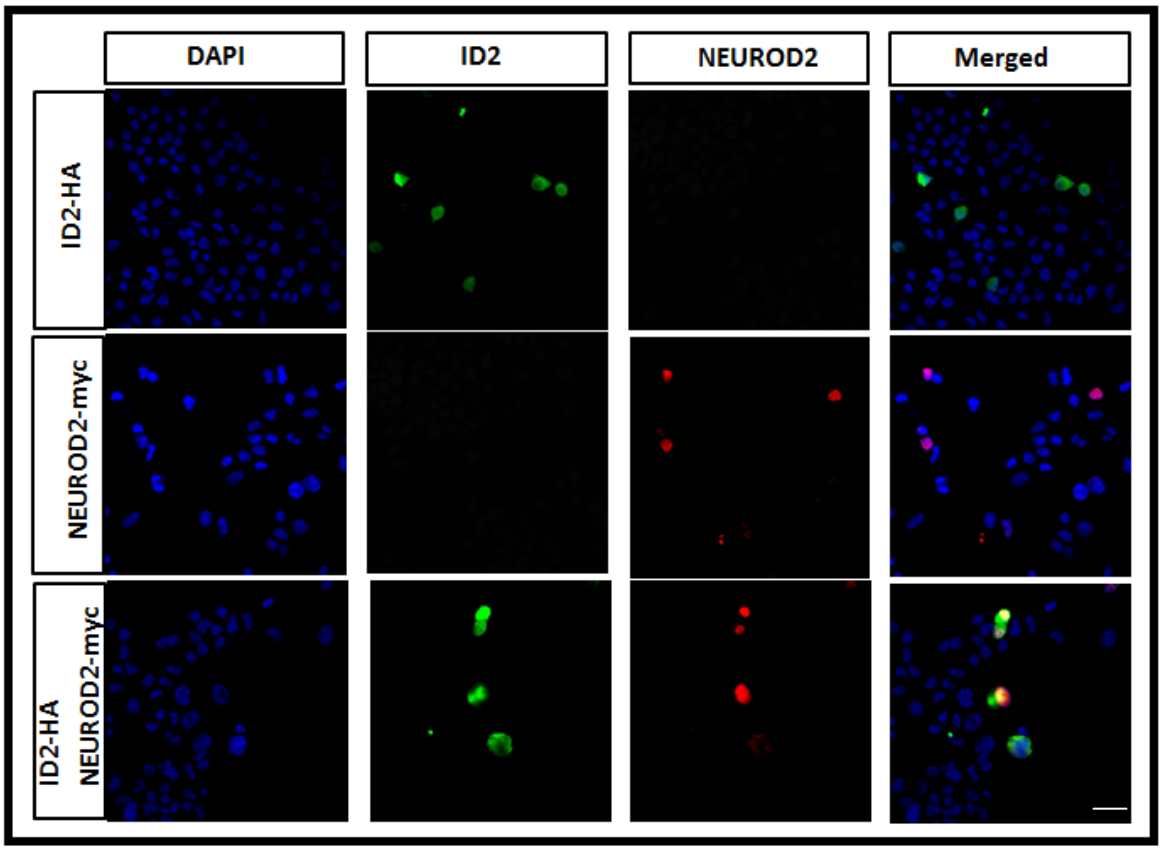

Figure 4.21 Immunofluorescence analysis of co-localization and expression of Id2-HA and NeuroD2-myc in Neuro2a cell line. Neuro2a cell line was co-transfected with Id2-HA and NeuroD2-myc constructs and immunostained with anti-HA and anti-myc antibodies. Id2 (green), NeuroD2 (red) and DAPI (blue). Scale bar, 10μm

4.17 Co-localization and expression of NeuroD2 and Id2 in primary cortical neurons

Next, we detected the localization and expression of endogenous Id2 and NeuroD2 in embryonic primary cortical cultures. I cultured E14 primary cortical neurons and fixed them at different time points at 1,3,5,7 div. Then, I did co-immunostaining with anti-NeuroD2 and anti-ID2 antibodies. DAPI was used to stain nuclei (Figure 4.22). My

immunofluorescence results revealed that NeuroD2 was expressed in the nucleus while Id2 localized both nucleus and cytoplasm of the cell. Also, although these two proteins were co-expressed in the same cells, they were not co-localized.

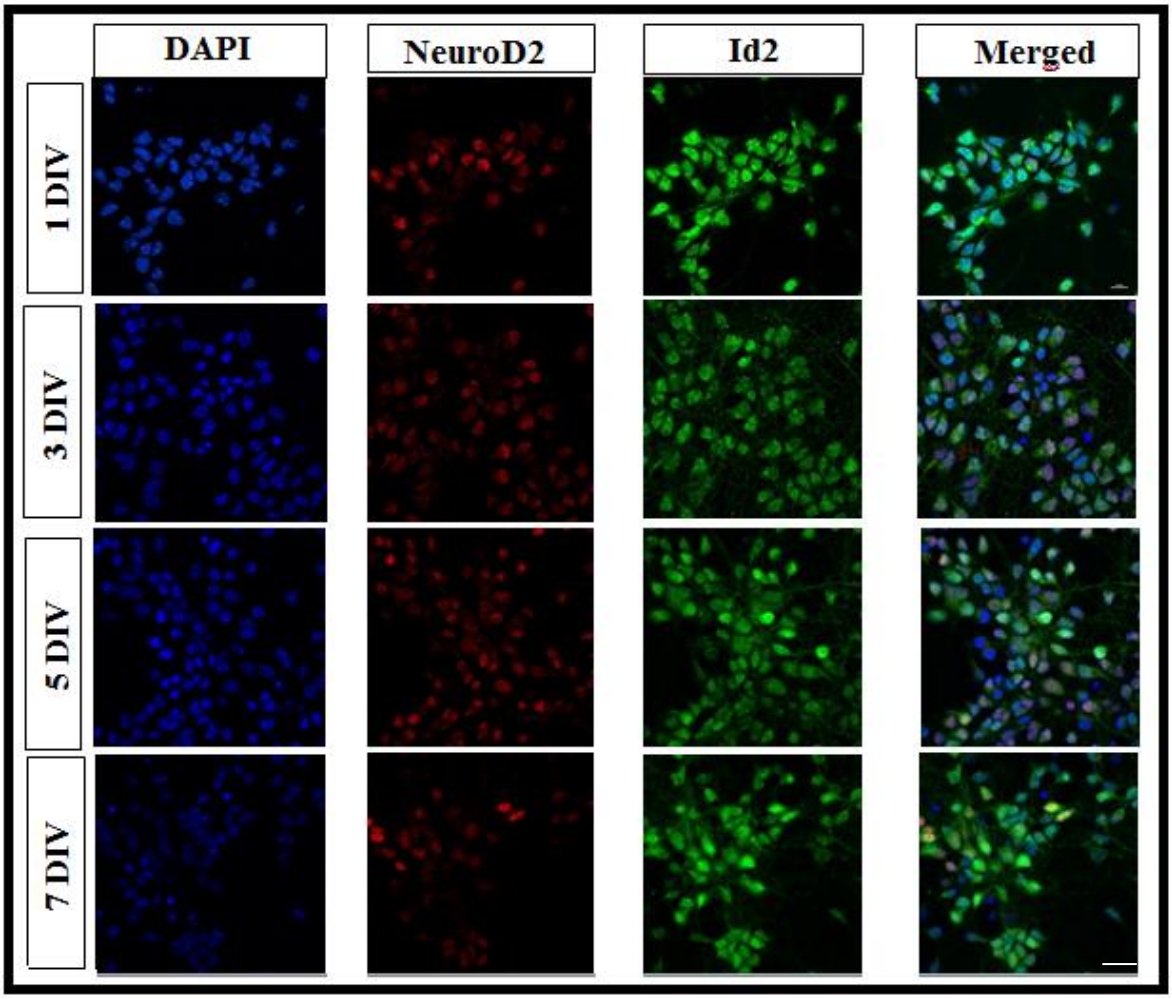

Figure 4.22 Immunofluorescence analysis of co-localization and expression of endogenous Id2 and NeuroD2 in 1,3,5,7 DIV E14 primary cortical neurons. Primary cortical neurons fixed at different time points were immunostained with anti-Id2 and anti-NeuroD2 antibodies. Id2 (green), NeuroD2 (red) and DAPI (blue). Scale bar, 10μm.

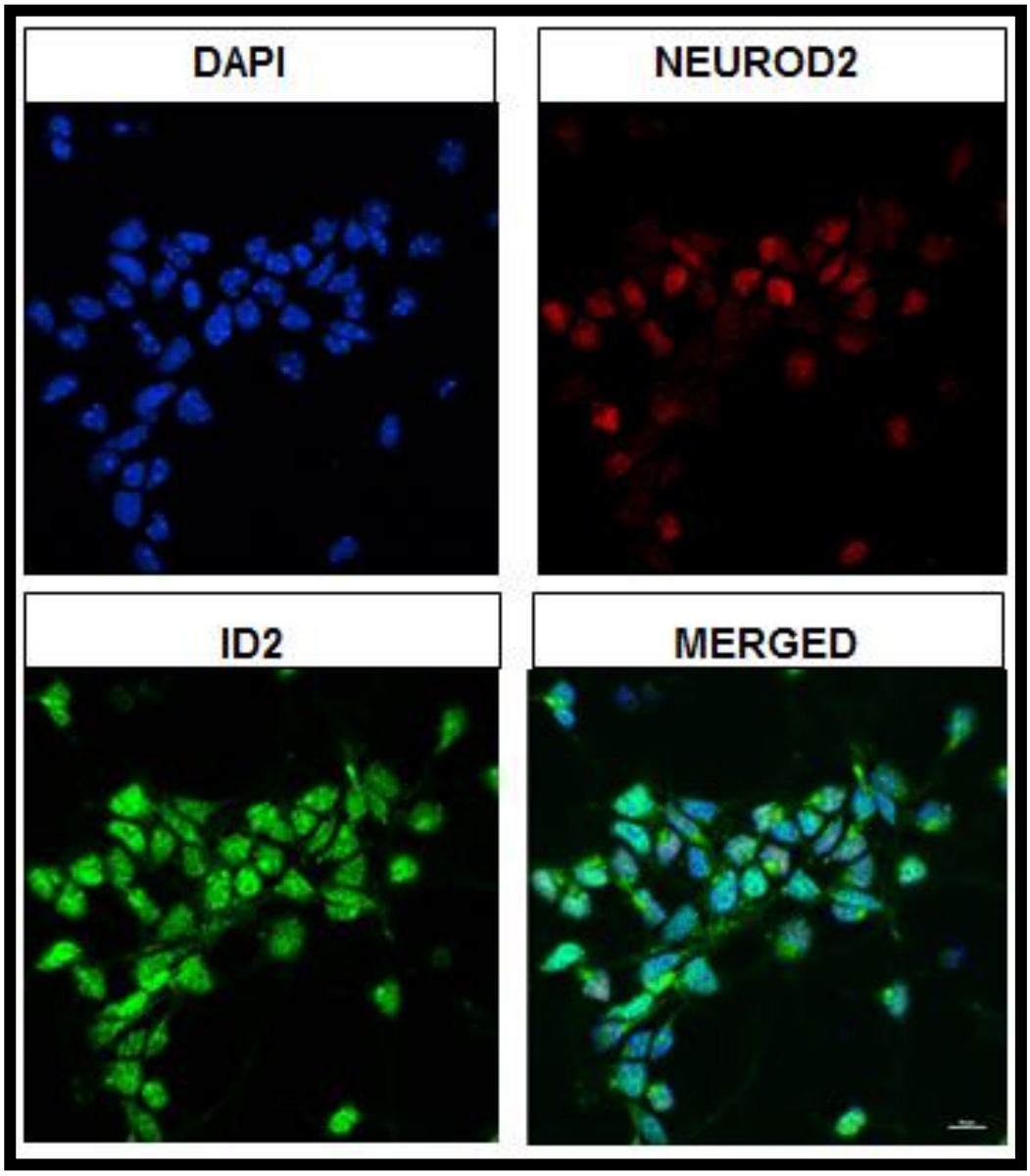

Figure 4.23 Higher magnification of expression of endogenous Id2 and NeuroD2 in 1DIV E14 primary cortical neurons. Scale bar, 10μm.

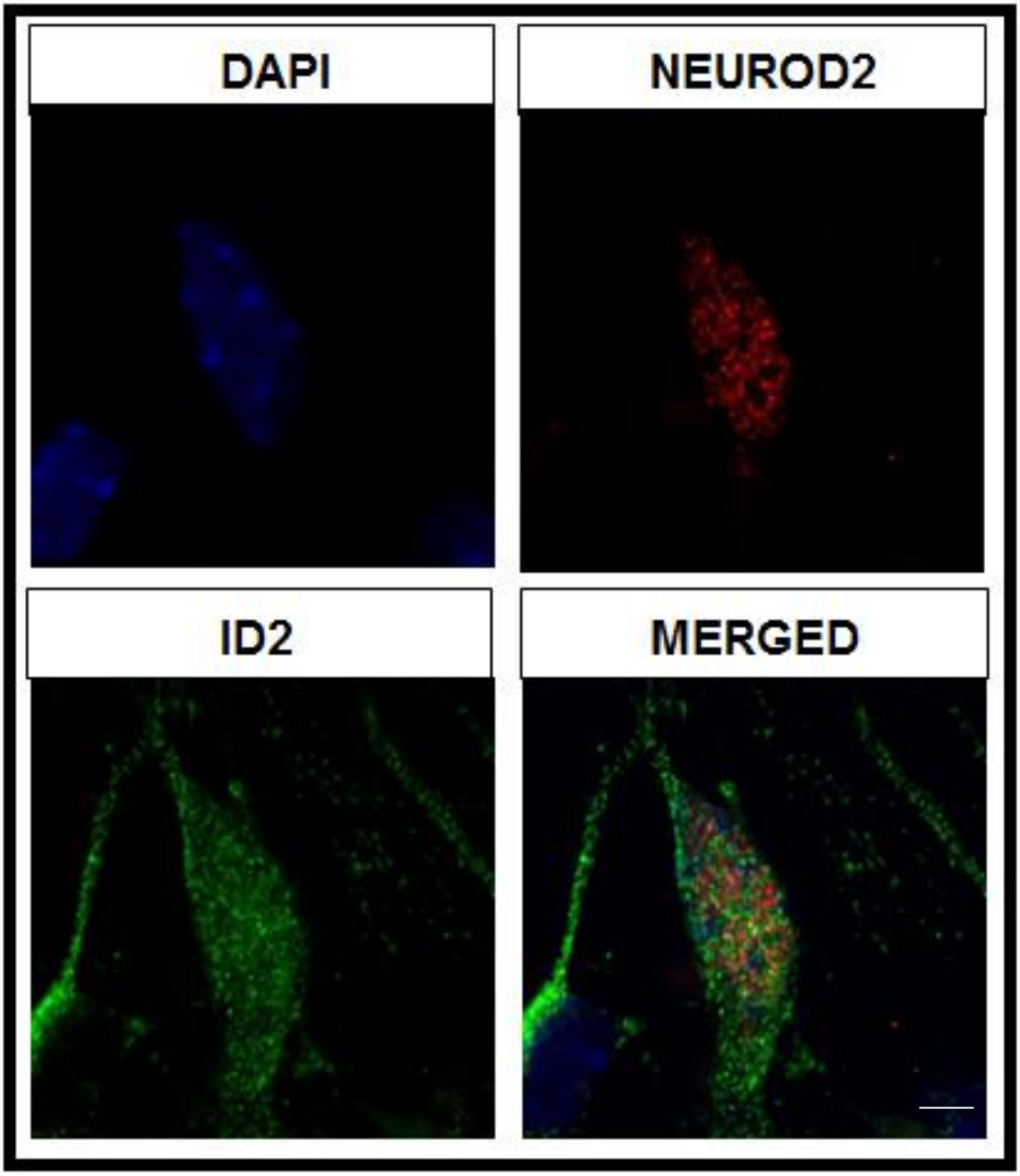

Figure 4.24 Higher magnification of localization of endogenous Id2 and NeuroD2 in 1DIV E14 primary cortical neuron. Scale bar, 10μm.

4.18 Expression of Id2 in NeuroD2 knockdown primary cortical neurons

In order to determine whether NeuroD2 was required for the expression of Id2, we first quantified its mRNA level by RT-qPCR after knockdown of NeuroD2 in embryonic primary cortical neurons. Our RT-qPCR results indicated that there was no change in the mRNA level of Id2 in NeuroD2 knockdown samples compared to wild-type (Figure 4.25).

In addition, we collected cell lysates of NeuroD2 knockdown E14 primary cortical neurons and did western blot to display the change at the protein level of Id2. The blot was incubated with anti-Id2 antibody and stripped to detect whether NeuroD2 was knocked down successfully and beta-actin was expressed for loading control (Figure 4.26). The results showed that NeuroD2 knockdown did not affect protein level of Id2 in primary cortical neurons.

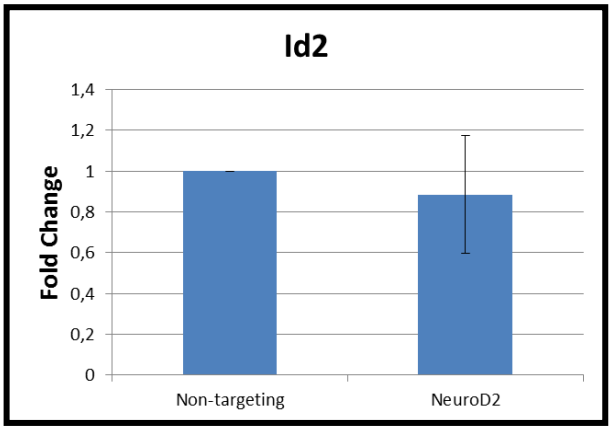

Figure 4.25 mRNA levels of *Id2* in NeuroD2 knocked down primary neurons. Reverse transcription and q-PCR analysis shows no reduction in mRNA levels of *Id2* gene. Data represents three biological and each has three technical replicates. Data is presented as fold change of control sample . A non-targeting shRNA was used as control. Bars are standard error of mean.

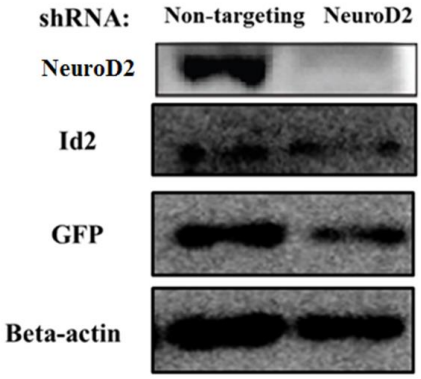

Figure 4.26 Western Blot analysis of Id2 expression in non-targeting and NeuroD2 shRNA transfected E14 primary cultures. The blot was incubated with anti-Id2, anti-GFP and anti-Beta-actin antibodies separately. Id2 was expressed both in E14 primary cortical neurons transfected with non-targeting and NeuroD2 shRNA.

4.19 Interaction between Id2 and NeuroD2

After showing that there was no co-localization between Id2 and NeuroD2 by immunofluorescence, we wanted to verify this result by co-immunoprecipitation (Co-IP). Therefore, we transfected Neuro2a cell line with Id2-pcDNA3-HA/FLAG and NeuroD2-pcDNA4-myc vectors and we collected cell lysates two days after transfection. We did immunoprecipitation with anti-myc antibody and western blot with anti-HA. Moreover, the cell lysates were immunoprecipitated with anti-HA antibody and after running on SDS-gel and the transfers, the blot was incubated with anti-myc antibody (Figure 4.27). Our Co-IP results demonstrated that NeuroD2 and Id2 do not interact with each other biochemically.

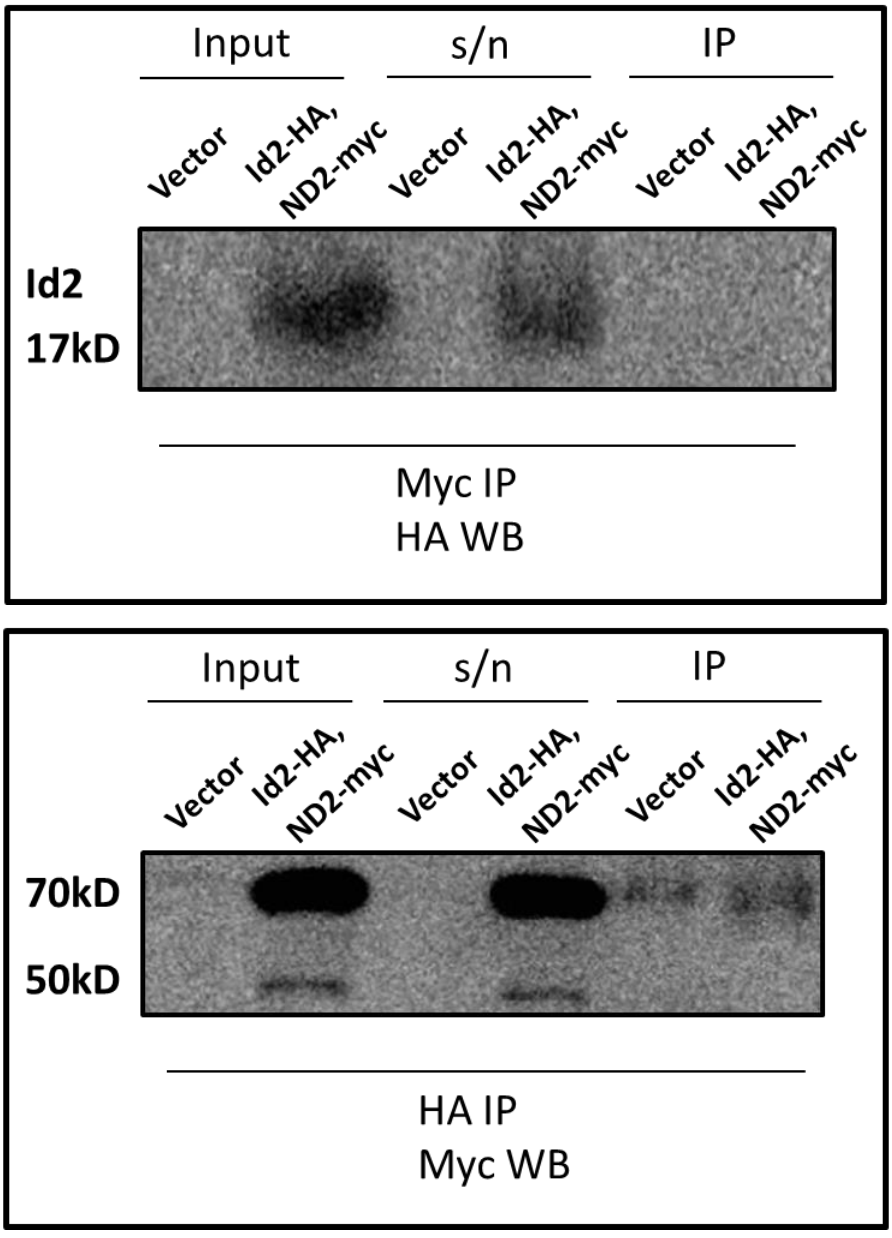

Figure 4.27 Co-immunoprecipitation of NeuroD2 and Id2 proteins. Co-immunoprecipitation was performed with two different antibodies. No association of Id2 with NeuroD2 was detected. (NeuroD2: 50kD and Id2: 17kD)

Chapter 5

DISCUSSION

This study reveals the analysis of binding profiles of NeuroD2 transcription factor along the genome as revealed by a previous Chromatin Immunoprecipitation followed by sequencing (ChIP-Seq) experiment conducted in our laboratory and identifies NeuroD2's mechanism of action in major pathways. The findings are important because NeuroD2 regulates a set of genes which function in neuronal migration, cortical layer identity, synaptogenesis, axonal path finding and dendritogenesis.

First, I demonstrated that the knockdown of NeuroD2 does not affect the dendrite morphology in primary cortical neuronal cultures. Moreover, I tested the requirement for NeuroD2 in individual calcium activated pathways. I chose CaM Kinase IV since its function in dendrite development is shown by several studies. I found that overexpression of the constitutively active form of CaM Kinase IV does not change the dendrite numbers and branches in NeuroD2 knocked down cultures compared to non-targeting shRNA transfected ones. A study showing the role of NeuroD2 in dendrite development displayed that oleic acid treatment of neurons provides the upregulation of NeuroD2 and growth of dendrites [26]. Another previous study demonstrated that development of dendrite arbors needs NeuroD2 (Ince Dunn, unpublished). They showed that dendritic growth and branching patterns dramatically decrease in *NeuroD2* knock out cortical neurons compared

to wild type neurons. In addition, they revealed the activation of NeuroD2 mediated transcription by CaM Kinase IV and requirement of NeuroD2 in CaM Kinase IV stimulated dendrite development. However, my results are not consistent with the findings that NeuroD2 required for CaM Kinase IV stimulated dendrite development. There may be some reasons due to the differences between knockout and knockdown conditions. Since NeuroD2 is continuously absent in knockout conditions, cells are affected by this absence much more easily. On the other hand, knockdown is an acute manipulation and it needs much more time to influence some developmental processes in the cell. In addition, there may be secondary effects of knockout conditions causing improper dendrite morphology. Taken together, it would be good to examine whether CaM Kinase IV directly regulate NeuroD2 by phosphorylating resulting that this regulation induces NeuroD2 activity in dendrite development. Also, other calcium activated pathways would be tested to control the function of NeuroD2 in dendrite morphology regulation.

I next analyzed the mechanism by which NeuroD2 regulates the expression of *Id2* gene. *Id2* is identified as a target gene of NeuroD2 by ChIP-Seq analysis conducted in our laboratory. I confirmed the enrichment in the promoter region of *Id2* gene due to NeuroD2 binding. Then, I tested whether NeuroD2 is necessary for the regulation of Id2 and whether there is a direct interaction between these two proteins. My results showed that the mRNA and protein levels of Id2 are not changed in NeuroD2 knocked down primary cortical neurons compared to wild-type neurons. Moreover, NeuroD2 and Id2 proteins do not directly interact with each other based on co-immunoprecipitation experiment and also they do not co-localized in the neurons by co-immunofluorescence. Id2 functions in the regulation of cell cycle, cell proliferation and differentiation. Wang et al. indicated that premature oligodendrocyte differentiation increase in the absence of Id2 in cultured precursor cells [68]. Microarray analysis from a previous study compared *NeuroD2*

knockout and wild-type cortical tissue and identified *Id2* as a being potential downstream target (Ince Dunn, unpublished). Furthermore, they supported this finding by demonstrating the dramatic decrease for the RNA level of Id2 in northern blot and *in-situ* hybridization results. I was not able to show the decrease in the mRNA and protein level of *Id2* in NeuroD2 knocked down conditions. This inconsistency might be due to weak effects of NeuroD2 knockdown in a restricted time scale. As I mentioned above, knockout is more effective process than the knockdown. Since NeuroD2 is completely deleted, the other genes regulated by NeuroD2 are altered in a fast manner. However, knockout of NeuroD2 might cause some secondary and non-specific effects in the cell that might lead to downregulation of other genes. Therefore, It would be good to examine the mRNA level of Id2 in NeuroD2 knocked down neurons that are cultured much longer after transfection.

Next I confirmed the genome-wide targets of NeuroD2 transcription factor both in embryonic and postnatal stages identified by a ChIP-Seq approach achieved by our laboratory. To have better understanding of function of NeuroD2 transcription factor through its direct target genes, gene ontology database DAVID was used. For the embryonic stage, my results revealed that NeuroD2 targets key components that play role in Reelin signaling, a pathway that control the migration of neurons to locate in the proper places of cortical layers. In addition, I found that NeuroD2 binds to promoter regions of a large set of genes that are responsible for cortical layer identity and axonal guidance. For the postnatal stage, my analysis illustrated that target genes of NeuroD2 regulate major pathways such as Wnt and mTOR signaling pathways. Furthermore, NeuroD2 targets genes most significantly involved in synapse formation.

A total explanation of NeuroD2 function comes to light after a complete understanding of its downstream targets. ChIP-Seq analysis from a previous study investigated genome-

wide targets of NeuroD2 using viral transduction in P19 cell line [62]. However, since this study was conducted in cell line, it might hard to reveal the accurate in vivo targets of NeuroD2 during cortical development. Therefore, genome-wide targets of NeuroD2 and their biological importance were largely unknown. Our laboratory analyzed the ChIP-Seq results of NeuroD2 by using ClosestGene method which give scores to each gene based on the number of associated peaks and their closeness to transcription start site [9] and selected putative target genes for confirmation. After high rate of confirmation, we identified top 1,045 genes for further analyses [9].

Our analysis revealed that Reelin pathway is one of the most targeted pathways of NeuroD2 transcription factor. *Fyn, Cdk5r1, Dab1* and *Lrp8* genes included in this pathway were identified as the target genes of NeuroD2 [9]. I also showed that NeuroD2 is necessary for the expression of both *Cdk5r1* and *Lrp8*. Reelin signaling has been suggested to be involved in several brain diseases. The expression of Reelin protein dramatically decreases in schizophrenia and bipolar disorder [70]. Also, total lack of reelin leads to lissencephaly, a rare brain formation disorder caused by defective neuronal migration. Reelin signaling also plays role in Alzheimer's disease and autism [71]. However, the causes of all these observations remain uncertain. Since our results strongly support NeuroD2 regulation of Reelin signaling pathway, NeuroD2 might have important roles in the formation of these diseases. It would be very interesting to investigate the functions of NeuroD2 and its targets by knocking them down during neuronal migration to show that they might be key regulators of mamalian brain development.

Consistent with a laminar positioning deficiency of postnatal neurons of *NeuroD2/6* double knockouts [56], *NeuroD6* is one of the most strongly targeted genes with *NeuroD2* gene expression and is confirmed to be a direct target gene of NeuroD2.

Neurons generated in the ventricular zone start to migrate through the intermediate zone and differentiate into future cortical projection neurons [27]. Previous studies illustrated that NeuroD2 is an effector transcription factor required for the neuronal differentiation. However, the entire mechanism controlled by NeuroD2 was not clear. In addition, the genetic programs of some layer specific transcription factors that regulate cortical projection neurons are still not fully understood. Based on our results, we hypothesized that NeuroD2 has an essential role in axon guidance of these cortical projection neurons by controlling layer specific transcription factors. We showed that NeuroD2 directly regulates both deep and upper layer markers of the neocortex. *Fezf2, Ctip2, Tbr1* are the deep layer markers that I confirmed as the targets of NeuroD2 while *Cux1* and *Satb2* are the upper layer markers. The layers of the cortex are created in an inside-out order; so later born neurons migrate radially into the cortical plate past the deep layer neurons, and become the upper layers [57]. *Fezf2* and its major downstream effector *Ctip2* regulate extension of axons toward subcortical targets. In *Fezf2* knockout neurons, the fate of callosal projection neurons is assessed by the acquisition of *Satb2* expression suggesting that deep and the upper layers are regulated differentially [72]. I asked how NeuroD2 targets both deep and upper layer neuronal markers while their regulation works in an opposite manner. The layer specific transcription factors might not be regulated at the same time which means that while NeuroD2 controls the deep layer markers, the upper layer marker promoters might be poised by NeuroD2. Furthermore, *Satb2* and *Tbr1* come out to be crucial for neurodevelopmental disorders like mental retardation and sleeping sickness [73]. In addition, *Tbr1* controls the development of dendritic arborization and spines of pyramidal neurons [74]. Taken together, it would be interesting to analyze the expression of these target genes and the kind of developmental processes they are required for. Also, NeuroD2 regulated *Tbr1* regulation on dendrite development would be investigated.

Given the confirmed target genes we were able to identify at postnatal stage, two major pathways are revealed: Wnt and mTOR signaling. Wnt signaling plays a critical role in the embryonic development, cell differentiation, cell proliferation and migration [75]. I confirmed *Fzd4, Fzd8, Fzd9, Dvl3* as the direct targets of NeuroD2. The secretion of Wnt proteins from neurons is regulated by synaptic activity. Therefore, it is expected that Wnt signaling contributes to the pathogenesis of disorders associated with abnormal neuronal activity. Consistent with its role in synaptic plasticity, some studies showed the regulatory function of Wnt signaling in learning and memory. Alzheimer's disease, the pathology of memory deficiency, occurs due to the abnormalities of the Wnt pathway [75]. In addition to the regulation of memory formation, recent findings suggested an association between Wnt signaling and psychiatric disorders. Peng et al. revealed the involvement of Wnt signaling in schizophrenia, while Zhang et al. showed their work on the contribution of Wnt signaling to autism. Since Wnt signaling is an important regulator of various neurological disorders, it would be significant to target NeuroD2 and its several components of this signaling pathway might lead to the development of novel drugs to treat the disorders.

The mechanistic target of rapamycin (mTOR) signaling pathway is a crucial cellular signaling hub that regulates the growth control, protein synthesis, gene expression, and metabolic balance [76]. *Eif3a, Tsc1, Rsb6kb1* and *Pkd1* are the key components of mTOR pathway that were listed in our ChIP-Seq analyses. The dysfunction of mTOR pathway is implicated in autism, epilepsy, and neurodegenerative disorders [76]. Early embryonic activation of this pathway causes the microcephaly whereas in post-mitotic neurons, the activity of mTOR leads to cortical hypertrophy. It also destroys the cortical lamination which is a neurodegeneration with inclusion bodies containing ubiquitinated proteins [77]. In addition, it has been shown that Wnt and mTOR pathways are associated with each other by the control of *Gsk3* and *Tsc1* proteins. Therefore, it would be very interesting to

examine the mechanism between these two major pathways whether they are regulated by NeuroD2.

Further supporting the information obtained from gene ontology, Stim1 protein was identified as the top target gene. Also, I demonstrated decrease in mRNA level of *Stim1* in NeuroD2 knocked down primary cultures. Stim1 mediates Ca+2 influx through store-operated Ca+2 channels by sensing decreased Ca+2 level in the ER [64]. Calcium influx is essential to regulate synaptic transmittance and activity. Since NeuroD2 is also calcium-regulated protein, there might be a mechanism by which NeuroD2 regulate Stim1 activity. Therefore, it would be good to examine their functions and interactions with each other.

In summary, the confirmations of direct target genes of NeuroD2 transcription factor at the stage embryonic day 14 and postnatal day 0 are reported in this study. I confirmed target gene binding and target gene expression regulation by ChIP-PCR and RT-PCR, respectively. The results demonstrated that NeuroD2 is the key regulator of major developmental pathways. It also controls the mechanisms of target genes playing role in neuronal migration, cortical layer identity, and axon pathfinding and synapse formation.

Future Aspect

To examine and understand the functional relationship between NeuroD2 and its target genes, in utero electroporation experiment will be performed. Non-targeting and Neurod2 shRNAs will be electroporated into embryonic mouse cortex and followed by primary neuronal cultures to detect the role of target genes during neuronal migration. In addition, immunofluorescent staining on coronal sections will be carried out to mark the neurons that completed their migration and settled down cortical plate. RNA-Seq analysis will be conducted to identify the genes that are affected by the knock down of NeuroD2 in primary cortical neurons and the candidate genes will be further confirmed by RT-qPCR. NeuroD2 mediated transcription is activated by calcium signaling and its target genes should be identified upon neuronal activity in primary neuronal cultures. The target genes of ChIP-Seq data that play role in major pathways will be further confirmed and tested to identify their functions.

BIBLIOGRAPHY

[1] a R. Desai and S. K. McConnell, “Progressive restriction in fate potential by neural progenitors during cerebral cortical development.,” *Development*, vol. 127, no. 13, pp. 2863–2872, 2000.

[2] K. M. Bishop, G. Goudreau, and D. D. O’Leary, “Regulation of area identity in the mammalian neocortex by Emx2 and Pax6.,” *Science*, vol. 288, no. 5464, pp. 344–349, 2000.

[3] J. E. Lee, “Basic helix-loop-helix genes in neural development,” *Curr. Opin. Neurobiol.*, vol. 7, no. 1, pp. 13–20, 1997.

[4] M. B. McCormick, R. M. Tamimi, L. Snider, a Asakura, D. Bergstrom, and S. J. Tapscott, “NeuroD2 and neuroD3: distinct expression patterns and transcriptional activation potentials within the neuroD gene family.,” *Mol. Cell. Biol.*, vol. 16, no. 10, pp. 5792–5800, 1996.

[5] L. de la Torre-Ubieta and A. Bonni, “Transcriptional Regulation of Neuronal Polarity and Morphogenesis in the Mammalian Brain,” *Neuron*, vol. 72, no. 1, pp. 22–40, 2011.

[6] S. V Puram and A. Bonni, “Cell-intrinsic drivers of dendrite morphogenesis.,” *Development*, vol. 140, no. 23, pp. 4657–71, 2013.

[7] B. Martynoga, D. Drechsel, F. Guillemot, A. Ochoa-espinosa, M. Affolter, A. Fedoriw, and J. Mugford, “Molecular Control of Neurogenesis : A View from the Mammalian Cerebral Cortex Molecular Control of Neurogenesis : AView from the Mammalian Cerebral Cortex,” 2013.

[8] M. E. Massari and C. Murre, “Helix-loop-helix proteins: regulators of transcription in eucaryotic organisms.,” *Mol. Cell. Biol.*, vol. 20, no. 2, pp. 429–440, 2000.

[9] Bayam et al., “Genome-wide target analysis of NeuroD2 reveals new insights into regulation of cortical projection neuron identity,” *BMC Genomics*, 2015.

[10] S. K. McConnell, “Constructing the cerebral cortex: neurogenesis and fate determination.,” *Neuron*, vol. 15, no. 4, pp. 761–768, 1995.

[11] M. Götz and W. B. Huttner, “The cell biology of neurogenesis.,” *Nat. Rev. Mol. Cell Biol.*, vol. 6, no. 10, pp. 777–788, 2005.

[12] E. Taverna, M. Götz, and W. B. Huttner, *The Cell Biology of Neurogenesis: Toward an Understanding of the Development and Evolution of the Neocortex.*, no. June. 2014.

[13] A. Murciano, J. Zamora, J. López-Sánchez, and J. M. Frade, “Interkinetic nuclear movement may provide spatial clues to the regulation of neurogenesis.,” *Mol. Cell. Neurosci.*, vol. 21, no. 2, pp. 285–300, 2002.

[14] E. Aaku-Saraste, B. Oback, A. Hellwig, and W. B. Huttner, “Neuroepithelial cells downregulate their plasma membrane polarity prior to neural tube closure and neurogenesis,” *Mech. Dev.*, vol. 69, no. 1–2, pp. 71–81, 1997.

[15] V. Busskamp, N. E. Lewis, P. Guye, A. H. M. Ng, S. L. Shipman, S. M. Byrne, N. E. Sanjana, J. Murn, Y. Li, and S. Li, “Rapid neurogenesis through transcriptional activation in human stem cells,” pp. 1–22, 2014.

[16] W. B. Huttner and Y. Kosodo, “Symmetric versus asymmetric cell division during neurogenesis in the developing vertebrate central nervous system,” *Curr. Opin. Cell Biol.*, vol. 17, no. 6, pp. 648–657, 2005.

[17] S. C. Noctor, a C. Flint, T. a Weissman, R. S. Dammerman, and a R. Kriegstein, “Neurons derived from radial glial cells establish radial units in neocortex.,” *Nature*, vol. 409, no. 6821, pp. 714–720, 2001.

[18] S. C. Noctor, V. Martínez-Cerdeño, L. Ivic, and A. R. Kriegstein, “Cortical neurons arise in symmetric and asymmetric division zones and migrate through specific phases.,” *Nat. Neurosci.*, vol. 7, no. 2, pp. 136–144, 2004.

[19] I. Imayoshi and R. Kageyama, “bHLH factors in self-renewal, multipotency, and fate choice of neural progenitor cells,” *Neuron*, vol. 82, no. 1, pp. 9–23, 2014.

[20] A. Kriegstein and A. Alvarez-Buylla, “The glial nature of embryonic and adult neural stem cells.,” *Annu. Rev. Neurosci.*, vol. 32, pp. 149–184, 2009.

[21] K. Y. Kwan, N. Sestan, and E. S. Anton, “Transcriptional co-regulation of neuronal migration and laminar identity in the neocortex,” *Development*, vol. 139, no. 9, pp. 1535–1546, 2012.

[22] A. S. Nord, K. Pattabiraman, A. Visel, and J. L. R. Rubenstein, “Review Genomic Perspectives of Transcriptional Regulation in Forebrain Development,” *Neuron*, vol. 85, no. 1, pp. 27–47, 2015.

[23] L. Sussel, O. Marin, S. Kimura, and J. L. Rubenstein, “Loss of Nkx2.1 homeobox gene function results in a ventral to dorsal molecular respecification within the basal telencephalon: evidence for a transformation of the pallidum into the striatum.,” *Development*, vol. 126, no. 15, pp. 3359–3370, 1999.

[24] A. Manuscript, “NIH Public Access,” *Changes*, vol. 29, no. 6, pp. 997–1003, 2012.

[25] B. J. Molyneaux, L. A. Goff, A. C. Brettler, H.-H. Chen, J. R. Brown, S. Hrvatin, J. L. Rinn, and P. Arlotta, “DeCoN: Genome-wide Analysis of In Vivo Transcriptional Dynamics during Pyramidal Neuron Fate Selection in Neocortex,” *Neuron*, vol. 85, no. 2, pp. 275–288, 2015.

[26] F. M. Rodríguez-tornos, B. Cubelos, and M. Nieto, “Cortical Development,” pp. 127–151, 2013.

[27] L. C. Greig, M. B. Woodworth, M. J. Galazo, H. Padmanabhan, and J. D. Macklis, “Molecular logic of neocortical projection neuron specification, development and diversity.,” *Nat. Rev. Neurosci.*, vol. 14, no. 11, pp. 755–69, 2013.

[28] B. Menn, J. M. Garcia-Verdugo, C. Yaschine, O. Gonzalez-Perez, D. Rowitch, and A. Alvarez-Buylla, “Origin of oligodendrocytes in the subventricular zone of the adult brain.,” *J. Neurosci.*, vol. 26, no. 30, pp. 7907–7918, 2006.

[29] P. J. Andres-Barquin, M. C. Hernandez, and M. a. Israel, “Id genes in nervous system development,” *Histol. Histopathol.*, vol. 15, no. 2, pp. 603–618, 2000.

[30] P. Mattar, L. M. Langevin, K. Markham, N. Klenin, S. Shivji, D. Zinyk, and C. Schuurmans, “Basic helix-loop-helix transcription factors cooperate to specify a cortical projection neuron identity.,” *Mol. Cell. Biol.*, vol. 28, no. 5, pp. 1456–1469, 2008.

[31] V. Ledent and M. Vervoort, “The basic helix-loop-helix protein family: Comparative genomics and phylogenetic analysis,” *Genome Res.*, vol. 11, no. 5, pp. 754–770, 2001.

[32] C. Schuurmans and F. Guillemot, “Molecular mechanisms underlying cell fate specification in the developing telencephalon,” *Curr. Opin. Neurobiol.*, vol. 12, no. 1, pp. 26–34, 2002.

[33] S. Willaime-Morawek, R. M. Seaberg, C. Batista, E. Labbé, L. Attisano, J. a. Gorski, K. R. Jones, A. Kam, C. M. Morshead, and D. Van Der Kooy, “Embryonic cortical neural stem cells migrate ventrally and persist as postnatal striatal stem cells,” *J. Cell Biol.*, vol. 175, no. 1, pp. 159–168, 2006.

[34] M. J. Eckler, W. L. Mckenna, S. Taghvaei, S. K. Mcconnell, and B. Chen, “Fezf1 and Fezf2 are required for olfactory development and sensory neuron identity,” *J. Comp. Neurol.*, vol. 519, no. 10, pp. 1829–1846, 2011.

[35] M. H. Farah, J. M. Olson, H. B. Sucic, R. I. Hume, S. J. Tapscott, and D. L. Turner, “Generation of neurons by transient expression of neural bHLH proteins in mammalian cells.,” *Development*, vol. 127, no. 4, pp. 693–702, 2000.

[36] G. Ince-Dunn, B. J. Hall, S. C. Hu, B. Ripley, R. L. Huganir, J. M. Olson, S. J. Tapscott, and A. Ghosh, “Regulation of thalamocortical patterning and synaptic maturation by NeuroD2,” *Neuron*, vol. 49, no. 5, pp. 683–695, 2006.

[37] Q. Ma, C. Fode, F. Guillemot, and D. J. Anderson, “NEUROGENIN1 and NEUROGENIN2 control two distinct waves of neurogenesis in developing dorsal root ganglia,” *Genes Dev.*, vol. 13, no. 13, pp. 1717–1728, 1999.

[38] Y. Sun, M. Nadal-Vicens, S. Misono, M. Z. Lin, A. Zubiaga, X. Hua, G. Fan, and M. E. Greenberg, “Neurogenin promotes neurogenesis and inhibits glial differentiation by independent mechanisms,” *Cell*, vol. 104, no. 3, pp. 365–376, 2001.

[39] S. Li, P. Mattar, R. Dixit, S. O. Lawn, G. Wilkinson, C. Kinch, D. Eisenstat, D. M. Kurrasch, J. a Chan, and C. Schuurmans, “RAS/ERK signaling controls proneural genetic programs in cortical development and gliomagenesis.,” *J. Neurosci.*, vol. 34, no. 6, pp. 2169–90, 2014.

[40] H. Oda, F. Fushimi, M. Kato, M. Kitagawa, K. Araki, N. Seki, and H. Ohkubo, "Microarray analysis of the genes induced by tetracycline-regulated expression of NDRF/NeuroD2 in P19 cells," *Biochem. Biophys. Res. Commun.*, vol. 335, no. 2, pp. 458–468, 2005.

[41] C. H. Lin, J. Stoeck, A. C. Ravanpay, F. Guillemot, S. J. Tapscott, and J. M. Olson, "Regulation of neuroD2 expression in mouse brain," *Dev. Biol.*, vol. 265, no. 1, pp. 234–245, 2004.

[42] P. Mattar, O. Britz, C. Johannes, M. Nieto, L. Ma, A. Rebeyka, N. Klenin, F. Polleux, F. Guillemot, and C. Schuurmans, "A screen for downstream effectors of Neurogenin2 in the embryonic neocortex," *Dev. Biol.*, vol. 273, no. 2, pp. 373–389, 2004.

[43] "Synaptic Activity and the Construction of Cortical Circuits Author (s): L . C . Katz and C . J . Shatz Published by : American Association for the Advancement of Science Stable URL : http://www.jstor.org/stable/2891573," *Adv. Sci.*, vol. 274, no. 5290, pp. 1133–1138, 2009.

[44] H. Aizawa, S.-C. Hu, K. Bobb, K. Balakrishnan, G. Ince, I. Gurevich, M. Cowan, and A. Ghosh, "Dendrite development regulated by CREST, a calcium-regulated transcriptional activator.," *Science*, vol. 303, no. 5655, pp. 197–202, 2004.

[45] L. Redmond, A. H. Kashani, and A. Ghosh, "Calcium regulation of dendritic growth via CaM kinase IV and CREB-mediated transcription," *Neuron*, vol. 34, no. 6, pp. 999–1010, 2002.

[46] T. Noda, R. Kawamura, H. Funabashi, M. Mie, and E. Kobatake, "Transduction of NeuroD2 protein induced neural cell differentiation," *J. Biotechnol.*, vol. 126, no. 2, pp. 230–236, 2006.

[47] J. M. Olson, a Asakura, L. Snider, R. Hawkes, a Strand, J. Stoeck, a Hallahan, J. Pritchard, and S. J. Tapscott, "NeuroD2 is necessary for development and survival of central nervous system neurons.," *Dev. Biol.*, vol. 234, no. 1, pp. 174–187, 2001.

[48] Z. Molnar, "Calcium and NeuroD2 Control," pp. 639–642, 2006.

[49] R. Erzurumlu, "Neural activity: sculptor of barrels in the neocortex," vol. 24, no. 10, pp. 589–595, 2013.

[50] M. C. Crair and R. C. Malenka, “A critical period for long-term potentiation at thalamocortical synapses.,” *Nature*, vol. 375, no. 6529. pp. 325–328, 1995.

[51] H. Nakata and S. Nakamura, “Brain-derived neurotrophic factor regulates AMPA receptor trafficking to post-synaptic densities via IP3R and TRPC calcium signaling,” *FEBS Lett.*, vol. 581, no. 10, pp. 2047–2054, 2007.

[52] S. a Wilke, B. J. Hall, J. K. Antonios, L. a DeNardo, S. Otto, B. Yuan, F. Chen, E. M. Robbins, K. Tiglio, M. E. Williams, Z. Qiu, T. Biederer, and A. Ghosh, “NeuroD2 regulates the development of hippocampal mossy fiber synapses,” *Neural Dev.*, vol. 7, no. 1, p. 9, 2012.

[53] R. Hand, D. Bortone, P. Mattar, L. Nguyen, J. I. T. Heng, S. Guerrier, E. Boutt, E. Peters, A. P. Barnes, C. Parras, C. Schuurmans, F. Guillemot, and F. Polleux, “Phosphorylation of neurogenin2 specifies the migration properties and the dendritic morphology of pyramidal neurons in the neocortex,” *Neuron*, vol. 48, no. 1, pp. 45–62, 2005.

[54] R. Mihrshahi, “The Corpus Callosum as an Evolutionary Innovation,” *J. Exp. Zool. B. Mol. Dev. Evol.*, vol. 306, no. 1, pp. 1–7, 2006.

[55] M. H. Schwab, S. Druffel-Augustin, P. Gass, M. Jung, M. Klugmann, a Bartholomae, M. J. Rossner, and K. a Nave, “Neuronal basic helix-loop-helix proteins (NEX, neuroD, NDRF): spatiotemporal expression and targeted disruption of the NEX gene in transgenic mice.,” *J. Neurosci.*, vol. 18, no. 4, pp. 1408–1418, 1998.

[56] I. Bormuth, K. Yan, T. Yonemasu, M. Gummert, M. Zhang, S. Wichert, O. Grishina, A. Pieper, W. Zhang, S. Goebbels, V. Tarabykin, K.-A. Nave, and M. H. Schwab, “Neuronal basic helix-loop-helix proteins Neurod2/6 regulate cortical commissure formation before midline interactions.,” *J. Neurosci.*, vol. 33, no. 2, pp. 641–51, 2013.

[57] B. J. Molyneaux, P. Arlotta, J. R. L. Menezes, and J. D. Macklis, “Neuronal subtype specification in the cerebral cortex.,” *Nat. Rev. Neurosci.*, vol. 8, no. 6, pp. 427–437, 2007.

[58] C.-H. Lin, S. Hansen, Z. Wang, D. R. Storm, S. J. Tapscott, and J. M. Olson, “The dosage of the neuroD2 transcription factor regulates amygdala development and

emotional learning.," *Proc. Natl. Acad. Sci. U. S. A.*, vol. 102, no. 41, pp. 14877–14882, 2005.

[59] S. M. Rodrigues, G. E. Schafe, and J. E. Ledoux, "Molecular mechanisms underlying emotional learning and memory in the lateral amygdala," *Neuron*, vol. 44, no. 1, pp. 75–91, 2004.

[60] D. L. Maier, S. Mani, S. L. Donovan, D. Soppet, L. Tessarollo, J. S. McCasland, and K. F. Meiri, "Disrupted cortical map and absence of cortical barrels in growth-associated protein (GAP)-43 knockout mice.," *Proc. Natl. Acad. Sci. U. S. A.*, vol. 96, no. 16, pp. 9397–9402, 1999.

[61] Y. Konishi, N. Ohkawa, Y. Makino, H. Ohkubo, R. Kageyama, T. Furuichi, K. Mikoshiba, and T. Tamura, "Transcriptional regulation of mouse type 1 inositol 1,4,5-trisphosphate receptor gene by NeuroD-related factor.," *J. Neurochem.*, vol. 72, no. 4, pp. 1717–1724, 1999.

[62] A. P. Fong, Z. Yao, J. W. Zhong, N. M. Johnson, G. H. Farr, L. Maves, and S. J. Tapscott, "Conversion of MyoD to a Neurogenic Factor: Binding Site Specificity Determines Lineage," *Cell Rep.*, vol. 10, no. 12, pp. 1937–1946, 2015.

[63] Z. Huang, "Molecular regulation of neuronal migration during neocortical development," *Mol. Cell. Neurosci.*, vol. 42, no. 1, pp. 11–22, 2009.

[64] G. Bai, N. Sheng, Z. Xie, W. Bian, Y. Yokota, R. Benezra, R. Kageyama, F. Guillemot, and N. Jing, "Id Sustains Hes1 Expression to Inhibit Precocious Neurogenesis by Releasing Negative Autoregulation of Hes1," *Dev. Cell*, vol. 13, no. 2, pp. 283–297, 2007.

[65] S.-H. Ghil, Y.-J. Jeon, and H. Suh-Kim, "Inhibition of BETA2/NeuroD by Id2.," *Experimental & molecular medicine*, vol. 34, no. 5. pp. 367–373, 2002.

[66] S. Jung, R.-H. Park, S. Kim, Y.-J. Jeon, D.-S. Ham, M.-Y. Jung, S.-S. Kim, Y.-D. Lee, C.-H. Park, and H. Suh-Kim, "Id proteins facilitate self-renewal and proliferation of neural stem cells.," *Stem Cells Dev.*, vol. 19, no. 6, pp. 831–841, 2010.

[67] B. J. Martinsen and M. Bronner-Fraser, "Neural crest specification regulated by the helix-loop-helix repressor Id2.," *Science*, vol. 281, no. 5379, pp. 988–991, 1998.

[68] S. Wang, A. Sdrulla, J. E. Johnson, Y. Yokota, and B. a. Barres, “A role for the helix-loop-helix protein Id2 in the control of oligodendrocyte development,” *Neuron*, vol. 29, no. 3, pp. 603–614, 2001.

[69] S. M. Ward, S. J. Fernando, T. Y. Hou, and G. E. Duffield, “The transcriptional repressor ID2 can interact with the canonical clock components CLOCK and BMAL1 and mediate inhibitory effects on mPer1 expression,” *J. Biol. Chem.*, vol. 285, no. 50, pp. 38987–39000, 2010.

[70] M. Shimabukuro, T. Sasaki, A. Imamura, T. Tsujita, C. Fuke, T. Umekage, M. Tochigi, K. Hiramatsu, T. Miyazaki, T. Oda, J. Sugimoto, Y. Jinno, and Y. Okazaki, “Global hypomethylation of peripheral leukocyte DNA in male patients with schizophrenia: A potential link between epigenetics and schizophrenia,” *J. Psychiatr. Res.*, vol. 41, no. 12, pp. 1042–1046, 2007.

[71] J. Mill, “Toward an integrated genetic and epigenetic approach to Alzheimer’s disease,” *Neurobiol. Aging*, vol. 32, no. 7, pp. 1188–1191, 2011.

[72] E. a. Alcamo, L. Chirivella, M. Dautzenberg, G. Dobreva, I. Fariñas, R. Grosschedl, and S. K. McConnell, “Satb2 Regulates Callosal Projection Neuron Identity in the Developing Cerebral Cortex,” *Neuron*, vol. 57, no. 3, pp. 364–377, 2008.

[73] S. Deborggraeve, V. Lejon, R. A. Ekangu, D. M. Ngoyi, P. P. Pyana, M. Ilunga, J. P. Mulunda, and P. Büscher, “Diagnostic accuracy of pcr in gambiense sleeping sickness diagnosis, staging and post-treatment follow-up: A 2-year longitudinal study,” *PLoS Negl. Trop. Dis.*, vol. 5, no. 2, pp. 1–7, 2011.

[74] K. R. Maynard and E. Stein, “DSCAM contributes to dendrite arborization and spine formation in the developing cerebral cortex.,” *J. Neurosci.*, vol. 32, no. 47, pp. 16637–50, 2012.

[75] Y. Komiya and R. Habas, “Wnt signal transduction pathways.,” *Organogenesis*, vol. 4, no. 2, pp. 68–75, 2008.

[76] J. O. Lipton and M. Sahin, “The Neurology of mTOR,” *Neuron*, vol. 84, no. 2, pp. 275–291, 2014.

[77] H. Kassai, Y. Sugaya, S. Noda, K. Nakao, T. Maeda, M. Kano, and A. Aiba, “Selective Activation of mTORC1 Signaling Recapitulates Microcephaly, Tuberous

Sclerosis, and Neurodegenerative Diseases," *Cell Rep.*, vol. 7, no. 5, pp. 1626–1639, 2014.

VITA

Gizem Güzelsoy was born on 14.06.1989, in Istanbul, Turkey. She received her major BSc degree in Molecular Biology and Genetics from Middle East Technical University (METU), Ankara in 2013. From September 2013 to September 2015 she worked as teaching and research assistant at Koç University. She worked on “Genome-wide target analysis of NEUROD2 transcription factor reveals potential roles in cortical migration and layer formation” during her MSc studies.

Appendix A: Generation of lentiviruses

NeuroD2 shRNA's were provided from pGIPZ lentiviral constructs (Figure A.1, Thermo Scientific Open Biosystems). HEK293T cells were needed for lentiviral particle production. HEK293T cells were split in proliferating state up to 9th or 10th passages. 4.5 millions of HEK293T cells were plated in 8 ml DMEM (Sigma Life Sciences, Cat. #D5671) containing 10% FBS, 1% P/S, 0.5% L-glutamine and 1mM Sodium-pyruvate per 100-mm plates. Next day, they are co-transfected with 225ng of VSV-G, 2250ng of GaqPol viral vectors and 2500ng lentiviral DNA of interest in 1.5ml OptiMEM and 30µ Lipofectamine reagent in 1.5ml OptiMEM. The media was sucked and 8ml OPTIMEM with (10%FBS, Lipofectamine and viral particles) was added very slowly into plate. After 12h incubation at 37°C, OPTiMEM was aspirated and fresh HEK media was put again very slowly into the plates and they were incubated for 48-72h at 37°C.

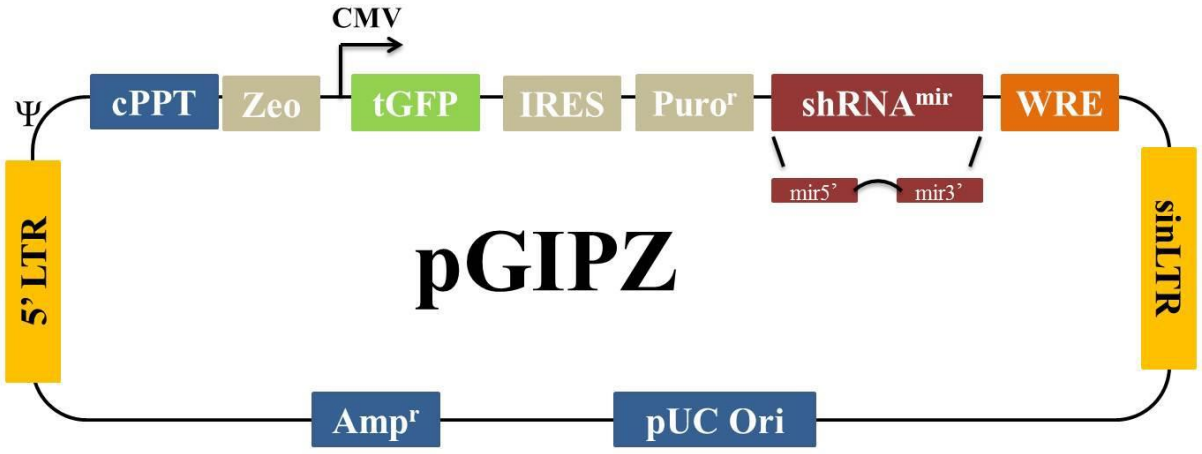

Figure A.1 pGIPZ lentiviral vector

48-hours later, cells were analyzed under fluorescence microscope to detect the transfection efficiency. Since the vector of shRNAs contains TurboGFP gene, transfected HEK293T cells were expected to be TurboGFP positive. After that, the medium of the plates were collected into 50-ml falcon tubes which mean that first harvesting. New fresh 8ml HEK media was added immediately and slowly onto the plates for additional 24hours incubation. After collection of second harvests, HEK293T cells were bleached and disposed. Harvested media were centrifuged at 1400 rpm for 5 minutes at 4°C and the supernatants were filtered through 0.45μm filters to new 50-ml falcon tubes. 50% (w/v) PEG in 1X PBS were added onto media to 20% (v/v) final concentration. The tubes were rotated 10 times to mix the media and PEG properly. These virus containing media were stored at 4°C for two days. Precipitates were observed at the bottom of the 50-ml falcon tubes. They were centrifuged at 2500 rpm for 20 minutes at 4°C. The supernatants were aspirated until 5ml media left in the tube. Then, the tubes were again centrifuged at 1500rpm for 5 min at 4°C. Rest of the media was sucked as much as possible. The pellets were dissolved by cold and sterile 1X PBS to make concentrated viruses. Then, they were aliquot in desired volume for further use and stored at -80°C immediately.

Appendix B: Viral Transduction of Primary Cortical Cultures

To find the most efficient condition of viral transduction, we tried three different conditions. After several experiments, we chose condition 1 which was applied after primary neuronal culture preparation (Figure A.2-A.6). Neurons were plated onto coated plates with BF media. Two hours later, BF media was changed with BNBF and desired amounts of viruses along with 6mg/ml polybrene were added onto cultures. After 5 hours, virus containing media were aspirated, wells were washed with BME twice and fresh BNBF were added. The media of culture were replenished in 1:1 ratios in every two days

until they were collected for further analyses. Western Blot analysis was performed and quantified by Image J software.

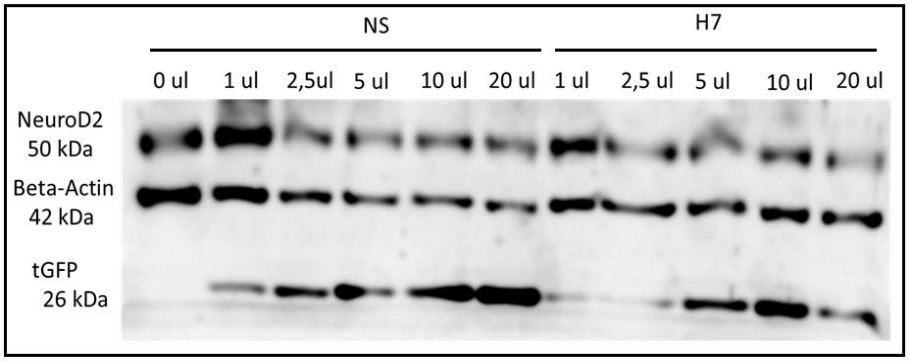

Figure A.2 Non-silencing (NS) and NeuroD2 shRNA (H7) containing viral construct transduction of 4 DIV E14 primary cortical neurons.

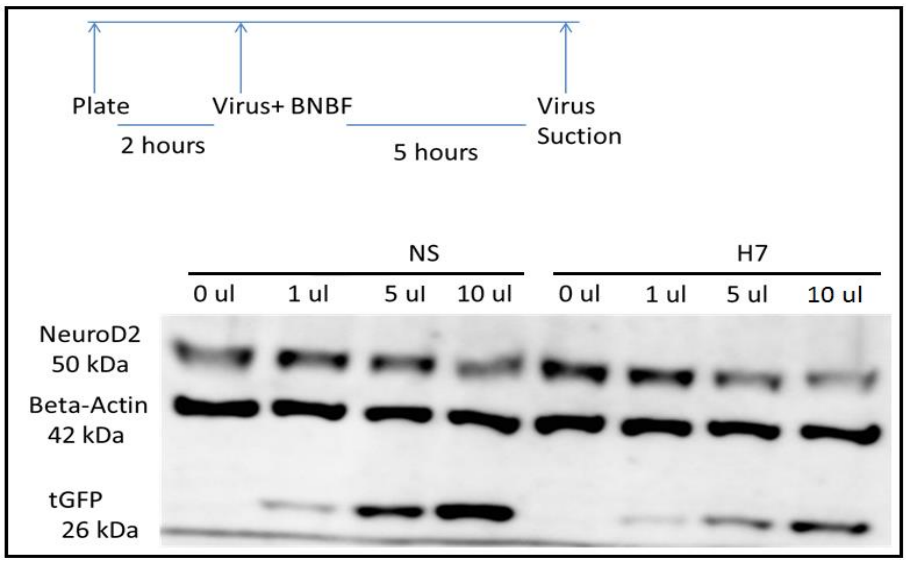

Figure A.3 Condition 1: Non-silencing (NS) and NeuroD2 shRNA (H7) containing viral construct transduction of 4 DIV E14 primary cortical neurons.

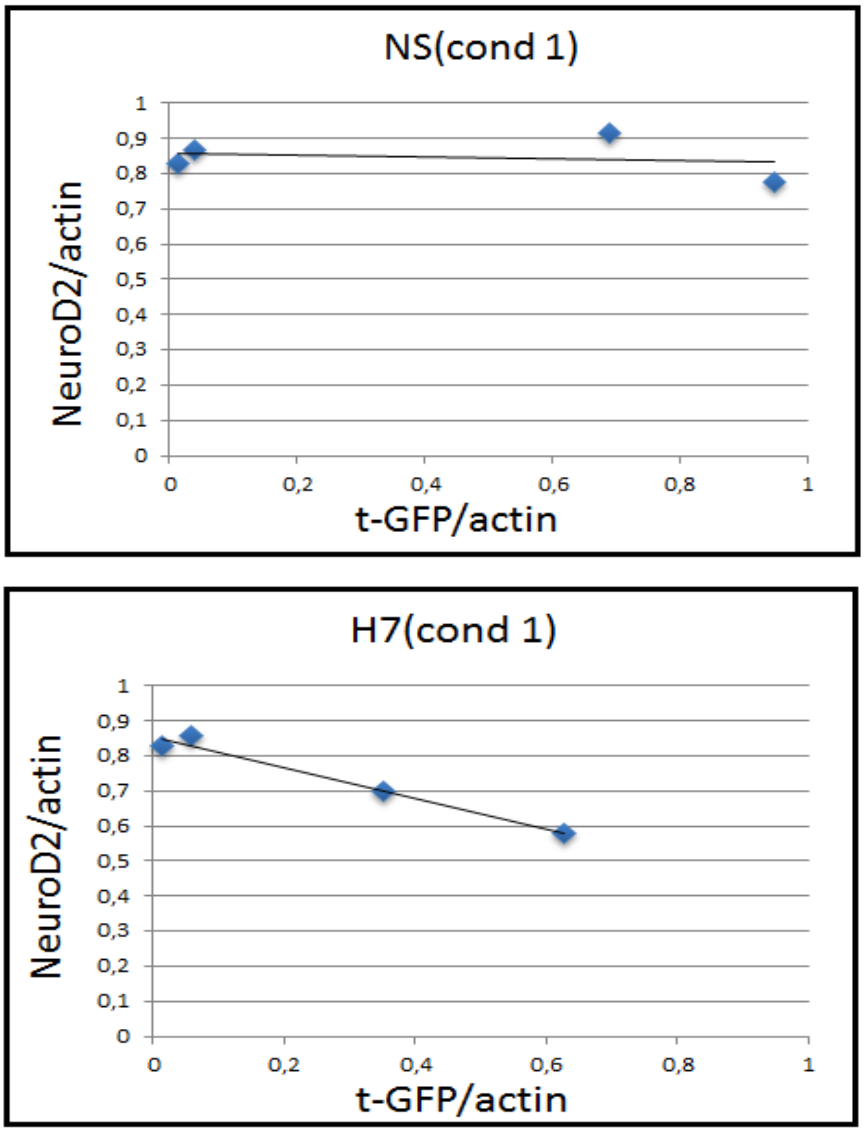

Figure A.4 Quantification of Western Blot analysis of Condition 1.

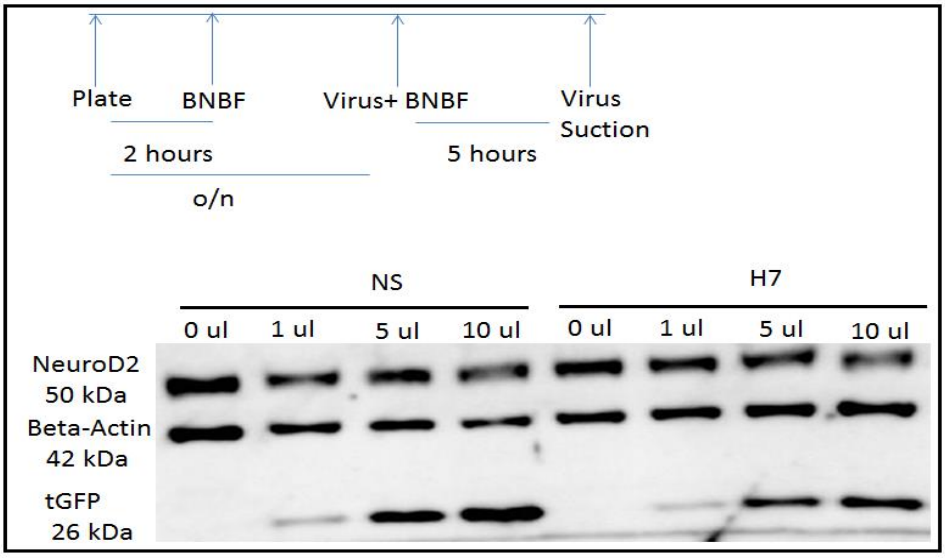

Figure A.5 Condition 2: Non-silencing (NS) and NeuroD2 shRNA (H7) containing viral construct transduction of 4 DIV E14 primary cortical neurons.

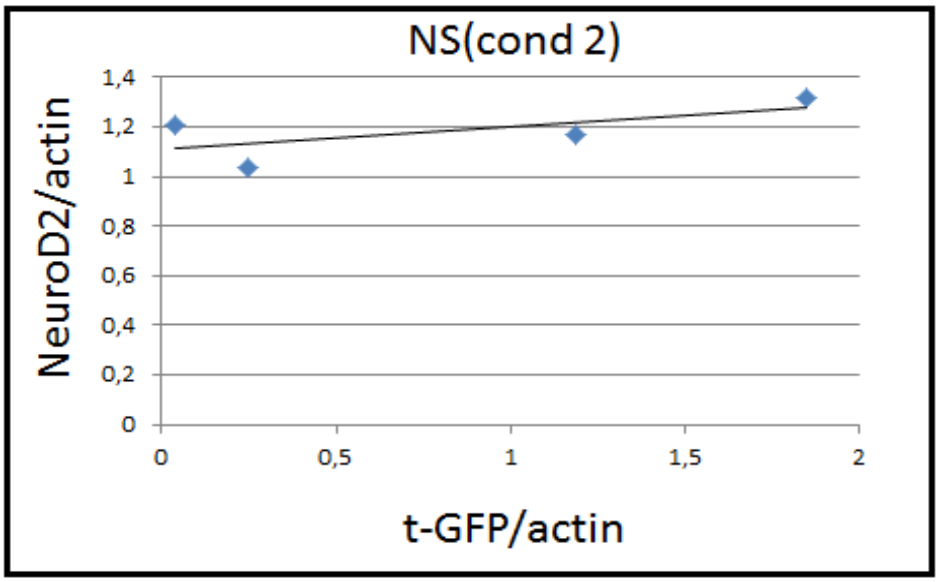

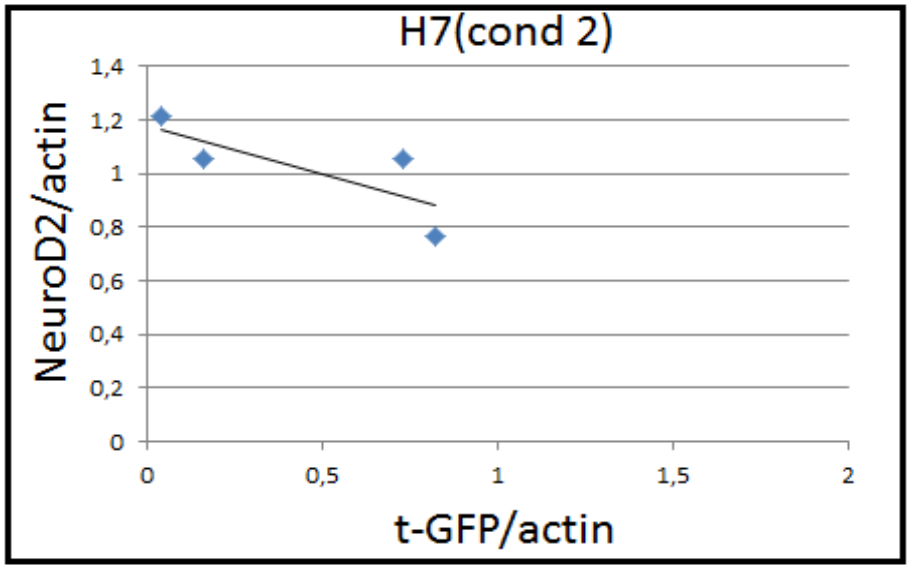

Figure A.6 Quantification of Western Blot analysis of Condition 2.

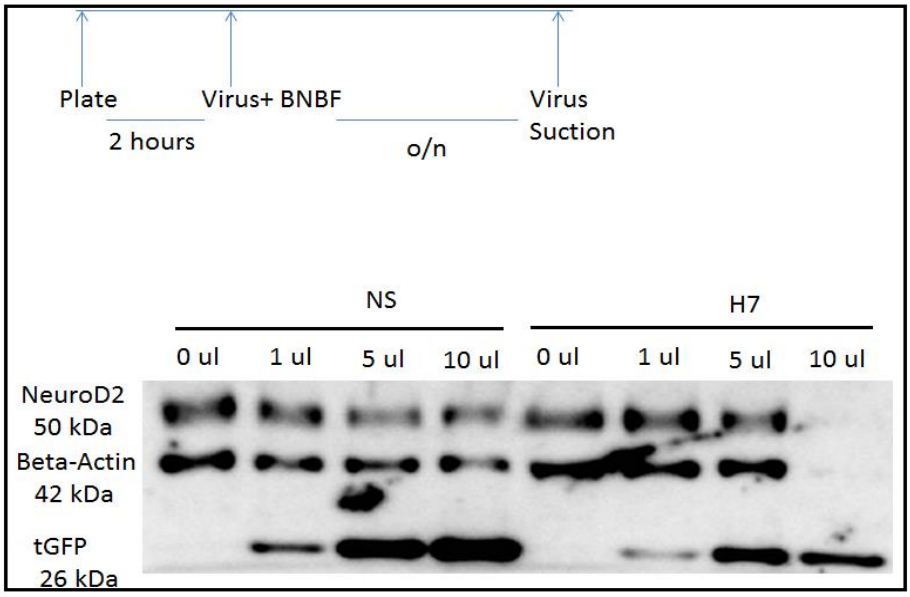

Figure A.7 Condition 3: Non-silencing (NS) and NeuroD2 shRNA (H7) containing viral construct transduction of 4 DIV E14 primary cortical neurons.

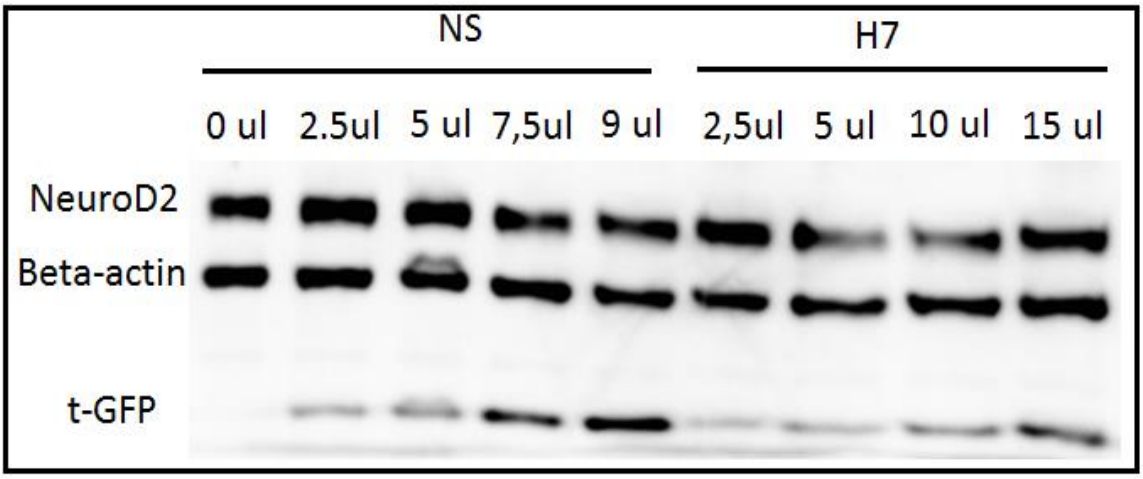

Figure A.8. Non-silencing (NS) and NeuroD2 shRNA (H7) containing viral transduction of 5 DIV E14 primary cortical neurons.

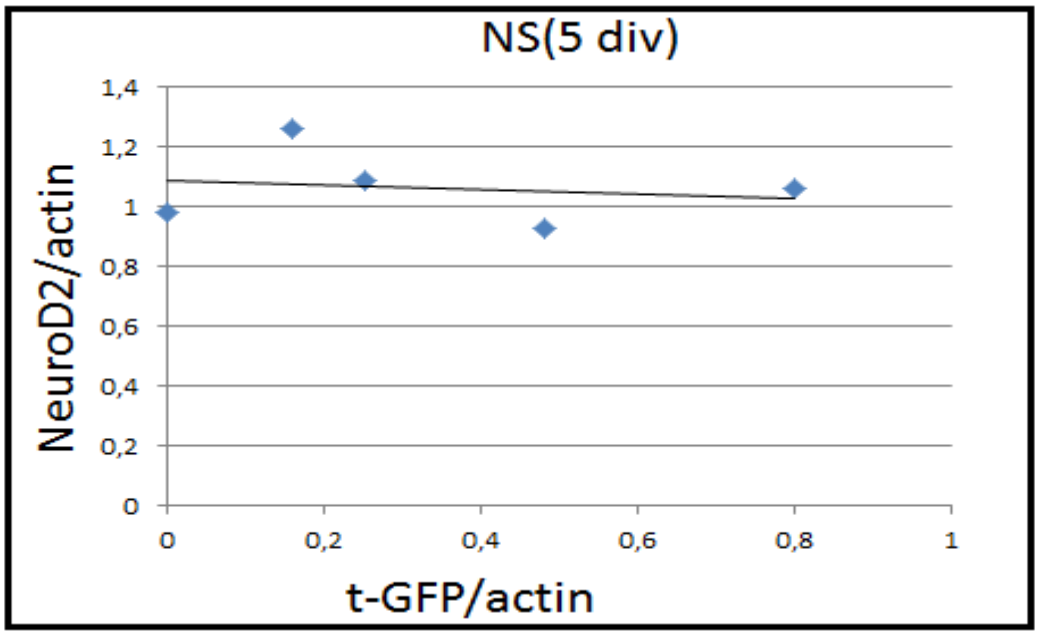

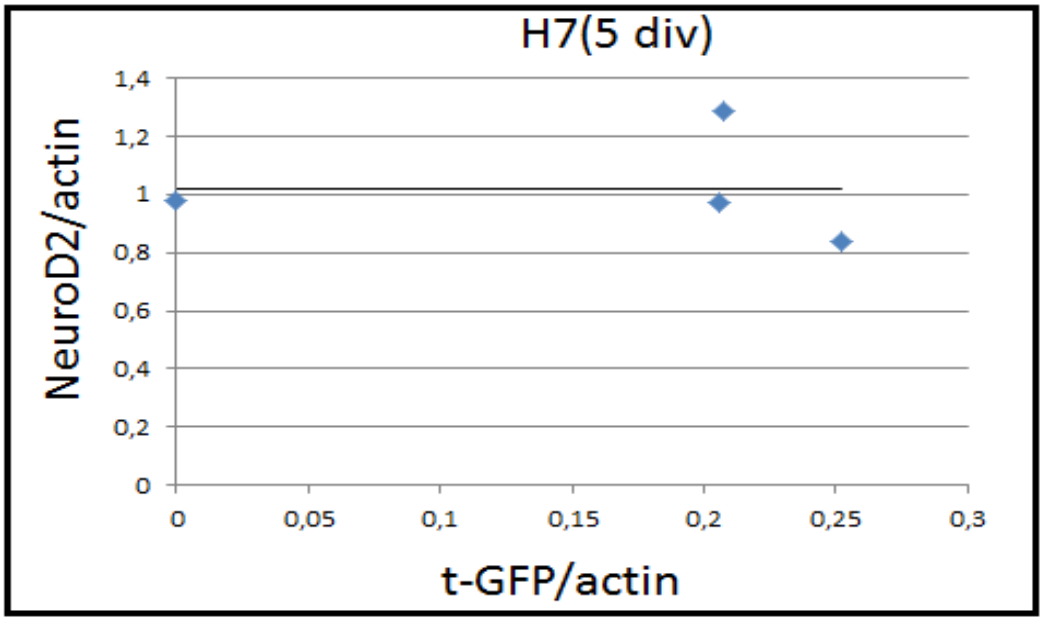

Figure A.9 Quantification of Western Blot analysis of 5 DIV E14 primary neurons.

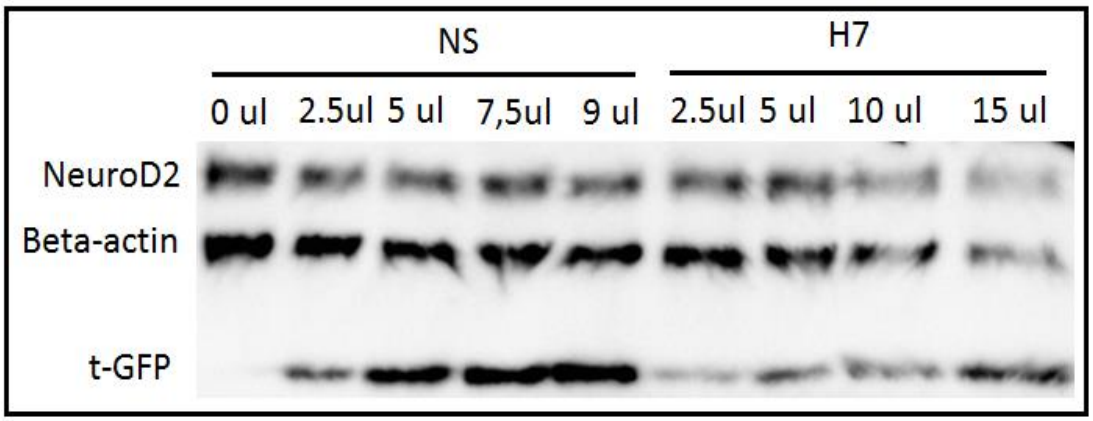

Figure A.10 Non-silencing (NS) and NeuroD2 shRNA (H7) containing viral construct transduction of 7 DIV E14 primary cortical neurons.

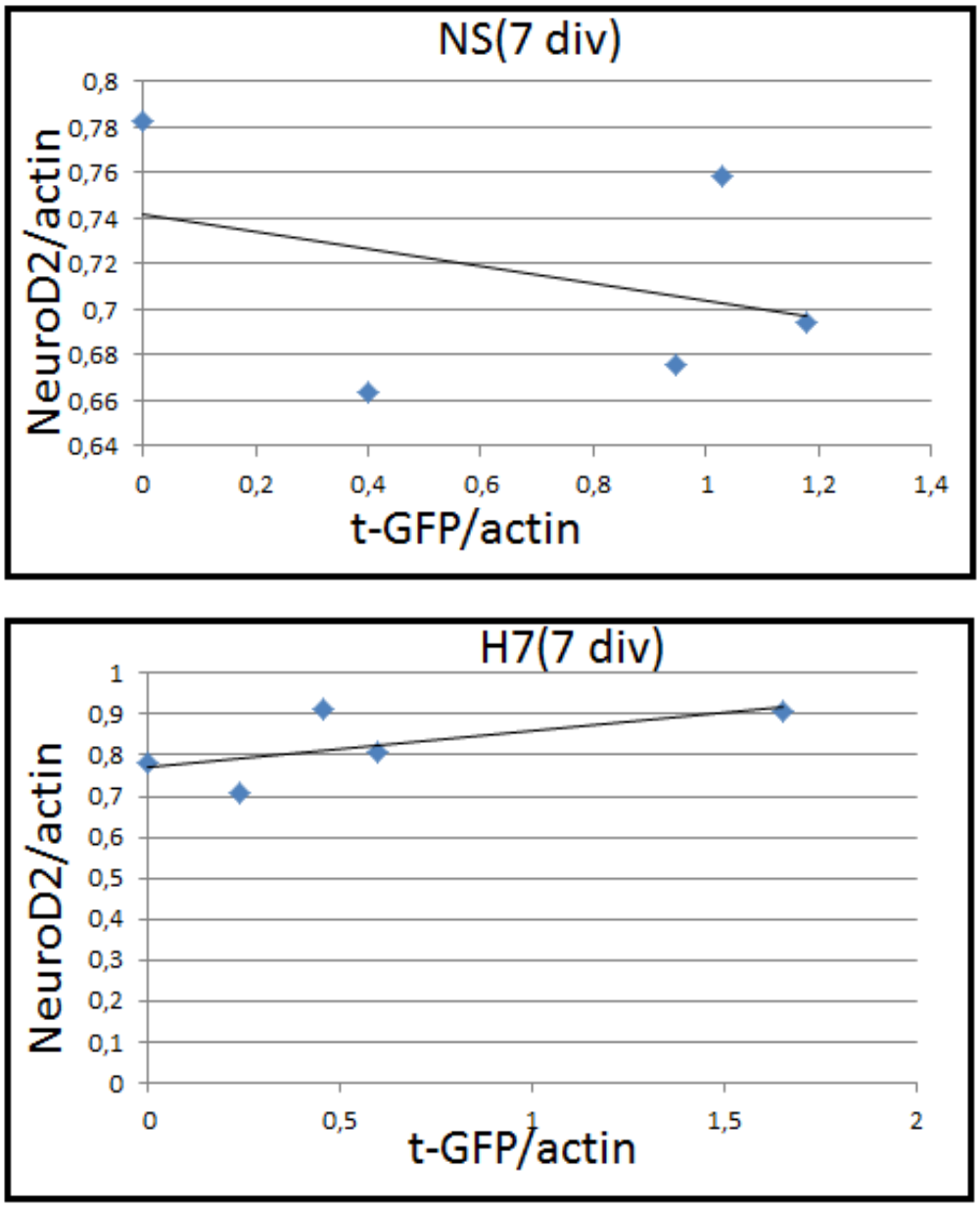

Figure A.11 Quantification of Western Blot analysis of 7 DIV E14 primary neurons.

Appendix C : Primer List

Primer Name	**Primer Sequence**
Id2-BamHI-F	5’-TCTAAGCTTATGAAAGCCTTCAGTCCGGTGAGG -3’
Id2-XhoI-R	5’-AAACTCGAGGCCACAGAGTACTTTGCTATCATTCG-3’
Id2-QPCR-F	5’-ATGAACGACTGCTACTCCAAGCTC-3’
Id2-QPCR-R	5’-TGCAAGGACAGGATGCTGATG-3’
Id2up-ChIP-F	5’-AATTGGAATAAGGCGGGCAC-3’
Id2up-ChIP-R	5’-CAGGCGAATTCTCCCATTGG -3’
Id2down-ChIP-F	5’-GAGAGAACAAGTTGCTGCCC-3’
Id2down-ChIP-R	5’-CCAGGGTGAAAGAATTGACTG-3’
NeuroD6- ChIP-F	5’-AACAGTTGCACCATTGGCAG-3’
NeuroD6- ChIP-R	5’-GCACTGATCATCTGGCATCC-3’
NeuroD6-QPCR-F	5’-CCCTCAGTTTGAAGGTCCCT-3’
NeuroD6-QPCR-R	5’-GATTGGCTGCGCAGATGTAA-3’
Nrcam-ChIP-F	5’-AAGCTTCGGAAACACGCAC-3’
Nrcam-ChIP-R	5’-GGCTCCTTGTTCTGCTCCAG-3’
Bhlhe22-ChIP-F	5’-GCCACACATGTCAAGCTAAAG-3’
Bhlhe22-ChIP-R	5’-GCCGCGAGTCTGAATAGTTTC-3’
Dvl3-ChIP-F	5’-GCGAGACCAAGATCATCTACC-3’
Dvl3-ChIP-R	5’-CAGAACGCCCTTAAAGTCCG-3’
Fzd4-ChIP-F	5’-CTCCGGACGTCTGATATCCC-3’
Fzd4-ChIP-R	5’-CTGCTCCCAACTCCGGATAG-3’
Fzd8-ChIP-F	5’-GCCACAACCCCTTCTTTAGC-3’
Fzd8-ChIP-R	5’-CGTTCCGGGTACTTAAAGCG-3’

Fzd9-ChIP-F	5’-CGCATGCCCAACCTACTG-3’
Fzd9-ChIP-R	5’-CTGGGATGGGAGTGGAGAC-3’
Dlx2-ChIP-F	5’-GACGGTTGCCTCCTTTCTTG-3’
Dlx2-ChIP-R	5’-GTCGAGTGCATATCAGCCAC-3’
Dlx2-QPCR-F	5’-TACTACACCAACCAGCAGCA-3’
Dlx2-QPCR-R	5’-TCGGATTTCAGGCTCAAGGT-3’
Gsx2-ChIP-F	5’-CAAAAGCCAGTTCTCTCCCG-3’
Gsx2-ChIP-R	5’-GGCTGGTGATGGTGATGATG-3’
Stim1-ChIP-F	5’-GTCCTGCTGCTGACTATGTG-3’
Stim1-ChIP-R	5’-CTAACCCTTTGCCCCTAACC-3’
Stim1-QPCR-F	5’-CCTCTCTTGACTCGGCATAATC-3’
Stim1-QPCR-R	5’-GACCTTCTCTACTTCCACAGTTC-3’
Lrp8-ChIP-F	5’-GTGAGTCTCCTTCTCCCGAG-3’
Lrp8-ChIP-R	5’-CATGATCCTGCTCTGTGTGC-3’
Lrp8-QPCR-F	5’-CTTGGTGTGGAGATGCGATG-3’
Lrp8-QPCR-R	5’-GTCCGCAGCTTAACTTCTCG-3’
Cdk5r1-ChIP-F	5’-GGAAGGCCACACTGTTTGAG-3’
Cdk5r1-ChIP-R	5’-CTTCTTCGCTGACACCGC-3’
Eif3a-ChIP-F	5’-CACGTGGTTCCTTCCTTTCC-3’
Eif3a-ChIP-R	5’-GGAAATAGGCCGGCATCTTG-3’
Eif3a-QPCR-F	5’-AAGACCCAGGGATGAAGGTG-3’
Eif3a-QPCR-R	5’-GAGCTTGCTTCTTCTCGCTC-3’
Rps6kb1-ChIP-F	5’-CCGGAGCTGAACTTGAGGAG-3’
Rps6kb1-ChIP-R	5’-CAAACACTCCTGCCATGTCC-3’
Rps6kb1-QPCR-F	5’-GCTTTTACCTAGCGCCTGAC-3’

Rps6kb1-QPCR-R	5’-GGCCCTCTGTTCACACTAGT-3’
Pkd1-ChIP-F	5’-CTCAACAGCCAGAGGACTTC-3’
Pkd1-ChIP-R	5’-CTTGAAGGTGGAGGAAGCTC-3’
Pkd1-QPCR-F	5’-CCATCTACCACCCACACCTT-3’
Pkd1-QPCR-R	5’-ATTGGTACCTTCAGCCAGCT-3’
Tsc1-ChIP-F	5’-GACTTCTTTCGGCCTCCTTC-3’
Tsc1-ChIP-R	5’-GAGTCTCAGCCTCTCCAGAC-3’
Tsc1-QPCR-F	5’-TGGTCCATCTTCATGCCAGT-3’
Tsc1-QPCR-R	5’-TGGTCCTTGGATCCAGTCAC-3’
Tbr1-ChIP-F	5’-GTCTAGTGAGGGGTCTGTGG-3’
Tbr1-ChIP-R	5’-CAAGACAAGCTCAGATCCGC-3’
Tbr1-QPCR-F	5’-GGAGCCCCTTTCTACCAGTT-3’
Tbr1-QPCR-R	5’-AAAAGGGAAACATGCGCCTT-3’
Satb2-ChIP-F	5’-GTTTCAGACAGACCGTGAGC-3’
Satb2-ChIP-R	5’-GCGAAAGATGTAGGGAGTGC-3’
Satb2-QPCR-F	5’-AGCAGTTGGATGGCTCTCTT-3’
Satb2-QPCR-R	5’-GATTATTCCTTGGGCCTGCG-3’
Fezf2-ChIP-F	5’-GCTCTTTCAGTGCCCAGTTC-3’
Fezf2-ChIP-R	5’-TGCCCTGGGACTATGAAAGG-3’
Fezf2-QPCR-F	5’-TCCAAGACGCTGCTCAGTTA-3’
Fezf2-QPCR-R	5’-GTAGTAGAGAGAGCCGCTGG-3’
Ctip2-ChIP-F	5’-CCAGAGCTGATACCCTGGAG-3’
Ctip2-ChIP-R	5’-TCTCCTCCTTTTCCCTCTGC-3’
Ctip2-QPCR-F	5’-ACATTCCTCTGAGAACGGCA-3’
Ctip2-QPCR-R	5’-CGCAGTACTCACATGTGTCG-3’

Cux1-ChIP-F	5’-GGTGACCGATAGCTTGCATC-3’
Cux1-ChIP-R	5’-AGTCTCCTTACAGTCCAGCG-3’
Cux1-QPCR-F	5’-ACCCTTTCTCCTCCTTCAGC-3’
Cux1-QPCR-R	5’-TCACTCCATGCCAGCTTGTA-3’
Tle1-ChIP-F	5’-GGCGGGATTCAAGTTGGAAG-3’
Tle1-ChIP-R	5’-CCGTCTAGACATCCAGTGGG-3’
Gapdh-QPCR-F	5’-CGACTTCAACAGCAACTCCCACTCTTCC-3’
Gapdh-QPCR-R	5’-TGGGTGGTCCAGGGTTTCTTACTCCTT-3’
Gad1-ChIP-F	5’-CCAGGGATCGTGCAAGCAA-3’
Gad1-ChIP-R	5’-GTGGTCTTGGGGTCTCTACG-3’
Calb2-ChIP-F	5’-ATGCGGGTAGGTATGCTTCG-3’
Calb2-ChIP-R	5’-CAGGGCGTTAGCTTGAAGGA-3’

Appendix D: CaM Kinase IV induced dendrite development in primary cortical neurons

I decided to test whether NeuroD2 play role in candidate kinase pathways to activate the dendritic growth. CaM Kinase IV was chosen since its role in dendrite development has been well documented [45]. In order to display that constitutively active form of CaM kinase IV was expressed successfully in primary cortical neurons, I transfected E14 cortical neurons with pcDNA4-myc and constitutively active CaM KinaseIV-pcDNA4-myc constructs at 2 DIV, collected cell lysates at 4 DIV and performed western blot with anti-myc antibody. Our results demonstrated that the construct were transfected and expressed successfully in primary cortical neurons (Figure A.12).

After confirmation of constituvely active form of CaM Kinase IV, we again cultured E14 primary cortical neurons and tranfected them with constituvely active form of CaM Kinase IV along with non-targeting shRNA, NeuroD2 shRNA and resistant form of NeuroD2 constructs at 2 div and fixed 4 div. Cultures were co-immunostained with anti-NeuroD2 and anti-GFP antibodies and DAPI staining was done for nuclei. Dendrites were analyzed using Scholl analysis (Figure A.13 and A.14).

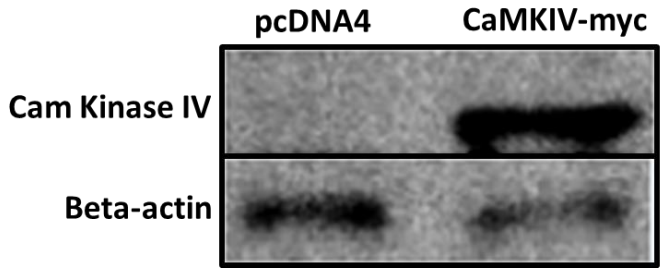

Figure A.12 Western Blot analysis of expression of constitutively active CaM Kinase IV-myc in primary cortical neurons. The membrane was blotted with anti-myc and anti-beta-actin antibodies separately. CaMKIV-pcDNA4-myc construct was successfully transfected to primary cortical neurons

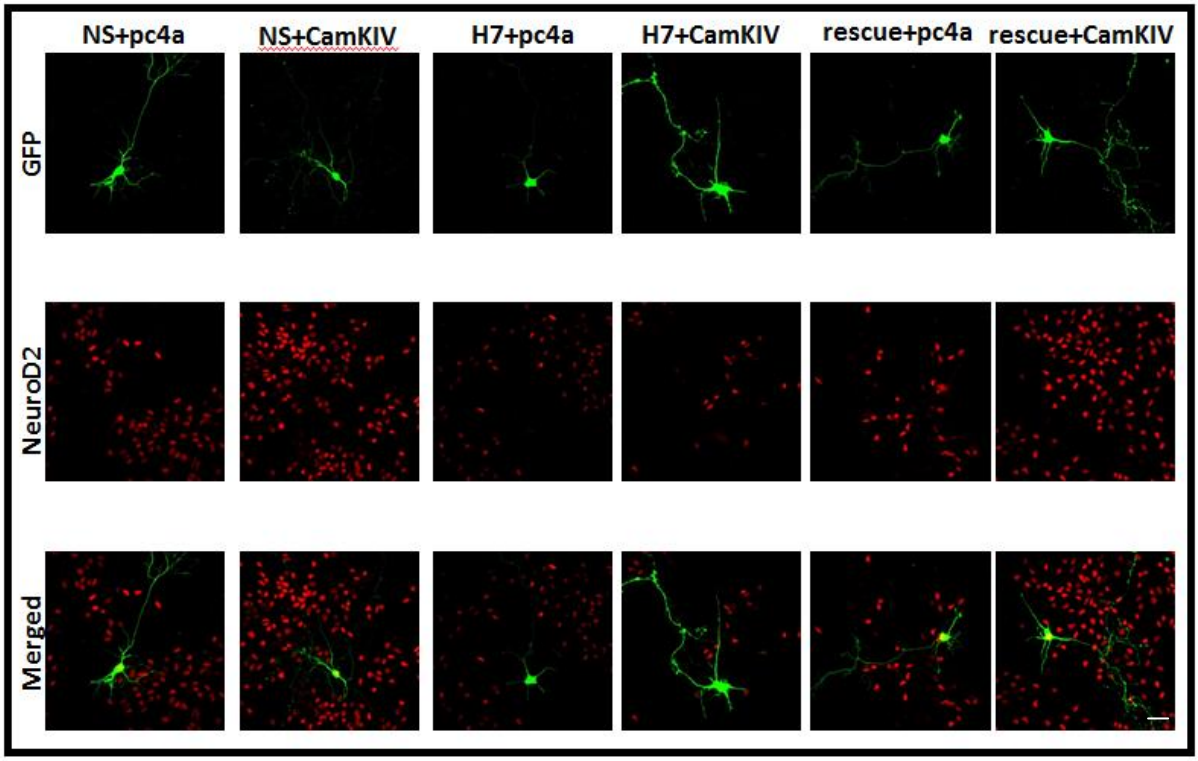

Figure A.13 Immunofluorescence analysis of dendrite morphology of both non-targeting (NS) , NeuroD2 shRNA (H7) and constitutively active CaM Kinase IV transfected E14 primary cortical neurons. 2 DIV E14 primary cortical neurons were transfected with non-targeting, NeuroD2 shRNA and both NeuroD2 shRNA and resistant NeuroD2 cDNA with constitutively active CaM Kinase IV construct. The neurons were fixed at 4 DIV and analyzed by Sholl analysis based on their dendrite morphology. GFP (green) and NeuroD2 (red). Scale bar, 10µm

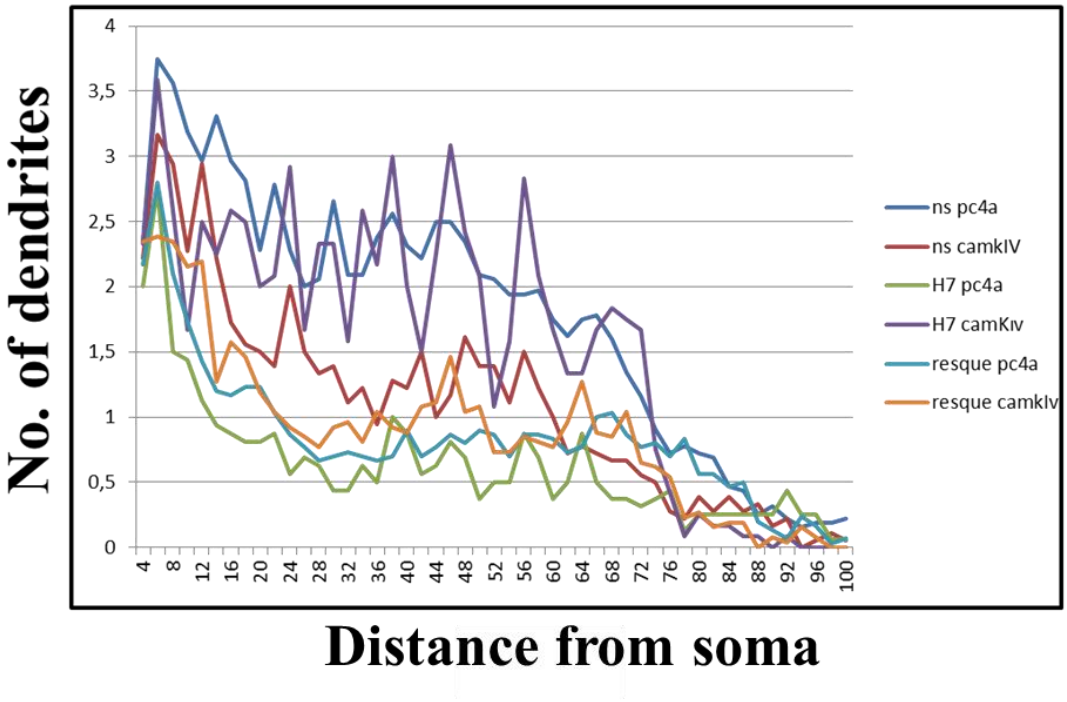

Figure A.14 Quantification of dendrite development of E14 primary cortical neurons. Sholl analysis plugin of ImageJ software was used to analyze the dendrite development of E14. Images were captured under 60X focus and they were 1024x1024 pixels. Unit scale: 1Pixel= 1,0 pixels.